To the Graduate Council:

I am submitting herewith a dissertation written by Oleg Burenko entitled "Dynamics and Feedback Control of Plasma Equilibrium Position in a Tokamak." I have examined the final copy of this dissertation for form and content and recommend that it be accepted in partial fulfillment of the requirements for the degree of Doctor of Philosophy, with a major in Engineering Science.

J Milton Bailey

J. Milton Bailey, Major Professor

We have read this dissertation
and recommend its acceptance:

J. Reece Roth

William J. Snyder

Marshall Pace

J M Forge

Accepted for the Council:

L Evans Roth

Vice Chancellor
Graduate Studies and Research

DYNAMICS AND FEEDBACK CONTROL OF PLASMA EQUILIBRIUM POSITION IN A TOKAMAK

A Dissertation

Presented for the

Doctor of Philosophy

Degree

The University of Tennessee, Knoxville

Oleg Burenko

June 1983

1 182885

To the Memory

of

FANTINA *and* VASIL

My Unforgettable Parents

ACKNOWLEDGMENTS

I wish to express my appreciation to Dr. J. Milton Bailey, my major adviser, and to Drs. Joseph M. Googe, Marshall O. Pace, J. Reece Roth, and William T. Snyder, my doctoral committee members, for their efforts to make presentation of this work a better one.

I would also like to thank the management of Oak Ridge National Laboratory Instrument and Electrical Engineering, Union Carbide Corporation Nuclear Division, for allowing use of Company equipment, supplies, and facilities in processing the manuscript.

ABSTRACT

A brief history of the beginnings of nuclear fusion research involving toroidal closed-system magnetic plasma containment is presented in Section 1.

In Section 2 a tokamak machine is defined mathematically for the purposes of plasma equilibrium position perturbation analysis.

The perturbation equations of a tokamak plasma equilibrium position are developed in Section 3.

Solution of the approximated perturbation equations of a tokamak plasma equilibrium position is carried out in Section 4. A *unique*, simple, and useful plasma displacement dynamics transfer function of a tokamak is developed. The dominant time constants of the dynamics transfer function are determined in a *symbolic* form. This symbolic form of the dynamics transfer function makes it possible to study the stability of a tokamak's plasma equilibrium position. Knowledge of the dynamics transfer function permits systematic syntheses of the required plasma displacement feedback control systems.

The major parameters governing the plasma equilibrium position stability of a tokamak are shown to be (1) external magnetic field decay index, (2) transformer iron core effect, (3) plasma current, (4) radial rate-of-change inductance parameter, (5) vertical rate-of-change inductance parameter, and (6) vacuum vessel eddy-current time constant. An *important* and *unique* result is derived, showing that for a *vacuum vessel eddy-current time constant* exceeding a certain value the vertical plasma equilibrium position is stable, in spite of an intentional vertical instability design represented by a negative decay index.

It is shown that a tokamak design having a theoretical set of positive decay index, negative radial rate-of-change inductance parameter, and positive vertical

rate-of-change inductance parameter is expected to have a better plasma equilibrium position stability tolerance than a tokamak design having the same set with the signs reversed.

In Section 5 a tokamak plasma displacement feedback control design is considered, Linear Optimal Control and the Optimality Condition are discussed, and a minimal hardware tokamak plasma displacement feedback control system is presented.

The ISX-A tokamak high-frequency oscillations and low-frequency dynamics functions are given numerically in Section 6, using the ISX-A tokamak numerical data given in the Appendix.

The results of an actual hardware ISX-A tokamak plasma displacement feedback control system design are presented in Section 7. It is shown that a theoretical design computer simulation and the actual hardware step function responses of the radial plasma displacement feedback control system are practically identical. The actual hardware vertical plasma displacement feedback control system performed just as well. Experimental results *support* all of the analytical developments.

TABLE OF CONTENTS

LIST OF FIGURES

1. INTRODUCTION

Nuclear fusion research originated after World War II. Basic nuclear fusion principles were studied and derived in the United States and other major nations. Early in the 1950's fusion research work for peaceful uses began independently in the United States, in Great Britain, in the Soviet Union, and in other nations. In the United States the fusion research work was done under Project Sherwood [1] of the Atomic Energy Commission. In Great Britain the work was carried out at the Atomic Energy Research Establishment, Harwell. The Soviet Union fusion research took place at the I. V. Kurchatov Institute of Atomic Energy in Moscow. Each of these nations had its projects classified "secret" until 1958, when a broad exchange of information took place at the Second International Conference on the Peaceful Uses of Atomic Energy in Geneva. It became known that, among several other magnetic plasma containment principles, the United States, Great Britain, and the Soviet Union all were developing *toroidal closed-system magnetic plasma containment*. The United States was experimenting with a toroidal machine called *Perhapsatron* [1; 5; 16, 7.122; 17, p.365], and Great Britain was developing a machine called ZETA [4; 6; 7; 14; 16, 7.131; 17, p.365], the letters standing for *zero-energy, thermonuclear assembly.* The Soviet Union was investigating a toroidal machine configuration [2, 8, 15]. All of these machines employed the transformer principle, with the one-turn secondary winding being a toroidal plasma ring. Perhapsatron employed also a one-turn primary winding (a metallic shell or closely spaced array of wires in parallel, over the outside of the toroidal vacuum chamber), while ZETA employed a multi-turn primary winding on two very large rings of wound steel tape (ten feet high and weighting 150 tons [14]). The Soviet Union toroidal device aiso employed a multi-turn primary winding. All of these machines employed a toroidal magnetic field (in the early days of fusion research called the axial, or longitudinal, magnetic field) for stabilization of *kink (wriggling) instabilities* of the plasma column. Several other nations also were experimenting with toroidal magnetic plasma containment [9-13].

The United States was also developing a toroidal machine called a *stellarator* [1; 16, 3.35; 17, p.349]. Several papers on stellarators were presented at the 1958 Geneva Second United Nations International Conference on the Peaceful Uses of Atomic Energy (Vol. 32: P/2170, p. 181; P/362, p. 201; P/358, p. 210; P/364, p. 217; P/359, p. 225).

Great Britain's experiments on ZETA continued into the early 1960's. A number of papers about ZETA experiments were presented at the 1961 Conference on Plasma Physics and Controlled Nuclear Fusion Research in Salzburg, Austria (Nuclear Fusion 1962 Supplement, Part 3: CN-10/54, p. 883; CN-10/57, p. 889; CN-10/58, p. 895; CN-10/60, p. 903).

The Soviet Union's toroidal machine configuration [2, 8, 15] was apparently named "tokamak" in the years 1959-1964. It appears that the name "tokamak" was first used by Lev A. Artsimovich at the Third International Conference on the Peaceful Uses of Atomic Energy in 1964 [23].

The results of experimental investigations on tokamak-type machines were presented at the 1965 Culham Conference on Controlled Nuclear Fusion Research (Proc. Vol. II: CN-21/147, p. 577; CN-21/245a, p. 595; CN-21/245b, p. 617; CN-21/246a, p. 629; CN-21/246b, p. 647; CN-21/144, p. 659).

A few papers on stellarator experiments were also presented at the 1965 Culham Conference [Proc. Vol. II: CN-21/119, CN-21/120, CN-21/50, CN-21/244, (pp. 673-733)], and there was one paper on ZETA (CN-21/32, p. 751).

1.1. Closed-System Magnetic Containment

A hot plasma at 200 million degrees Kelvin cannot be contained by any material walls; the plasma would rapidly melt the walls and add impurities. One general approach to the plasma containment problem is to use a magnetic field to contain the hot plasma. A magnetic field exerts an effective pressure on the contained plasma,

$$p_m = \frac{B^2}{2\mu_0} \quad (\text{newton/meter}^2)\,. \tag{1.1}$$

As long as this pressure is larger than the internal pressure of the plasma, plasma containment is possible. There are, however, practical limits on the production of strong magnetic fields over large volumes; this places an upper limit on the obtainable plasma pressure and hence on the density of hot plasma. Since a hot plasma behaves as a perfect gas, its kinetic pressure is given by

$$p_k\,(\text{N/m}^2) = k(n_e T_e + n_i T_i + n_{imp} T_{imp}) \quad , \tag{1.2}$$

where $k = 1.3804 \times 10^{-23}$(joules/kelvin) is the Boltzmann constant;

n_e, n_i, and n_{imp} are the plasma electron, ion, and impurity densities, respectively, per cubic meter;

T_e, T_i, and T_{imp} are the kinetic temperatures of electrons, ions, and impurities, respectively, in degrees Kelvin.

The ratio of the contained *plasma pressure* to the confining *magnetic field pressure* is a useful parameter, a *plasma stability index*

$$\beta = \frac{p_k}{p_m} = \frac{2\mu_0 p_k}{B^2} \quad , \tag{1.3}$$

where $\mu_0 = 4\pi \times 10^{-7}$ (henry/meter) is the vacuum permeability.

In a closed-system magnetic containment device, the magnetic lines do not depart from the plasma region but rather close on themselves within that region. Ultimately these magnetic lines map out a surface in a closed volume. Most often this surface is a toroidal shell, with different toroidal surfaces nested within each other.

Two general categories of closed-system magnetic containment devices have been predominantly under study in the late 1950's and in the 1960's: stellarators and tokamaks.

1.1.1. Stellarators

In a stellarator the confining magnetic field is generated by a set of toroidal and helical coils arranged around the outside of a toroidal chamber. The plasma is created and heated by inducing an electric current through a gas that fills the toroidal chamber. The arrangement of coils creates what has been called a *rotational transform* , an internal magnetic field with magnetic lines that form a closed path inside the torus while twisting about the magnetic axis of the torus. Each magnetic line makes repeated revolutions inside the torus and thereby generates a toroidal magnetic surface. There is an inherent tendency for a plasma with an induced current to become unstable and move across the magnetic field to the chamber wall. This plasma *kink instability* can be suppressed to some extent by using special external windings that cause the different (nested) magnetic surfaces to have different twist rates, a condition called *shear* . The use of complex external windings necessitated construction of a stellarator torus with a large aspect ratio (the ratio of the major radius of the torus to the minor radius). For these reasons poor containment properties have been observed in stellarators.

The stellarator originally was proposed by Lyman Spitzer, Jr., at Princeton University in 1951. Since that time the investigation of the properties of plasma in stellarators was a key element in the research program on controlled nuclear fusion in the United States. In the late 1960's ($\approx$1969) the research emphasis in the United States (and world-wide) was shifted to "tokamaks" after Lev Artsimovich at the I. V. Kurchatov Institute of Atomic Energy in Moscow, USSR, reported impressive results in experiments conducted in a comparatively simple toroidal magnetic-containment device, which he called a *tokamak.*

1.1.2. Tokamaks

In a tokamak, external windings around the outside of a toroidal chamber serve only to create an external magnetic field that points around the torus, the toroidal magnetic field. The necessary rotational transform (magnetic line twist about the central axis of the torus) and shear (different twists of magnetic lines of two nested magnetic surfaces) are contributed entirely by another field created by a plasma current flowing in the direction of the toroidal magnetic field. Just as in a stellarator, a tokamak plasma with an induced current may develop a *kink instability.* This instability may be suppressed in a tokamak by satisfying the Kruskal-Shafranov condition [24, (6.1)]

$$aB_T > RB_P \tag{1.4}$$

where a (meters) is the plasma minor radius,

B_T (tesla) is the external toroidal magnetic field,

R (meters) is the plasma major radius, and

B_P (tesla) is the poloidal magnetic field.

The Kruskal-Shafranov condition (1.4) places a limit on the allowable magnitude of B_P, for a given set of a, R, and B_T. Since B_P is directly proportional to a plasma current, this places a limit on the plasma current. This Kruskal-Shafranov limit is stated as a stability, or "safety factor"

$$q = \frac{aB_T}{RB_P} > 1 \; . \tag{1.5}$$

The safety factor q, (1.5), is defined as the number of times a magnetic field line (the net field line of both the toroidal and poloidal magnetic fields) travels around the major circumference of the torus while making one complete revolution about its minor axis.

For a given safety factor q (1.5) the maximum plasma current satisfying the stabilty requirement (1.4) is [24, (6.16)],

$$\left(I_p\right)_{\max} = \frac{2\pi a^2 B_T}{\mu_0 q R} \text{ (amperes)} \; , \tag{1.6}$$

where a, B_T, and R are as defined for eq. (1.4) and

$\mu_0 = 4\pi \times 10^{-7}$(henry/meter) is the vacuum permeability.

The tokamak originated in the USSR in the late 1950's. The first tokamak machine came into operation in 1957 [15]. The first significant experimental tokamak results were presented in 1965 at the Culham Conference on Plasma Physics and Controlled Nuclear Fusion Research. And today, about two decades later, major tokamak projects are being conducted by the United States, the Soviet Union, the European Economic Community, Japan, and China.

1.1.3. Plasma Instabilities and their Control

Generation of a plasma, its properties, and its magnetic containment methods have been extensively studied both theoretically and experimentally for over the past three decades [16-19; 24; 34; 65-67].

An equilibrium state of a plasma in any of the practical magnetic containment schemes has been found to be basically a non-stationary equilibrium. Attempts were made to control some of the plasma's instabilities via feedback systems: the flute instability in the magnetic mirror traps [28,29] and the sausage instability in the linear magnetic pinch devices via employment of a sensor-based computer control system [38].

In a tokamak plasma instabilities such as the flute (or ripple, or interchange) and the sausage (or necking-off), are suppressed or inhibited [30], while the kink (or helical) instability may be prevented from developing by satisfying the Kruskal-Shafranov condition [24], (1.4).

The toroidal geometry of the tokamak plasma current, however, creates forces acting to expand the plasma torus, to increase its major radius, and to decrease its minor radius. The equilibrium position of the plasma torus in the tokamak, defined by its major radius and out-of-plane displacement, is also subject to variation as a result of changes in the parameters of the plasma: the plasma pressure, the torus minor radius, and the plasma current.

If the outer casing of the tokamak (toroidal) vacuum chamber is made of copper [21] (or similar conducting material), the rate of change of the plasma torus displacement position (the major radius of the torus and the out-of-plane displacement) is greatly decreased by an interaction of the plasma current and the Foucault (eddy) current in the conducting outer casing. The conducting outer casing also serves to stabilize plasma instabilities, especially the kink (helical) instability [30]. The conducting outer casing makes a longer plasma discharge time possible. A practical fusion reactor of the tokamak type will have a plasma discharge (burn) time which will be considerably longer than that allowed by use of the conducting outer casing. For this and other technical reasons, it becomes necessary to replace the tokamak conducting outer casing with the feedback control of the plasma torus equilibrium position.

According to the published available records, the first successful attempt to control the plasma equilibrium position in the tokamak via an inductive feedback was performed in the USSR TO-1 tokamak [33, 36]. In this case a system of coils and two-terminal negative impedance regulators (regenerative circuits) effectively simulated the tokamak conducting outer casing, the effective time constant of which could be adjusted to be as large as 150-200 ms.

The tokamak plasma equilibrium position was successfully controlled employing an active feedback control system in the CLEO tokamak, United Kingdom [37, 39], and in the Oak Ridge Tokamak, ORMAK, United States of America [42, 44]. For the CLEO tokamak a quasi-classical method of analysis was employed, while the ORMAK analysis was in the domain of the optimal (modern) control theory and Kalman filtering.

The tokamak plasma equilibrium position feedback control via application of classical and/or modern control methods has been considered in several other works [45-50, 59-63]. The majority of references given above, and dealing with the tokamak plasma equilibrium position feedback control, emphasize on applications of the optimal control theory and Kalman filtering. None of them specifically states the fact that once a mathematical model of the tokamak has been developed, the task of applying optimal control theory is relatively straightforward; if the model is simplified by removing insignificant time constants, resorting to Kalman filtering [42, 48, 62] may not be necessary.

Analytical investigations of stability and analytical syntheses of feedback control of a system require knowledge of the system's dynamics and its perturbations in an analytical form. The equations necessary for a derivation of the tokamak's plasma equilibrium position perturbation dynamics have long been available [16-19; 24; 30; 33; 34; 39]. A need for simpler analytical models of the tokamak plasma equilibrium perturbation dynamics is well illustrated by the complexity and difficulty of applying both the classical and modern optimization methods to a very large system [48]: the understanding of the basic physical phenomenon is much more difficult, the sensitivity analysis becomes too complex, and unnecessarily complex controllers may be indicated. For these reasons development of a simpler analytical model of a tokamak plasma equilibrium position dynamics function is one of the objects of this work.

1.1.4. Simplifying Assumptions

For purposes of this work, it is assumed that a tokamak plasma column is stable. That is, it is assumed that there are no plasma disruptions of any sort and that none of the known (or unknown) plasma instabilities are present.

For considerations of forces acting on a plasma column, a plasma current is assumed to be a circular filament current having its radius equal to the major radius of a toroidal plasma column.

Effects of a transformer iron core magnetic flux return yoke (if there is one) and of its stray magnetic field are assumed to produce a (small) local steady-state deformation of plasma column; they are therefore assumed to be negligible.

2. TOKAMAK MACHINE

The tokamak approach was proposed in the early 1950's by Igor E. Tamm and Andrei D. Sakharov in Moscow, USSR. The tokamak was developed in the USSR by Lev A. Artsimovich at the I. V. Kurchatov Institute of Atomic Energy. The name "tokamak" may have come from the beginnings of the Russian words for toroidal [to], chamber [ka], magnetic [ma], and coil [k].

The tokamak is basically a transformer having a toroidal plasma ring (column) as its secondary winding. The current in the plasma ring is induced by the primary (ohmic heating) coil; the induced plasma current ohmically heats the plasma and produces the poloidal magnetic field; the external toroidal field coils produce the toroidal magnetic field; the toroidal and poloidal magnetic fields combine to form a helical field that shapes a toroidal magnetic container for holding the plasma away from the material walls of the tokamak toroidal vacuum chamber.

Figure 2.1 shows basic definition of the tokamak. The x-y plane is the equatorial plane of the plasma torus; the major radius of the plasma torus is always parallel to and nominally in the x-y plane; the motion of the plasma torus parallel to or in this plane is referred to as the "radial" or "equatorial" motion. The z-axis is the axis of symmetry of the plasma torus; normally it is the vertical axis (normal to the x-y plane); it is also the center line of the transformer iron core (some tokamaks have no iron cores); the motion of the plasma torus along the z-axis is referred to as the "vertical" or "axial" motion.

As shown in fig. 2.1, the vacuum vessel (chamber) is a circular toroid with minor radius b (m); it may, however, be a toroid of any other suitable cross section. The major radius of the toroidal plasma column is R (m) while its minor radius is a (m); Δ (m) is the plasma column displacement in the radial direction

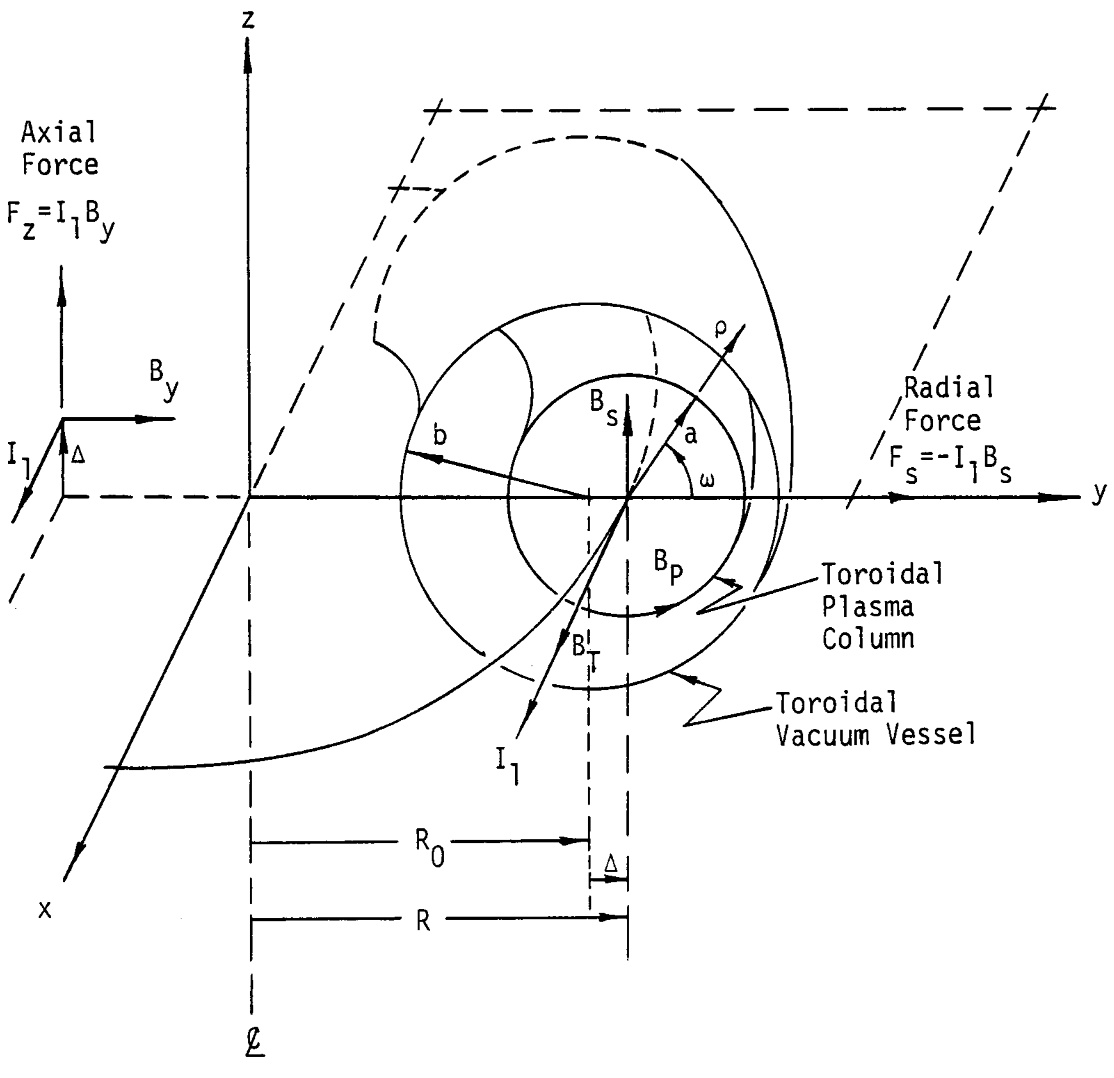

Figure 2.1. Tokamak basic definitions.

from its steady-state major radius R_0 (m), $R = R_0 + \Delta$. Displacement of the plasma column in a positive vertical direction (z-axis) is also designated by Δ. The plasma current I_1 (A) produces the poloidal magnetic field B_P (T). The externally generated toroidal magnetic field is B_T (T).

2.1. Radial Forces Acting on the Plasma

The mass of the toroidal plasma column is

$$M_T\,(\mathrm{kg}) = V_T(m_e n_e + m_i n_i)\,, \tag{2.1}$$

$$V_T = 2\pi R \times \pi a^2\,(\mathrm{m}^3) \tag{2.2}$$

is the column's volume, m_e (kg) is the mass of an electron, m_i (kg) is the mass of a plasma ion (nucleus) and, referring to eq. (1.56), for a clean hydrogen isotope plasma (which is of primary interest here),

$$n_e = n_i = n \quad ,$$

$$n_e + n_i = n_{ei} = 2n \quad , \tag{2.3}$$

$$n_{imp} = 0 \quad .$$

The plasma column length is $2\pi R$ (m) ; therefore, using equations (2.1)-(2.3), the plasma mass per unit length of the plasma column is

$$M\,(\mathrm{kg/m}) = \pi a^2 n(m_e + m_i)\,. \tag{2.4}$$

The plasma current mass element M has a positive displacement Δ (m) and velocity $\dot{\Delta}$ (m/s) . Therefore its momentum is, per unit length of the plasma column,

$M\,\dot{\Delta}$ (kg m/s/m) ,

and the equation of motion of the mass element is

$$\dot{M}\,\dot{\Delta} + M\,\ddot{\Delta} = \sum_{k=i,t}^{r,v,h,e} F_k \quad \text{(N/m)}\,, \tag{2.5}$$

where F_k are the forces acting on the plasma current mass element M. All of these forces are defined to be positive in the positive Δ-direction (y-direction) of fig. 2.1.

2.1.1. Internal Expansion Force

A toroidal plasma column tends to expand in major radius and to contract in minor radius under the action of plasma current and the other changing parameters of the plasma. Effectively, the internal expansion force (per unit length of the plasma column) acting on the plasma current mass element M is written

$$F_i\,\text{(N/m)} = I_1 B_i \ . \tag{2.6}$$

In (2.6) the effective internal expansion magnetic field is [34, (37)]

$$B_i\,\text{(T)} = \frac{\mu_0}{4\pi}\frac{I_1}{R}\Gamma \ , \tag{2.7}$$

$$\Gamma = \ln\frac{8R}{a} + \Lambda - \frac{1}{2} \ , \tag{2.8}$$

$$\Lambda = \beta_I + \frac{1}{2}l_i - 1 \ , \tag{2.9}$$

In (2.9), β_I is a plasma stability index (1.3). It is a dimensionless ratio of the plasma kinetic pressure p_k, averaged over the plasma cross section, to the poloidal magnetic field pressure (1.1),

$$\beta_I = \frac{2\mu_0 <p_k>}{B_P^2} \quad . \tag{2.10}$$

Referring to fig. 2.1, under the assumption of a cylindrical plasma column and an infinitely long plasma current filament, the plasma surface poloidal magnetic field is, at $\rho = a$,

$$B_P = \frac{\mu_0 I_1}{2\pi a} \quad . \tag{2.11}$$

Referring to (1.2) and (2.3), let an average plasma particle energy (temperature) of a clean plasma be, $n_{imp} = 0$,

$$T\ (\text{kelvin}) = \frac{(n_e T_e + n_i T_i)}{n_{ei}} \quad , \tag{2.12}$$

T_e and T_i being given in kelvin ; the plasma average kinetic pressure (energy density, joule/m^3 = newton/m^2) is then written

$$<p_k> = <n_{ei} kT> = <2nkT> \quad . \tag{2.13}$$

Substituting (2.11) and (2.13) into (2.10),

$$\beta_I = \frac{8\pi^2}{\mu_0} \frac{<n_{ei} kT> a^2}{I_1^2} = \frac{8\pi^2}{\mu_0} \frac{<2nkT> a^2}{I_1^2} \quad . \tag{2.14}$$

For a hydrogen isotope plasma equation (2.12) is simply

$$T\ (\text{kelvin}) = \frac{1}{2}(T_e + T_i) \quad . \tag{2.15}$$

The electron energy T_e, as determined by the bremsstrahlung and synchrotron radiation, can be related to the ion (nucleus) energy T_i [17, (11.20), (11.86)].

For the purposes of this work, however, it is convenient to assume that T_e and T_i are simply related to each other by a parameter μ_e,

$$T_e = \mu_e T_i \quad , \tag{2.16}$$

such that, using (2.15),

$$T_e \text{ (kelvin)} = \frac{2T\mu_e}{(\mu_e+1)} \quad , \tag{2.17}$$

$$T_e \text{ (kelvin)} = \frac{1}{2}(\mu_e+1)T_i \quad . \tag{2.18}$$

In (2.9), l_i is the plasma column internal inductance per unit length of the plasma column [34, (25)],

$$l_i = \frac{\overline{B_\omega^2}}{B_p^2} = \left\{ \int_0^a \left(\int_0^{2\pi} [B_\omega(\rho,\omega)]^2 \ \rho \ d\omega \right) d\rho \right\} \left(\pi a^2 B_p^2\right)^{-1} \quad . \tag{2.19}$$

Under an assumption of a cylindrical plasma column, $a \ll R$, and a constant plasma current density, J (A/m^2) $= (I_1/\pi a^2)$, the plasma internal poloidal magnetic field is, using (2.11),

$$B_\omega = B_p \frac{\rho}{a} \quad . \tag{2.20}$$

Substituting (2.20) into (2.19), the value of l_i is evaluated to be 0.5. In view of this result it is reasonable to assume that l_i is a constant equal to 0.5. Using this value of l_i in (2.9), equation (2.8) becomes

$$\Gamma = \ln\left(\frac{8R}{a}\right) + \beta_I - 1.25 \quad . \tag{2.21}$$

2.1.2. Transformer Iron Core Force

The interaction between the plasma current I_1 and a transformer iron core, if there is one, manifests itself in a force which attracts the plasma current to the core. Local effects of a transformer magnetic flux return yoke (if there is one) and of its stray magnetic field are assumed to be negligible. Then, assuming an infinitely long cylindrical iron core of radius r_c (m), aligned with the z-axis of fig. 2.1, the iron core force is proportional to a function of the ratio R/r_c [34, (75)] ,

$$f_t = 0.9 + 22.0 \exp\left[-1.6 \left(\frac{R}{r_c}\right)\right] \quad . \tag{2.22}$$

An effective magnetic field of the transformer iron core, at the plasma current element location R (m), fig. 1, is then (due to the iron core image of the plasma current element I_1)

$$B_t\,(\text{Tesla}) = \rho\frac{\mu_0}{4\pi}\frac{2I_1}{R}f_t \quad , \tag{2.23}$$

where $0 \leqslant \rho \leqslant 1.0$ has been introduced to account for different effects of various transformer core materials.

The iron core transformer force F_t (N/m), at the plasma current element location R (m), fig. 2.1, is generated by the poloidal magnetic flux lines passing through the vacuum vessel into the iron core. Therefore the force is

$$F_t + \tau_t\dot{F}_t = -I_1B_t \quad , \tag{2.24}$$

where τ_t(s) is the vacuum vessel penetration time constant for the force of transformer iron core.

2.1.3. Vacuum Vessel Eddy-Current Force

As the plasma current element I_1 moves within the vacuum vessel in the radial (y,R) direction, a vacuum vessel eddy current produces a time-delayed magnetic field B_r at the plasma current element location,

$$B_r + \tau_r \dot{B}_r = \frac{\mu_0}{4\pi} K_r I_1 \dot{\Delta} \quad , \tag{2.25}$$

where τ_r (s) is the eddy-current time constant, and K_r (s/m^2) is a vacuum vessel geometry gain constant. The eddy current force is then

$$F_r \ (\mathrm{N/m}) = -I_1 B_r \ . \tag{2.26}$$

2.1.4. Vacuum Vessel Induced-Current Force

In the case of a toroidally continuous vacuum vessel there will be a current induced in the vacuum vessel walls which is due to the ohmic heating magnetic flux time rate of change. Similarly, in the case of a toroidally split vacuum vessel an effect of currents induced in all the separate sections of the vacuum vessel may be attributed to a single effective toroidal current. In either case, it is assumed that an effective vacuum vessel induced current,

I_2 (A),

generates a force

$$F_v = I_1 B_v \quad , \tag{2.27}$$

where

$$B_v = \frac{\mu_0}{4\pi} K_v I_2 \quad , \tag{2.28}$$

and K_v (1/m) is an effective gain constant of the vacuum vessel geometry.

2.1.5. *Ohmic Heating Force*

The primary coil of the tokamak (transformer) induces the plasma current. Since the plasma current heats up the plasma ohmically, the primary coil is called also the *ohmic heating coil*. The ohmic heating coil current,

I_4 (A) ,

generates a force acting on the plasma current mass element M, the ohmic heating force,

$$F_h = I_1 B_h \quad , \tag{2.29}$$

where the effective magnetic field B_h had to penetrate the vacuum vessel to arrive at the plasma current element location ; therefore

$$B_h + \tau_k \dot{B}_h = \frac{\mu_0}{4\pi} K_h I_4 \quad , \tag{2.30}$$

where τ_k (s) is the vacuum vessel penetration delay time constant for a magnetic field, and K_h (1/m) is an effective gain constant of the tokamak coil geometry.

2.1.6. *External Magnetic Field Force*

The equilibrium of a plasma torus in its equatorial plane (x-y plane, fig. 2.1) is maintained by an external magnetic field B_s , which is perpendicular to the radial plane as it is shown in fig. 2.1. This field is normally designed to be slightly concave towards the z-axis. Such a curved shape of the external magnetic field makes the plasma torus stable relative to the vertical (z-axis) displacement. The *barrel* shape of such a field is generally characterized by the *decay index* [34, (38)]

$$N = -\frac{R}{B_s}\frac{\partial B_s}{\partial R} \quad , \tag{2.31}$$

and the condition of vertical (z-axis) stability of the plasma torus is written then as [34, (39)]

$$N > 0 \quad . \tag{2.32}$$

Integration of equation (2.31) results in

$$B_s = f_s R^{-N} \quad , \tag{2.33}$$

where f_s is a function of integration. In view of (2.6), it is logical to let f_s be a function directly proportional to the plasma current,

$$f_s = K_s I_1 \quad ; \tag{2.34}$$

equation (2.33) is then written

$$B_s = K_s I_1 R^{-N} \quad , \tag{2.35}$$

where K_s is a proportionality constant. Denoting the steady-state equilibrium quantities by a subscript zero, using (2.35),

$$B_{s0} = K_s (I_1)_0 R_0^{-N} \quad , \tag{2.36}$$

from which

$$K_s = B_{s0}\left(I_1^{-1}\right)_0 R_0^N \quad . \tag{2.37}$$

Substituting (2.37) into (2.35),

$$B_s \;=\; B_{s0}\,\frac{I_1}{(I_1)_0}\left(\frac{R}{R_0}\right)^{-N} \quad . \tag{2.38}$$

The external magnetic field has to penetrate the vacuum chamber to arrive at the plasma location ; therefore (2.38) is correctly written as

$$B_s \;+\; \tau_k \dot{B}_s \;=\; B_{s0}\,\frac{I_1}{(I_1)_0}\left(\frac{R}{R_0}\right)^{-N} \quad , \tag{2.39}$$

where τ_k (s) is the vacuum chamber penetration delay time constant for a magnetic field.

The external magnetic field force acting on the plasma current mass element M in the radial direction is then

$$F_s \;=\; -I_1 B_s \quad . \tag{2.40}$$

In a steady-state radial equilibrium of the plasma torus, the sum of all forces acting on the plasma current mass element M is zero. Adding the steady-state values of the equations (2.7) [(2.6)], (2.23) [(2.24)], (2.25) [(2.26)], (2.28) [(2.27)], (2.30) [(2.29)], and (2.40), a steady-state value of the external magnetic field is

$$B_{s0} \;=\; \frac{\mu_0}{4\pi}\left\{ \left(\frac{I_1}{R}\right)_0 \left[\; \Gamma_0 - 2\rho(f_t)_0 \;\right] \;+\; K_v(I_2)_0 \;+\; K_h(I_4)_0 \right\} \quad . \tag{2.41}$$

The radial plasma equilibrium can be controlled by a vertical magnetic field (fig. 2.1) $B_s \;=\; B_{s0}$, (2.41), at the effective plasma current I_1. In such a case B_{s0} is simply preprogrammed and is generated as a function of time by an automatic sequencer; all the steady-state quantities of (2.41) must be precalculated as functions of time. This type of the radial plasma equilibrium control is referred to as the *open-loop* control. Obviously an open-loop control cannot take into account the inaccuracies of precalculations and the instantaneous unpredictable deviations of the variables from equation (2.41) from their precalculated steady-state values.

A *closed-loop* (feedback) control of the radial plasma equilibrium position is afforded by use of equation (2.38) [(2.39)]. To the first order of (binomial series) approximation, equation (2.38) can be written

$$B_s = B_{s0} \frac{I_1}{(I_1)_0}\left(1 - \frac{N}{R_0}\Delta\right) \quad . \tag{2.42}$$

If the plasma current I_1 is measured (Rogowski coil) and if the plasma column displacement Δ is measured (position pickup coils), then the external vertical magnetic field B_s can be (feedback) adjusted using equation (2.42), to minimize the displacement of the plasma column due to inaccurate precalculations and unpredictable deviations of the variables [equation (2.41)] from their precalculated steady-state values [39]. In this case of the feedback control, just as in the case of the open-loop control, B_{s0} is preprogrammed and is instrumented using a time-function generator.

While in either of the above two cases, the open-loop and the closed-loop controls, the plasma column equilibrium position conditions may be satisfied at some instances, the stability of the plasma equilibrium position remains analytically unknown and undefined, except for some experimental results [39, 42].

To control the plasma equilibrium position and its stability, it is practical to introduce an external vernier vertical magnetic control field

$$B_c = -K_c I_3 \quad , \tag{2.43}$$

such that equation (2.39) becomes

$$B_e + \tau_k \dot{B}_e = B_{s0} \frac{I_1}{(I_1)_0} \left(\frac{R}{R_0} \right)^{-N} - K_c I_3 \quad , \tag{2.44}$$

where

$$B_e = B_s + B_c \quad , \tag{2.45}$$

K_c (T/A) is the magnetic control field gain constant, and I_3 (A) is the magnetic control field current.

The external magnetic field force acting on the plasma current mass element M in the radial direction, (2.40), becomes then

$$F_e = -I_1 B_e \quad . \tag{2.46}$$

2.2. Interacting Electric Circuits

Four electric circuits are assumed to be interacting. All circuits are assumed to be characterized by their respective applied voltages (volt), resistances (ohm), self-inductances (henry), and mutual inductances (henry), as depicted schematically in fig. 2.2, where numbers and subscripts denote circuits and their respective quantities as follows:

plasma, 1;

vacuum vessel, 2;

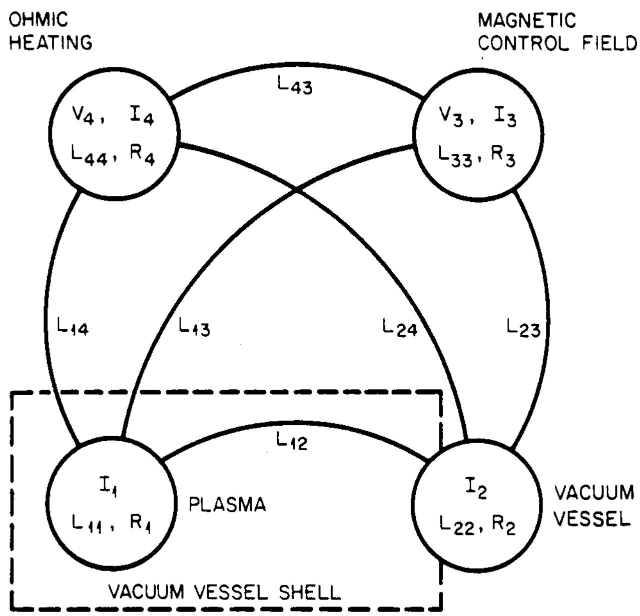

Figure 2.2. Interacting electric circuits.

control field, 3;

ohmic heating, 4.

As is shown in fig. 2.2, magnetic fluxes involving mutual inductances L_{13} and L_{14} must penetrate the vacuum vessel shell. This fact is taken into account in the appropriate circuit equations.

2.2.1. *Magnetic Flux of Electric Circuits*

Referring to figures 2.1, 2.2, and A1, it is assumed that all four electric circuits are located in parallel planes and that the directions of their positive currents are the same as that of the plasma current I_1. A magnetic flux linking a jth electric circuit is then

$$\Phi_j = \sum_{k=1}^{4} \Phi_{jk} \quad , \tag{2.47a}$$

$$\Phi_{jk} = L_{jk} I_k \quad , \tag{2.47b}$$

$$j = 1,\ 2,\ 3,\ 4 \ .$$

Referring to fig. 2.2, magnetic fluxes $\Phi_{13} = \Phi_{31}$ and $\Phi_{14} = \Phi_{41}$ must penetrate the vacuum vessel shell, with magnetic field penetration delay time constant of τ_k (s). Therefore, at the plasma current I_1 location the magnetic fluxes Φ_{13} and Φ_{14} must satisfy their respective first order differential equations,

$$\Phi_{13} + \tau_k \dot{\Phi}_{13} = L_{13} I_3 \quad , \tag{2.48}$$

$$\Phi_{14} + \tau_k \dot{\Phi}_{14} = L_{14} I_4 \quad . \tag{2.49}$$

Similarly, at the control field current I_3 location,

$$\Phi_{31} + \tau_k \dot{\Phi}_{31} = L_{13} I_1 \quad , \tag{2.50}$$

and at the ohmic heating current I_4 location,

$$\Phi_{41} + \tau_k \dot{\Phi}_{41} = L_{14} I_1 \quad . \tag{2.51}$$

An external voltage applied to a jth electric circuit is then written, using (2.47)-(2.51),

$$V_j = R_j I_j + \dot{\Phi}_j \quad . \tag{2.52}$$

2.2.2. Plasma Circuit

The resistivity of a clean (assumed to have no impurities) hydrogen isotope plasma column has been calculated to be [17, (8.51); 18]

$$\rho_1 = 3.346 \times 10^{-33} \; Z \; \ln\lambda \; (kT_e)^{-3/2} \, (\Omega\text{-m}) \, , \tag{2.53}$$

where T_e (kelvin) is the electron temperature (energy), $Z = n_e/n_i$ is the ionic charge number (equal to unity for hydrogen) and [17, (8.18)]

$$\lambda = 12\pi \left(\frac{\epsilon_0}{e^2} \right)^{3/2} \left(\frac{(kT_e)^3}{n_e} \right)^{1/2} \quad . \tag{2.54}$$

Substituting into (2.54) the permittivity of vacuum $\epsilon_0 = 8.854 \times 10^{-12}$ (farad/meter) and the charge of proton $e = 1.602 \times 10^{-19}$ (Coulomb),

$$\lambda = 24.158 \times 10^{40} \left(\frac{(kT_e)^3}{n_e} \right)^{1/2} \quad . \tag{2.55}$$

Substituting (2.55) into (2.53),

$$\rho_1 = 3.346\times10^{-33}(kT_e)^{-1.5}\left(95.288+\frac{3}{2}\ln(kT_e)-\frac{1}{2}\ln(n_e)\right)(\Omega\text{-m}) . \tag{2.56}$$

The resistance of the toroidal plasma (column) circuit is then

$$R_1(\Omega) = \rho_1\frac{2\pi R}{\pi a^2} . \tag{2.57}$$

The self-inductance of the toroidal plasma (column) circuit is [34, (17)],

$$L_{11} = K_i\mu_0 R\left[\ln\left(8\frac{R}{a}\right) - 2\right] , \tag{2.58}$$

where

$$K_i = (13.223\rho + 1) \tag{2.59}$$

accounts for a transformer iron core effect, ρ being an iron core parameter

$$0 \leqslant \rho \leqslant 1.0 , \tag{2.60}$$

$\rho=1.0$ for an entire transformer iron core effect.

Using equations (2.47)-(2.49) and (2.52), $j=1$, the plasma circuit equations are then

$$0 = R_1 I_1 + \frac{d}{dt}\sum_{k=1}^{2} L_{1k}I_k + \dot{\Phi}_{13} + \dot{\Phi}_{14} , \tag{2.61}$$

$$\Phi_{13} + \tau_k\dot{\Phi}_{13} = L_{13}I_3 , \tag{2.62}$$

$$\Phi_{14} + \tau_k\dot{\Phi}_{14} = L_{14}I_4 , \tag{2.63}$$

where all quantities, except τ_k, are time-varying functions.

2.2.2.1. Plasma Energy Injection

The average plasma energy density is given by (2.13). The average plasma particle energy is given by either (2.12), (2.15), or (2.18); it may also be written as

$$kT\,(\text{joules}) \;=\; kT_0 \;+\; kT_1 \;+\; kT_{ext} \quad , \tag{2.64}$$

where

kT_0 is the initial, steady-state value of the particle energy,

$$kT_1(n\times 2\pi R\times \pi a^2) \;=\; \int_0^t I_1^2 R_1 \; dt \tag{2.65}$$

is the ohmic heating generated particle energy, and

$$kT_{ext}(n\times 2\pi R\times \pi a^2) \;=\; E_{ext} \;=\; \int_0^t P_{ext} \; dt \tag{2.66}$$

is the plasma energy supplied by some external means, such as by *neutral beam injection* .

A neutral beam injector is assumed to be characterized by the power it can deliver to the plasma, P_{ext} (joules/second), and the associated number of neutral particles, K_p (neutral particles/joule). Each neutral particle is assumed to be simply a hydrogen isotope atom, splitting after injection into the plasma into an electron of mass m_e (kg) and an ion of mass m_{iext} (kg); therefore, referring to the equations (2.1)-(2.4) and (2.66), the injected plasma density is

$$n_{ext} \;=\; \frac{2K_p E_{ext}}{2\pi R\times \pi a^2} \quad , \tag{2.67}$$

and the injected plasma mass per unit length of the plasma column is

$$M_{ext}\,(\text{kg/m}) \;=\; \pi a^2 n_{ext}(m_e \;+\; m_{iext}) \quad . \tag{2.68}$$

The time derivative of equation (2.63) is, using (2.65) and (2.66),

$$k\dot{T} = \frac{(I_1^2 R_1 + P_{ext})}{(n \times 2\pi R \times \pi a^2)} - (kT_1 + kT_{ext})\left(\frac{\dot{n}}{n} + \frac{\dot{R}}{R} + 2\frac{\dot{a}}{a}\right) \quad . \tag{2.69}$$

The time derivative of equation (2.67) is

$$\dot{n}_{ext} = \frac{K_p}{\pi^2 R a^2}\left[P_{ext} - \left(\frac{\dot{R}}{R} + 2\frac{\dot{a}}{a}\right)E_{ext}\right] \quad . \tag{2.70}$$

2.2.3. *Vacuum Vessel Circuit*

Using equations (2.47) and (2.52), $j=2$, the vacuum vessel circuit equation is

$$0 = I_2 R_2 + \frac{d}{dt}\sum_{k=1}^{4} L_{2k} I_k \quad , \tag{2.71}$$

2.2.4. *Control Field Circuit*

Using equations (2.47), (2.50), and (2.52), $j=3$, the control field circuit equations are

$$V_3 = I_3 R_3 + \frac{d}{dt}\sum_{k=2}^{4} L_{3k} I_k + \dot{\Phi}_{31} \quad , \tag{2.72}$$

$$\Phi_{31} + \tau_k \dot{\Phi}_{31} = L_{13} I_1 \quad , \tag{2.73}$$

where V_3 is an externally applied control field voltage, and R_3, L_{23}, L_{33}, L_{34}, and τ_k are constants; all other quantities are time-varying functions.

2.2.5. *Ohmic Heating Circuit*

Using equations (2.47), (2.51), and (2.52), $j=4$, the ohmic heating circuit equations are

$$V_4 = I_4 R_4 + \frac{d}{dt} \sum_{k=2}^{4} L_{4k} I_k + \dot{\Phi}_{41} \quad , \tag{2.74}$$

$$\Phi_{41} + \tau_k \dot{\Phi}_{41} = L_{14} I_1 \quad , \tag{2.75}$$

where V_4 is an externally applied ohmic heating voltage, and R_4, L_{24}, L_{34}, L_{44}, and τ_k are constants; all other quantities are time-varying functions.

3. PERTURBATION EQUATIONS

Equations of the forces and interacting electric circuits involve quantities which are functions of a number of variables. Applying Taylor's theorem for several variables, to the first order of approximation the perturbation of a quantity Q of n variables is found to be

$$\delta Q = \sum_{j=1}^{n} \delta x_j \left[\frac{\partial Q(X)}{\partial x_j}\right]_{X=X_0} , \tag{3.1a}$$

where

$Q = Q(X)$, X is a set of n variables, which are in general functions of time,

δQ is a perturbation increment of Q,

x_j is a jth member of the set X,

δx_j is a perturbation increment of x_j,

X_0 is a steady-state set of the set X.

Equation (3.1a) also applies to time derivatives of a quantity Q. A time-rate-of-change of a perturbation of a quantity Q is equal to the perturbation of the time-rate-of-change of the quantity Q,

$$\frac{d}{dt}[\delta Q(t)] = \delta\left[\frac{dQ(t)}{dt}\right] = \delta\left[\dot{Q}(t)\right] . \tag{3.1b}$$

Since any perturbation of a quantity at "zero" time is equal to zero, $\delta Q(0)|=|0$, Laplace transformation of equation (3.1b) is simply ("s" designates the complex frequency)

$$s\left[\delta Q(s)\right] = \delta\left[sQ(s)\right] = \delta\left[\dot{Q}(s)\right] . \tag{3.1c}$$

3.1. Toroidal Flux Conservation

Perturbation equations for the forces and interacting electric circuits are derived under an assumption that a plasma toroidal flux is conserved. Referring to fig. 2.1, according to Ampère's law

$$B_T R = \frac{\mu I}{2\pi} \quad , \tag{3.2}$$

where I is the current enclosed. If this current is constant, then

$$B_T R = (B_T)_0 R_0 \quad . \tag{3.3}$$

Toroidal flux conservation requires that

$$\Phi = \pi a^2 B_T = \pi a_0^2 (B_T)_0 \quad . \tag{3.4}$$

Substituting (3.3) into (3.4),

$$a^2 R_0 = a_0^2 R \tag{3.5}$$

is a statement of the toroidal flux consevation.

3.2. Total and Perturbation Quantities

For simplicity of notation, the same quantity symbols used up to now to designate total quantities are used from now on to designate their perturbation quantities, the equilibrium (steady-state) quantities being distiguished by a subscript zero. To illustrate the point, in equation (3.5) a_0 and R_0 are the steady-state values (quantities) of the total quantities a and R, respectively,

$$a = a_0 + \delta a \quad , \tag{3.6}$$

$$R = R_0 + \delta R \quad , \tag{3.7}$$

and δa and δR are the perturbation quantities of a and R, respectively. Applying (3.1) to equation (3.5),

$$\delta a \left(2aR_0 \right)_{a=a_0} = \delta R(a_0^2) \quad ,$$

$$\delta a(2a_0R_0) = \delta R(a_0^2) \quad ,$$

$$\delta a = \frac{a_0}{2R_0}\delta R \quad , \tag{3.8}$$

or

$$a = \frac{a_0}{2R_0}R \tag{3.9}$$

is the perturbation equation of equation (3.5), a and R being now the perturbation quantities.

From fig. 2.1 and equation (3.7),

$$\delta R = \Delta \quad ; \tag{3.10}$$

therefore the perturbation equation (3.9) may also be written

$$a = \frac{a_0}{2R_0}\Delta \quad . \tag{3.11}$$

All perturbation equations are Laplace transformed, with s designating the complex frequency.

3.2.1. Internal Expansion Force Perturbation

Applying equations (3.1), (3.10), and (3.11) to equations (2.6), (2,7), (2.14), and (2.21), the perturbation equations of the internal expansion force are

$$F_i = (B_i)_0 I_1 + (I_1)_0 B_i \quad , \tag{3.12}$$

$$B_i = \frac{\mu_0}{4\pi}\left[\left(\frac{\Gamma}{R}\right)_0 I_1 - \left(\frac{I_1}{R^2}\Gamma\right)_0 \Delta + \left(\frac{I_1}{R}\right)_0 \Gamma \right] \quad , \tag{3.13}$$

$$\Gamma = \frac{1}{2R_0}\Delta + \beta_I \quad , \tag{3.14}$$

$$\beta_I = (\beta_I)_0 \left[\frac{1}{R_0}\Delta - \frac{2}{(I_1)_0} I_1 + \frac{1}{(n_{ei})_0} n_{ei} + \frac{1}{kT_0} kT \right] \quad . \tag{3.15}$$

Substituting equations (3.13)-(3.15) into equation (3.12),

$$F_i = B_{11} I_1 + B_{12}\Delta + B_{13} n_{ei} + B_{14} kT \quad , \tag{3.16}$$

where

$$B_{11} = \frac{\mu_0}{4}\pi\left(\frac{2I_1}{R}\right)_0 \left(\ln\frac{8R_0}{a_0} + \frac{1}{2}l_i - 1.5 \right) \quad , \tag{3.17}$$

$$B_{12} = \frac{\mu_0}{4\pi}\left(\frac{I_1^2}{R^2}\right)_0 \left(2.0 - \frac{1}{2}l_i - \ln\frac{8R_0}{a_0} \right) \tag{3.18}$$

$$B_{13} = 2\pi\left(\frac{I_1}{R}\right)_0 kT_0 a_0^2 \quad , \tag{3.19}$$

$$P_{17} = 2\pi\left(\frac{I_1}{R}\right)_0 (n_{ei})_0 a_0^2 \quad . \tag{3.20}$$

3.2.2. Transformer Iron Core Force Perturbation

Applying equations (3.1) and (3.10) to equations (2.22)-(2.24), the perturbation equations of the transformer iron core force are

$$F_t + \tau_t \dot{F}_t = -(B_t)_0 I_1 - (I_1)_0 B_t \quad , \tag{3.21}$$

$$B_t = \rho\frac{\mu_0}{2\pi}\left[\left(\frac{f_t}{R}\right)_0 I_1 - \left(\frac{I_1}{R^2}\right)_0 \left(f_t\right)_0 \Delta + \left(\frac{I_1}{R}\right)_0 \left(\frac{\partial f_t}{\partial R}\right)_0 \Delta\right] \quad ,$$

or

$$(1 + \tau_t s)F_t = B_{21} I_1 + B_{22}\Delta \quad , \tag{3.22}$$

where

$$B_{21} = -\rho\frac{\mu_0}{4\pi}\left(\frac{4I_1}{R}\right)_0 (f_t)_0 \quad , \tag{3.23}$$

$$B_{22} = \rho\frac{\mu_0}{4\pi}\left(\frac{2I_1^2}{R}\right)_0 \left[\frac{1}{R_0}(f_t)_0 - \left(\frac{\partial f_t}{\partial R}\right)_0\right] \quad . \tag{3.24}$$

3.2.3. Vacuum Vessel Eddy-Current Force Perturbation

Applying equations (3.1) and (3.10) to equations (2.25) and (2.26), the perturbation equations of the vacuum vessel eddy current force are

$$F_r = -(B_r)_0 I_1 - (I_1)_0 B_r \quad , \tag{3.25}$$

$$B_r + \tau_r \dot{B}_r = \frac{\mu_0}{4\pi}K_r\left[(I_1)_0 \dot{\Delta} + (\dot{\Delta})_0 I_1\right] \quad . \tag{3.26}$$

Since in steady-state $(\dot{\Delta})_0 = 0$, $(B_r)_0 = 0$,

$$F_r = -(I_1)_0 B_r \quad , \tag{3.27}$$

$$(1 + \tau_r s) B_r = \frac{\mu_0}{4\pi} K_r (I_1)_0 s \Delta \quad . \tag{3.28}$$

Substituting (3.28) into (3.27),

$$(1 + \tau_r s) F_r = B_{31} s \Delta \quad , \tag{3.29}$$

$$B_{31} = -\frac{\mu_0}{4\pi} K_r (I_1^2)_0 \quad . \tag{3.30}$$

3.2.4. Vacuum Vessel Induced-Current Force Perturbation

Applying equation (3.1) to equations (2.27) and (2.28), the perturbation equations of the vacuum vessel induced-current force are

$$F_v = (B_v)_0 I_1 + (I_1)_0 B_v \quad , \tag{3.31}$$

$$B_v = \frac{\mu_0}{4\pi} K_v I_2 \quad . \tag{3.32}$$

Substituting (3.32) into (3.31),

$$F_v = B_{41} I_1 + P_{12} I_2 \quad , \tag{3.33}$$

$$B_{41} = (B_v)_0 = \frac{\mu_0}{4\pi} K_v (I_2)_0 \quad , \tag{3.34}$$

$$P_{12} = \frac{\mu_0}{4\pi} K_v (I_1)_0 \quad . \tag{3.35}$$

3.2.5. Ohmic Heating Force Perturbation

Applying equation (3.1) to equations (2.29) and (2.30), the perturbation equations of the ohmic heating force are

$$F_h = (B_h)_0 I_1 + (I_1)_0 B_h \quad , \tag{3.36}$$

$$(1 + \tau_k s)B_h = \frac{\mu_0}{4\pi} K_h I_4 \quad ; \tag{3.37}$$

substituting (3.37) into (3.36),

$$F_h = B_{51} I_1 + \frac{B_{52}}{(1+\tau_k s)} I_4 \quad , \tag{3.38}$$

$$B_{51} = (B_h)_0 = \frac{\mu_0}{4\pi} K_h (I_4)_0 \quad , \tag{3.39}$$

$$B_{52} = \frac{\mu_0}{4\pi} (I_1)_0 K_h \quad . \tag{3.40}$$

3.2.6. External Magnetic Field Force Perturbation

Applying equations (3.1) and (3.10) to equations (2.44) and (2.46), the perturbation equations of the external magnetic field force are

$$F_e = -(B_e)_0 I_1 - (I_1)_0 B_e \quad , \tag{3.41}$$

$$(1 + \tau_k s)B_e = B_{s0} \left[\frac{1}{(I_1)_0} I_1 - \frac{N}{R_0} \Delta \right] - K_c I_3 \quad ; \tag{3.42}$$

substituting (3.42) into (3.41), noting that $(B_e)_0 = B_{s0}$,

$$(1 + \tau_k s)F_e = (1 + 0.5\tau_k s) B_{61} I_1 + B_{62} \Delta + B_{63} I_3 \quad , \tag{3.43}$$

$$B_{61} = -2B_{s0} \quad , \tag{3.44}$$

$$B_{62} = NB_{s0} \left(\frac{I_1}{R}\right)_0 \quad , \tag{3.45}$$

$$B_{63} = (I_1)_0 K_c \quad . \tag{3.46}$$

3.2.7. Newton's Force Equation Perturbation

Equation (2.5) is the Newton's (second Law) force equation; its perturbation equation is simply

$$s^2 \Delta M_0 = \sum_{K=i,t}^{r,v,h,e} F_k \quad , \tag{3.47}$$

since $(\dot{M})_0 = 0$, $(\dot{\Delta})_0 = 0$, and $(\ddot{\Delta})_0 = 0$.

Substituting equations (3.16), (3.22), (3.29), (3.33), (3.38), and (3.43) into equation (3.47), using (2.3), the perturbation equation of Newton's force is

$$\begin{aligned} s^2 \Delta M_0 = & \left[B_{11} + \frac{B_{21}}{1+\tau_t s} + B_{41} + B_{51} + \frac{(1+0.5\tau_k s)B_{61}}{1+\tau_k s} \right] I_1 \\ & + \left[B_{12} + \frac{B_{22}}{1+\tau_t s} + \frac{sB_{31}}{1+\tau_r s} + \frac{B_{62}}{1+\tau_k s} \right] \Delta \\ & + 2B_{13} n + P_{17} kT + P_{12} I_2 \\ & + \frac{B_{63}}{1+\tau_k s} I_3 + \frac{B_{52}}{1+\tau_k s} I_4 \quad . \end{aligned} \tag{3.48}$$

3.2.8. Plasma Circuit Perturbation

A plasma circuit is described by equations (2.53)-(2.63). Applying equation (3.1) to these equations, using (3.11), the plasma circuit perturbation equations are

$$R_1 = A_{12} kT_e + A_{14} n_e \quad , \tag{3.49}$$

$$A_{12} = 3K_{R1}(1 - \ln\lambda_0) \quad , \tag{3.50}$$

$$A_{14} = -K_{R1}\left(\frac{kT_e}{n_e}\right)_0 \quad , \tag{3.51}$$

$$K_{R1} = 3.346 \times 10^{-33} \frac{R_0}{[(kT_e)^{2.5}]_0 a_0^2} \quad , \tag{3.52}$$

$$L_{11} = L_{11d}\Delta \quad , \tag{3.53a}$$

$$L_{11d} = \left(\frac{dL_{11}}{dR}\right)_0 = K_i \mu_0 \left[\ln\left(\frac{8R_0}{a_0}\right) - 1.5 \right] \quad , \tag{3.53b}$$

$$\dot{L}_{11} = L_{11d}\,\dot{\Delta} \quad , \tag{3.53c}$$

$$\begin{aligned} 0 = (R_1)_0 I_1 + (I_1)_0 R_1 \\ &+ (\dot{L}_{11})_0 I_1 + (I_1)_0 s L_{11} + (L_{11})_0 s I_1 + (\dot{I}_1)_0 L_{11} \\ &+ (\dot{L}_{12})_0 I_2 + (I_2)_0 s L_{12} + (L_{12})_0 s I_2 + (\dot{I}_2)_0 L_{12} \\ &+ s\Phi_{13} + s\Phi_{14} \quad , \end{aligned} \tag{3.54}$$

$$(1+\tau_k s)s\Phi_{13} = (\dot{I}_3)_0 L_{13} + (I_3)_0 s L_{13} + (L_{13})_0 s I_3 + (\dot{L}_{13})_0 I_3 \quad , \tag{3.55}$$

$$(1+\tau_k s)s\Phi_{14} = (\dot{I}_4)_0 L_{14} + (I_4)_0 s L_{14} + (L_{14})_0 s I_4 + (\dot{L}_{14})_0 I_4 \quad . \tag{3.56}$$

In equations (3.54)-(3.56), under the steady-state conditions of the "burn" phase (which is of major interest here),

$$(\dot{L}_{11})_0 = (\dot{L}_{12})_0 = (\dot{L}_{13})_0 = (\dot{L}_{14})_0 = 0 \quad , \tag{3.57}$$

since they all are proportional to $(\dot{\Delta})_0$, and $(\dot{\Delta})_0$ is zero;

$$(\dot{I}_1)_0 = (\dot{I}_2)_0 = (\dot{I}_3)_0 = 0 \quad , \tag{3.58}$$

they may, however, have constant values during "start up" and "shut down" phases;

$$(L_{11})_0 = (L_{12})_0 = (L_{22})_0 \quad , \tag{3.59}$$

since the plasma column is centered in the vacuum vessel, $(\Delta)_0$ being zero.

Similar to equations (3.53a), (3.53b), and (3.53c),

$$L_{12} = L_{12d}\Delta \quad , \tag{3.60a}$$

$$L_{12d} = \left(\frac{\partial L_{12}}{\partial R}\right)_0 \quad , \tag{3.60b}$$

$$\dot{L}_{12} = L_{12d}\,\dot{\Delta} \quad , \tag{3.60c}$$

$$L_{13} = L_{13d}\Delta \quad , \tag{3.61a}$$

$$L_{13d} = \left(\frac{\partial L_{13}}{\partial R}\right)_0 \quad , \tag{3.61b}$$

$$\dot{L}_{13} = L_{13d}\,\dot{\Delta} \quad , \tag{3.61c}$$

$$L_{14} = L_{14d}\Delta \quad , \tag{3.62a}$$

$$L_{14d} = \left(\frac{\partial L_{14}}{\partial R} \right)_0 \quad , \tag{3.62b}$$

$$\dot{L}_{14} = L_{14d} \, \dot{\Delta} \quad , \tag{3.62c}$$

Substituting equations (3.53), (3.57), and (3.60)-(3.62) into equations (3.54)-(3.56),

$$\begin{aligned} 0 = {} & (R_1)_0 I_1 + (I_1)_0 R_1 \\ & + (I_1)_0 L_{11d} s\Delta + (L_{11})_0 s I_1 + (\dot{I}_1)_0 L_{11d} \Delta \\ & + (I_2)_0 L_{12d} s\Delta + (L_{12})_0 s I_2 + (\dot{I}_2)_0 L_{12d} \Delta \\ & + s\Phi_{13} + s\Phi_{14} \quad , \end{aligned} \tag{3.63}$$

$$(1 + \tau_k s) s\Phi_{13} = (I_3)_0 L_{13d} s\Delta + (L_{13})_0 s I_3 + (\dot{I}_3)_0 L_{13d} \Delta \quad , \tag{3.64}$$

$$(1 + \tau_k s) s\Phi_{14} = (I_4)_0 L_{14d} s\Delta + (L_{14})_0 s I_4 + (\dot{I}_4)_0 L_{14d} \Delta \quad . \tag{3.65}$$

Substituting (3.64) and (3.65) into (3.63), the plasma circuit perturbation equation is

$$\begin{aligned} 0 = {} & (I_1)_0 R_1 + \Big[(R_1)_0 + s(L_{11})_0 \Big] I_1 \\ & + \left[A_{26} + sA_{27} + \frac{(A_{28} + sA_{29})}{(1+\tau_k s)} \right] \Delta \\ & + s(L_{12})_0 I_2 + \frac{s(L_{13})_0}{(1+\tau_k s)} I_3 + \frac{s(L_{14})_0}{(1+\tau_k s)} I_4 \quad , \end{aligned} \tag{3.66}$$

where

$$A_{26} = (\dot{I}_1)_0 L_{11d} + (\dot{I}_2)_0 L_{12d} \quad , \tag{3.67}$$

$$A_{27} = (I_1)_0 L_{11d} + (I_2)_0 L_{12d} \quad , \tag{3.68}$$

$$A_{28} = (\dot{I}_3)_0 L_{13d} + (\dot{I}_4)_0 L_{14d} \quad , \tag{3.69}$$

$$A_{29} = (I_3)_0 L_{13d} + (I_4)_0 L_{14d} \quad . \tag{3.70}$$

3.2.8.1. Plasma Energy and Density Perturbation

Applying equation (3.1) to equations (2.69) and (2.70), their perturbation equations are (assuming n, R, and a constant), respectively,

$$skT = K_e P_{ext} - P_{61} I_1 - P_{68} R_1 \quad , \tag{3.71}$$

$$sn_{ext} = K_n P_{ext} \quad , \tag{3.72}$$

where $K_e = (2\pi^2 n_0 R_0 a_0^2)^{-1}$ and

$$P_{61} = -(2 I_1 R_1)_0 K_e \quad , \tag{3.73}$$

$$P_{68} = -(I_1^2)_0 K_e \quad , \tag{3.74}$$

$$K_n = \frac{K_p}{\pi^2 R_0 a_0^2} \quad . \tag{3.75}$$

Referring to equations (2.1)-(2.4) and applying equations (3.1), (3.10), and (3.11), for a constant total mass of the plasma column, (2.1), the plasma density perturbation and its time derivative are, respectively,

$$n = G_{54} \Delta \quad , \tag{3.76}$$

$$sn = G_{54} s \Delta \quad , \tag{3.77}$$

where

$$G_{54} = -\frac{2n_0}{R_0} \quad . \tag{3.78}$$

Adding equations (3.72) and (3.77), using $n = n_{ext} + n$,

$$sn = K_n P_{ext} - P_{75}\Delta \ , \qquad P_{75} = -sG_{54} \ . \tag{3.79}$$

Referring to equations (2.3), (2.17), and (3.49)-(3.52),

$$R_1 = -P_{87}kT - P_{86}n \quad , \tag{3.80}$$

where

$$P_{86} = K_{R1} \frac{2\mu_e}{(\mu_e+1)} \left[\frac{kT}{n}\right]_0 \quad . \tag{3.81}$$

$$P_{87} = - \frac{2\mu_e}{(\mu_e+1)} A_{12} \quad , \tag{3.82}$$

Equations (3.71), (3.79), and (3.80) are the plasma (average) energy and density perturbation equations. From these equations, the plasma circuit resistance perturbation, required in equation (3.66), is

$$R_1(s + A_{11}) = A_{21}P_{ext} + A_{13}I_1 + A_{22}s\Delta \quad , \tag{3.83}$$

where

$$A_{11} = -P_{68}P_{87} \quad , \tag{3.84}$$

$$A_{13} = P_{61}P_{87} \quad , \tag{3.85}$$

$$A_{21} = -(P_{86}K_n + P_{87}K_e) \quad , \tag{3.86}$$

$$A_{22} = -P_{86}G_{54} \quad . \tag{3.87}$$

Also, substituting (3.83) into (3.71),

$$skT(s + A_{11}) = (s + A_{23})K_eP_{ext} - P_{61}sI_1 + A_{24}s\Delta \quad , \tag{3.88}$$

where

$$A_{23} = K_nP_{68}P_{86}K_e^{-1} \quad , \tag{3.89}$$

$$A_{24} = -P_{68}A_{22} \quad . \tag{3.90}$$

Substituting (3.83) into (3.66), the plasma circuit perturbation equation may be written

$$\begin{aligned} A_{25}P_{ext} = & \left\{ (I_1)_0A_{13} + (s + A_{11})\left[(R_1)_0 + s(L_{11})_0 \right] \right\}I_1 \\ & + \left\{ s(I_1)_0A_{22} + (s + A_{11})\left[A_{26} + sA_{27} + \frac{(A_{28}+sA_{29})}{(1+\tau_k s)} \right] \right\}\Delta \\ & + s(s + A_{11})(L_{12})_0I_2 + \frac{s(s+A_{11})(L_{13})_0}{(1+\tau_k s)}I_3 \\ & + \frac{s(s+A_{11})(L_{14})_0}{(1+\tau_k s)}I_4 \quad , \end{aligned} \tag{3.91}$$

where

$$A_{25} = -(I_1)_0A_{21} \quad . \tag{3.92}$$

3.2.9. Vacuum Vessel Circuit Perturbation

Applying equation (3.1) to equation (2.71), the vacuum vessel circuit perturbation equation is, using (3.60),

$$0 = (L_{12})_0 sI_1 + L_{12d}\Big[(\dot{I}_1)_0 + s(I_1)_0 \Big]\Delta \tag{3.93}$$

$$+ (R_2 + sL_{22})I_2 + L_{23}sI_3 + L_{24}sI_4 \quad .$$

3.2.10. Control Field Circuit Perturbation

Applying equation (3.1) to equations (2.72) and (2.73), the control field circuit perturbation equations are, using (3.61),

$$V_3 = L_{23}sI_2 + (R_3 + sL_{33})I_3 + L_{34}sI_4 + \dot{\Phi}_{31} \quad , \tag{3.94}$$

$$(1 + \tau_k s)\,\dot{\Phi}_{31} = (L_{13})_0 sI_1 + L_{13d}\Big[(\dot{I}_1)_0 + s(I_1)_0 \Big]\Delta \quad . \tag{3.95}$$

Substituting (3.95) into (3.94), the perturbation equation of the control field circuit is

$$V_3 = \frac{s(L_{13})_0}{(1+\tau_k s)} I_1 + \frac{L_{13d}\Big[(\dot{I})_{10} + s(I_1)_0\Big]}{(1+\tau_k s)}\Delta \tag{3.96}$$

$$+ L_{23}sI_2 + (R_{33} + sL_{33})I_3 + L_{34}sI_4 \quad .$$

3.2.11. Ohmic Heating Circuit Perturbation

Applying equation (3.1) to equations (2.74) and (2.75), the ohmic heating circuit perturbation equations are, using (3.62),

$$V_4 = L_{24}sI_2 + L_{34}sI_3 + (R_4 + sL_{44})I_4 + \dot{\Phi}_{41} \quad , \tag{3.97}$$

$$(1 + \tau_k s)\,\dot{\Phi}_{41} = (L_{14})_0 sI_1 + L_{14d}\Big[(\dot{I}_1)_0 + s(I_1)_0 \Big]\Delta \quad . \tag{3.98}$$

Substituting (3.98) into (3.97), the perturbation equation of the ohmic heating circuit is

$$V_4 = \frac{s(L_{14})_0}{(1+\tau_k s)} I_1 + \frac{L_{14d}\Big[(\dot{I})_{10} + s(I_1)_0\Big]}{(1+\tau_k s)}\Delta \tag{3.99}$$

$$+ L_{24}sI_2 + L_{34}sI_3 + (R_4 + sL_{44})I_4 \quad .$$

4. SOLUTION OF PERTURBATION EQUATIONS

Equations (3.48), (3.66), (3.71), (3.79), (3.80), (3.93), (3.96), and (3.99) form a plasma perturbation model of a tokamak. It is convinient to write these equations in vector-matrix form,

$$\begin{bmatrix} 0 \\ 0 \\ 0 \\ V_3 \\ V_4 \\ K_e P_{ext} \\ K_n P_{ext} \\ 0 \end{bmatrix} = \begin{bmatrix} P_{11} & P_{12} & P_{13} & P_{14} & P_{15} & P_{16} & P_{17} & 0 \\ P_{21} & P_{22} & P_{23} & P_{24} & P_{25} & 0 & 0 & P_{28} \\ P_{31} & P_{32} & P_{33} & P_{34} & P_{35} & 0 & 0 & 0 \\ P_{41} & P_{42} & P_{43} & P_{44} & P_{45} & 0 & 0 & 0 \\ P_{51} & P_{52} & P_{53} & P_{54} & P_{55} & 0 & 0 & 0 \\ P_{61} & 0 & 0 & 0 & 0 & 0 & P_{67} & P_{68} \\ 0 & 0 & 0 & 0 & P_{75} & P_{76} & 0 & 0 \\ 0 & 0 & 0 & 0 & 0 & P_{86} & P_{87} & P_{88} \end{bmatrix} \begin{bmatrix} I_1 \\ I_2 \\ I_3 \\ I_4 \\ \Delta \\ \eta \\ kT \\ R_1 \end{bmatrix} , \quad (4.1)$$

which is abbreviated as $$\bar{\mathrm{V}}_{\mathrm{i}} = \mathbf{P}\bar{\mathrm{V}}_0 \quad . \quad (4.2)$$

The non-zero elements of the matrix $\mathbf{P}$ are, referring to (3.48),

$$P_{11} = B_{11} + \frac{B_{21}}{(1+\tau_t s)} + B_{41} + B_{51} + \frac{(1+0.5\tau_k s)B_{61}}{(1+\tau_k s)} \quad , \quad (4.3)$$

$$P_{12} = \frac{\mu_0}{4\pi} K_v (I_1)_0 \quad , \quad (4.4)$$

$$P_{13} = \frac{B_{63}}{(1+\tau_k s)} \quad , \quad (4.5)$$

$$P_{14} = \frac{B_{52}}{(1+\tau_k s)} \quad , \quad (4.6)$$

$$P_{15} = B_{12} + \frac{B_{22}}{(1+\tau_t s)} + \frac{sB_{31}}{(1+\tau_r s)} + \frac{B_{62}}{(1+\tau_k s)} - s^2 M_0 \quad , \tag{4.7}$$

$$P_{16} = 2B_{13} \quad , \tag{4.8}$$

$$P_{17} = 4\pi \left(\frac{I_1}{R} \right)_0 n_0 a_0^2 \quad ; \tag{4.9}$$

referring to (3.66),

$$P_{21} = (R_1)_0 + s(L_{11})_0 \quad , \tag{4.10}$$

$$P_{22} = s(L_{12})_0 \quad , \tag{4.11}$$

$$P_{23} = \frac{s(L_{13})_0}{(1+\tau_k s)} \quad , \tag{4.12}$$

$$P_{24} = \frac{s(L_{14})_0}{(1+\tau_k s)} \quad , \tag{4.13}$$

$$P_{25} = A_{26} + sA_{27} + \frac{(A_{28}+sA_{29})}{(1+\tau_k s)} \quad , \tag{4.14}$$

$$P_{28} = (I_1)_0 \quad ; \tag{4.15}$$

referring to (3.93),

$$P_{31} = s(L_{12})_0 \quad , \tag{4.16}$$

$$P_{32} = R_2 + sL_{22} \quad , \tag{4.17}$$

$$P_{33} = sL_{23} \quad , \tag{4.18}$$

$$P_{34} = sL_{24} \quad , \tag{4.19}$$

$$P_{35} = L_{12d}[(\dot{I}_1)_0 + s(I_1)_0] \quad ; \tag{4.20}$$

referring to (3.96),

$$P_{41} = \frac{s(L_{13})_0}{(1+\tau_k s)} \quad , \tag{4.21}$$

$$P_{42} = sL_{23} \quad , \tag{4.22}$$

$$P_{43} = R_3 + sL_{33} \quad , \tag{4.23}$$

$$P_{44} = sL_{34} \quad , \tag{4.24}$$

$$P_{45} = \frac{L_{13d}[(\dot{I}_1)_0+s(I_1)_0]}{(1+\tau_k s)} \quad ; \tag{4.25}$$

referring to (3.99),

$$P_{51} = \frac{s(L_{14})_0}{(1+\tau_k s)} \quad , \tag{4.26}$$

$$P_{52} = sL_{24} \quad , \tag{4.27}$$

$$P_{53} = sL_{34} \quad , \tag{4.28}$$

$$P_{54} = R_4 + sL_{44} \quad , \tag{4.29}$$

$$P_{55} = \frac{L_{14d}[(\dot{I}_1)_0+s(I_1)_0]}{(1+\tau_k s)} \quad ; \tag{4.30}$$

referring to (3.71),

$$P_{61} = -2(I_1R_1)_0K_e \quad , \tag{4.31}$$

$$P_{67} = s \quad , \tag{4.32}$$

$$P_{68} = -(I_1^2)_0 K_e \quad ; \tag{4.33}$$

referring to (3.79),

$$P_{75} = -sG_{54} \quad , \tag{4.34}$$

$$P_{76} = s \quad , \tag{4.35}$$

$$P_{88} = 1 \quad . \tag{4.36}$$

These equations can be used in a computer simulation of tokamak plasma perturbation dynamics. If solved explicitly, the characteristic equation of the solution will be (approximately) of the fourteenth order. Such a complex solution is not very useful for explicit analytical studies of a tokamak plasma equilibrium position stability, and it is not acceptable for systematic analytical syntheses of plasma displacement feedback control systems of minimal hardware complexity. For these purposes simplified approximated solutions must be considered.

4.1. Approximated Radial Plasma Equilibrium Perturbation Model

Consideration of the plasma perturbation model (4.1) for the steady-state "burn" phase operation of a tokamak leads to a conclusion that for an infinitesimal plasma displacement perturbation Δ the following perturbations may be assumed to be zero: I_1, I_4, n, T, and R_1. Under these assumptions the approximated plasma equilibrium perturbation model results in, using equations (3.48), (3.93), and (3.96),

$$\begin{bmatrix} 0 \\ 0 \\ V_3 \end{bmatrix} = \begin{bmatrix} P_{12} & P_{13} & P_{15} \\ P_{32} & P_{33} & P_{35} \\ P_{42} & P_{43} & P_{45} \end{bmatrix} \begin{bmatrix} I_2 \\ I_3 \\ \Delta \end{bmatrix} \quad , \tag{4.37}$$

where $[(\dot{I})_0 = 0, \ (3.58)]$

$$P_{12} = \frac{\mu_0}{4} \pi K_v (I_1)_0 \quad , \tag{4.38}$$

$$P_{13} = \frac{B_{63}}{(1+\tau_k s)} = B_{63k} \quad , \tag{4.39}$$

$$P_{15} = -(s^2 M_0 + sB_{31r} + B_{tk}) \quad , \tag{4.40}$$

$$B_{31r} = \frac{-B_{31}}{(1+\tau_r s)} \quad , \tag{4.41a}$$

$$B_{tk} = -(B_{12} + B_{22t} + B_{62k}) \quad , \tag{4.41b}$$

$$B_{22t} = \frac{B_{22}}{(1+\tau_t s)} \quad , \tag{4.41c}$$

$$B_{62k} = \frac{B_{62}}{(1+\tau_k s)} \quad , \tag{4.41d}$$

$$P_{32} = R_2 + sL_{22} = R_2(1+\tau_{vv} s) \quad , \tag{4.42}$$

$$\tau_{vv} = L_{22} R_2^{-1} \quad , \tag{4.43}$$

$$P_{33} = sL_{23} \quad , \tag{4.44}$$

$$P_{35} = s(I_1)_0 L_{12d} \quad , \tag{4.45}$$

$$P_{42} = sL_{23} \quad , \tag{4.46}$$

$$P_{43} = R_3 + sL_{33} = R_3(1 + \tau_{cc}s) \quad , \tag{4.47}$$

$$\tau_{cc} = L_{33}R_3^{-1} \quad , \tag{4.48}$$

$$P_{45} = \frac{s(I_1)_0 L_{13d}}{(1+\tau_k s)} = s(I_1)_0 L_{13dk} \quad . \tag{4.49}$$

4.1.1. Solution of Approximated Radial Plasma Equilibrium Perturbation Model

Solution of equation (4.37) is simple, in principle at least,

$$I_2 D = V_3(P_{15}P_{33} - P_{13}P_{35}) \quad , \tag{4.50}$$

$$I_3 D = V_3(P_{12}P_{35} - P_{15}P_{32}) \quad , \tag{4.51}$$

$$\Delta D = V_3(P_{13}P_{32} - P_{12}P_{33}) \quad , \tag{4.52}$$

$$D = P_{45}(P_{13}P_{32} - P_{12}P_{33}) + P_{35}(P_{12}P_{43} - P_{13}P_{42}) + P_{15}(P_{33}P_{42} - P_{32}P_{43}) \quad . \tag{4.53}$$

Using equations (4.38)-(4.49) in equations (4.50)-(4.53):

$$I_2 D = -sV_3\Big(s^2 L_{23} M_0 + sL_{23} B_{31r} + [\ (I_1)_0 L_{12d} B_{63k} + B_{tk} L_{23}\ ]\Big) \quad , \tag{4.54}$$

$$I_3 D = V_3 R_2\Big(s^3 \tau_{vv} M_0 + s^2(M_0 + \tau_{vv} B_{31r}) + s[\ B_{31r} + \tau_{vv} B_{tk} - P_{12}(I_1)_0 R_2^{-1} L_{12d}\ ] + B_{tk}\Big) \quad , \tag{4.55}$$

$$\Delta D = V_3 R_2[\ B_{63k} + s(\tau_{vv} B_{63k} - P_{12} L_{23} R_2^{-1})\ ] \quad , \tag{4.56}$$

$$D = R_2R_3\Big\{ s^4M_0\tau_{vv}\tau_{cc}(1-k^2) \tag{4.57}$$

$$+ s^3[M_0(\tau_{vv}+\tau_{cc}) + B_{31r}\tau_{vv}\tau_{cc}(1-k^2)]$$

$$+ s^2[M_0 + B_{31r}(\tau_{vv}+\tau_{cc}) + B_{tk}\tau_{vv}\tau_{cc}(1-k^2)$$

$$+ L_{12d}(I_1)_0R_2^{-1}(P_{12}\tau_{cc}-B_{63k}L_{23}R_3^{-1})$$

$$+ L_{13dk}(I_1)_0R_3^{-1}(B_{63k}\tau_{vv}-P_{12}L_{23}R_2^{-1})]$$

$$+ s[B_{31r} + B_{tk}(\tau_{vv}+\tau_{cc}) + L_{12d}(I_1)_0R_2^{-1}P_{12}$$

$$+ L_{13dk}(I_1)_0R_3^{-1}B_{63k}] + B_{tk}\Big\} .$$

In equation (4.57) an inductive coupling coefficient of the vaccum vessel and control field circuits is given by

$$k = \frac{L_{23}}{\sqrt{L_{22}L_{33}}} . \tag{4.58}$$

Of primary interest are the approximated perturbation dynamics functions of Δ/V_3, Δ/I_3, and I_3/V_3, ratios of (4.56)/(4.57), (4.56)/(4.55), and (4.55)/(4.57), respectively:

Δ/V_3 is a function simple enough to permit an ordered analytical synthesis of a plasma displacement control system using a control voltage drive;

Δ/I_3 is a function which could be used for an analytical design of a plasma displacement feedback control system utilizing a control current (I_3) drive;

I_3/V_3 can be used in computer simulations for determination of the control current I_3, which may be used in an implementation of the control voltage drive.

Use of the function Δ/I_3 may not be practical, however. By virtue of a tokamak design, a control current drive must operate into a highly inductive load and thus may require impractically high voltage sources. For this reason the first function, Δ/V_3, is of a more practical value.

4.1.1.1. Radial High-Frequency Solution

The characteristic equation of the functions Δ/V_3 and I_3/V_3 is given by equation (4.57). It is observed that the highest order term of (4.57) is directly proportional to M_0. The plasma current mass element M_0 is extremely small, on the order of 10^{-10} kg/m. Its presence in the characteristic equation (4.57) [and in equations (4.54) and (4.55)] gives rise to a group of high-frequency roots. If M_0 is assumed to be zero, then a group of low-frequency roots is represented by the resulting characteristic equation. Assuming that a separation ratio of the high-frequency roots to the low-frequency roots is large (>10.0), the high-frequency roots are represented with sufficient accuracy by a polynomial of higher order terms of (4.57), the last term of this polynomial being the first higher-order non-zero term of (4.57) under an assumption of M_0=0 in that term — the third order term of (4.57). It is recalled that equation (4.57) involves three time constants which are not explicitly shown in the equation. They are incorporated into the terms B_{63k}, B_{31r}, B_{tk}, and L_{13dk}, defined by equations (4.39), (4.41a), (4.41b), and (4.49), respectively. These time constants, τ_t, τ_k, and τ_r, must be considered in the evaluation of high-frequency roots. Multiplying equation (4.57) by $(1+\tau_t s)(1+\tau_k s)(1+\tau_r s)$, dividing by the highest order coefficient obtained, neglecting insignificant terms, and using (3.18) and (3.30), a second order equation describing high-frequency roots of the characteristic equation (4.57) is obtained,

$$s^2 + s[\ \tau_t^{-1} + \tau_k^{-1} + \tau_r^{-1} + (\tau_{vv}^{-1} + \tau_{cc}^{-1})(1-k^2)^{-1}\ ] \tag{4.59}$$

$$+ \frac{1}{M_0}\ \frac{\mu_0}{4\pi}(I_1)_0^2 \left[\frac{K_r}{\tau_r} + \frac{1}{R_0^2}\left(\ln\frac{8R_0}{a_0} + \frac{1}{2}l_i - 2.0 \right) + \frac{L_{12d}K_v}{L_{22}(1-k^2)} \right] = 0 \ .$$

Writing this equation in a conventional form

$$s^2 + 2\zeta\omega_n s + \omega_n^2 = 0 \ , \tag{4.60}$$

with roots defined by

$$s_{1,2} = Re \pm j\omega_h \ , \tag{4.61}$$

the following is immediately obtained, by comparison with equation (4.59):

$$Re\ (\text{rad/s}) = -\frac{1}{2}\left[\ \tau_t^{-1} + \tau_k^{-1} + \tau_r^{-1} + (\tau_{vv}^{-1} + \tau_{cc}^{-1})(1-k^2)^{-1}\ \right] \tag{4.62}$$

is an approximated real part of the roots, and their complex frequency is

$$\omega_h\ (\text{rad/s}) = (\omega_n^2 - Re^2)^{1/2} \ , \tag{4.63}$$

where

$$\omega_n^2 = \frac{1}{M_0} \frac{\mu_0}{4\pi}(I_1)_0^2 \left[\frac{K_r}{\tau_r} + \frac{1}{R_0^2} \left(\ln\frac{8R_0}{a_0} + \frac{1}{2}l_i - 2.0 \right) + \frac{L_{12d}K_v}{L_{22}(1-k^2)} \right] = 0 \quad , \tag{4.64}$$

and the damping factor is simply

$$\zeta = - \frac{Re}{\omega_n} \quad . \tag{4.65}$$

In a similar manner, considering the high-frequency roots of equation (4.55), it is found that in this case,

$$Re \text{ (rad/s)} = -0.5(\tau_t^{-1} + \tau_k^{-1} + \tau_r^{-1} + \tau_{vv}^{-1}) \quad , \tag{4.66}$$

$$\omega_n^2 = \frac{1}{M_0} \frac{\mu_0}{4\pi}(I_1)_0^2 \left[\frac{K_r}{\tau_r} + \frac{1}{R_0^2} \left(\ln\frac{8R_0}{a_0} + \frac{1}{2}l_i - 2.0 \right) + \frac{L_{12d}K_v}{L_{22}} \right] = 0 \quad . \tag{4.67}$$

It is of interest to note that there is very little difference between equations (4.66) and (4.62). In (4.66), as compared to (4.62), τ_{cc}^{-1} and k^2 are zero, and Re of (4.66) will have a lower value than that of (4.62), if $k^2 \ll 1.0$.

There is an insignificant difference between equations (4.67) and (4.64). In (4.67), as compared to (4.64), k^2 is zero, ω_n^2 of (4.67) will be nearly the same as that of (4.64), if $k^2 \ll 1.0$.

Referring to equation (4.58), it is expected that for a practical tokamak a value of k^2 will be much less than 1.0.

It is also expected that for other parameter values of a practical tokamak the real part of the roots Re will be very small as compared to the roots' very large frequency ω_h. The damping factor of the roots ζ will also be very small, the roots will be very lightly damped, and the amplitude of plasma's displacement oscillation will be infinitesimal.

It is noted that if the transformer iron core is absent the equations derived remain the same, except τ_t^{-1} in (4.59), (4.62), and (4.66) is set to zero, so the real part of the roots will decrease somewhat.

4.1.1.2. Radial Low-Frequency Solution

High-frequency oscillatory roots, considered in the previous section, are due to a very low plasma mass. As the plasma mass element M_0 approaches zero, these roots approach infinity. High-frequency roots, real at a virtual infinity, or oscillatory positively damped, however lightly, do not influence the low-frequency stability of plasma motion if the separation ratio of the high-frequency to low-frequency roots is very large. Reference to equations (4.59)-(4.67) suggests that this is so in a case of a practical tokamak.

4.1.1.2.1. Radial Low-Frequency Characteristic Equation

Letting M_0 be equal to zero in equation (4.57) results in a characteristic equation representing low-frequency roots,

$$D = R_2R_3\Big[s^3\tau_{vv}\tau_{cc}B_{31r} + s^2(\tau_{vv}B_d + \tau_{cc}B_{31r}) + s(B_d + \tau_{vv}B_{tk}) + B_{tk} + Y_1\Big] \quad , \tag{4.68}$$

where

$$B_d = B_{31r} + \tau_{cc}B_{tk} + L_{13dk}(I_1)_0R_3^{-1}B_{63k} \quad , \tag{4.69}$$

$$Y_1 = -s^2\tau_{vv}\tau_{cc}(sB_{31r} + B_{tk})k^2 + s^2Y_2 + sY_3 \quad , \tag{4.70}$$

$$Y_2 = (I_1)_0R_2^{-1}\Big[\tau_{cc}L_{12d}P_{12} - L_{23}R_3^{-1}(P_{12}L_{12dk} + B_{63k}L_{12d}) \Big] , \tag{4.71}$$

$$Y_3 = (I_1)_0R_2^{-1}L_{12d}P_{12} \quad . \tag{4.72}$$

The polynomial Y_1, (4.70), is negligible in (4.68) if

$$k^2 = L_{23}^2(L_{22}L_{23})^{-1} \ll 1.0 \quad , \tag{4.73}$$

$$|Y_2|_{s=0} \ll |\tau_{vv}B_d + \tau_{cc}B_{31r}|_{s=0} \quad , \tag{4.74}$$

$$|Y_3|_{s=0} \ll |B_d + \tau_{vv}B_{tk}|_{s=0} \quad . \tag{4.75}$$

Conditions stated by (4.73)-(4.75) are expected to be satisfied for nearly all practical tokamaks.

Assuming the polynomial Y_1 is negligible in equation (4.68), the approximated equation (4.68) becomes

$$D = R_2R_3(1+\tau_{vv}s)(s^2\tau_{cc}B_{31r} + sB_d + B_{tk}) \quad . \tag{4.76}$$

Let it be assumed that quadratic roots of equation (4.76) are real and widely separated, with a separation ratio larger than 10.0. Then equation (4.76) is approximated as

$$D = R_2R_3\tau_{cc}B_{31r}(1+\tau_{vv}s)(s-S_1)(s-S_{22s}) \quad , \tag{4.77}$$

$$S_1 = -\frac{B_{tk}}{B_d} \quad , \tag{4.78}$$

$$S_{22s} = -\frac{B_d}{\tau_{cc} B_{31r}} \quad . \tag{4.79}$$

For validity of this approximation the separation ratio must be

$$\left| \frac{S_{22s}}{S_1} \right|_{s=0} = \left| \frac{B_d^2}{\tau_{cc} |B_{31r}| |B_{tk}|} \right|_{s=0} > 10.0 \quad . \tag{4.80}$$

It is assumed that this separation ratio condition will be satisfied for all parameter values of practical tokamaks.

The quantities B_{31r}, B_{tk}, and B_d, defined by equations (4.41a), (4.41b), and (4.69), respectively, involve the time constants τ_r, τ_t, and τ_k in such a manner that the magnitudes of these quantities are maximum at zero frequency. In general the time constants τ_t and τ_k are expected to be relatively small, making their effect on the quantities B_{tk} and B_d negligible at low frequencies. Therefore it is logical to assume that in equations (4.78) and (4.79) B_{tk} and B_d are constants independent of frequency,

$$B_{tk} = -(B_{12} + B_{22} + B_{62}) \quad , \tag{4.81}$$

$$B_d = -B_{31} + \tau_{cc} B_{tk} + L_{13d} (I_1)_0 R_3^{-1} B_{63} \quad . \tag{4.82}$$

Using equations (3.18), (3.24), and (3.45), dividing by $(I_1)_0^2 \times 10^{-10}$ for convenience, equation (4.81) is written as

$$E_{ra}\ (\mathrm{m}^{-2}) \equiv E_r = A_{e1} + \rho A_{e2} - E_a \equiv B_{tk} (I_1)_0^{-2} \times 10^{10} \quad , \tag{4.83}$$

where

$$A_{e1} = \left[\ln\left(\frac{8R_0}{a_0}\right) + 0.5l_i - 2.0 \right]\frac{10^3}{R_0^2} \quad , \tag{4.84}$$

$$A_{e2} = \frac{2.0\times10^3}{R_0^2}\left[R_0\left(\frac{\partial f_t}{\partial R}\right)_0 - (f_t)_0 \right] \quad , \tag{4.85}$$

$$E_a = -\left[A_{e3} + \rho A_{e4} + A_{e5}(I_1)_0^{-2}\times10^{10} + A_{e6}\right]N \quad , \tag{4.86}$$

$$A_{e3} = -A_{e1} - \frac{10^3}{2R_0^2} \quad , \tag{4.87}$$

$$A_{e4} = \frac{2.0\times10^3}{R_0^2}(f_t)_0 \quad , \tag{4.88}$$

$$A_{e5} = -4\pi\left(\frac{nkTa^2}{R^2}\right)_0 = -2\pi\left(\frac{n_{ei}kTa^2}{R^2}\right)_0 \quad , \tag{4.89}$$

$$A_{e6} = -\frac{10^3}{(I_1R)_0}[K_v(I_2)_0 + K_h(I_4)_0] \quad . \tag{4.90}$$

Using equations (3.30) and (3.46) in equation (4.82), dividing by $(I_1)_0^2\times10^{-10}$ and substituting (4.83) and (4.48), equation (4.82) is written as

$$M_{ra}\ (\mathrm{s/m^2}) = (K_r + L_{13d}K_kR_3^{-1})\times10^3 + L_{33}R_3^{-1}E_{ra} \tag{4.91}$$

$$\equiv B_d(I_1)_0^{-2}\times10^{10} \quad ,$$

where

$$K_k\ (\mathrm{m^{-1}}) = \frac{4\pi}{\mu_0}K_c \quad . \tag{4.92}$$

Substituting (4.83) and (4.91) into equation (4.78),

$$S_1 = -\frac{E_{ra}}{M_{ra}} \quad . \tag{4.93}$$

Using equations (4.41a) and (4.91) in equation (4.79),

$$S_{22s} = \frac{M_{ra}(1+\tau_r s)}{\tau_{cc} B_{31}(I_1)_0^{-2} \times 10^{10}} \quad , \tag{4.94}$$

and using (3.30) this becomes

$$S_{22s} = \frac{-M_{ra}(1+\tau_r s)}{\tau_{cc} K_r \times 10^3} \quad . \tag{4.95}$$

Letting

$$S_{22} = \frac{-M_{ra}}{\tau_{cc} K_r \times 10^3} \quad , \tag{4.96}$$

(4.95) becomes

$$S_{22s} = S_{22}(1+\tau_r s) \quad . \tag{4.97}$$

Using (4.97), a term in equation (4.77) is

$$(s-S_{22s}) = (s-S_2)(1-S_{22}\tau_r) \quad , \tag{4.98}$$

where

$$S_2 = \frac{S_{22}}{(1-S_{22}\tau_r)} \quad . \tag{4.99}$$

Substituting (4.91) and (4.48) into equation (4.96),

$$S_{22} = -(R_3 + L_{13d} K_k K_r^{-1}) L_{33}^{-1} - E_{ra} K_r^{-1} \times 10^{-3} \quad . \tag{4.100}$$

Substituting into equation (4.77) equations (4.48), (4.41a), (3.30), and (4.98), the approximated low-frequency characteristic equation is

$$D \;=\; R_2 L_{33} \frac{\mu_0}{4\pi} K_r (1-S_{22}\tau_r)(I_1)_0^2 \, \frac{(1+\tau_{vv}s)}{(1+\tau_r s)} (s-S_1)(s-S_2) \quad . \tag{4.101}$$

4.1.1.2.2. Radial Low-Frequency Dynamics Function Δ/V_3

Refer to equation (4.56); it is expected that in this equation

$$\left| \, \tau_{vv} B_{63k} \, \right|_{s=0} \gg \left| \, P_{12} L_{23} R_2^{-1} \, \right| \quad , \tag{4.102}$$

for all the parameter values of practical tokamaks. Then equation (4.56) is approximated, using (4.39) and (3.46),

$$\Delta D \;=\; V_3 R_2 (I_1)_0 K_c \frac{(1+\tau_{vv}s)}{(1+\tau_k s)} \quad . \tag{4.103}$$

Substituting equation (4.101) into (4.103), an approximated low-frequency dynamics function is

$$\Delta (s-S_1)(s-S_2)(1+\tau_k s) \;=\; V_3 G_0 (1+\tau_r s) \quad , \tag{4.104}$$

where

$$G_0 \;=\; \frac{G_1}{(1-S_{22}\tau_r)} \quad , \tag{4.105}$$

$$G_1 \;\; (\mathrm{m/Vs^2}) \;=\; \frac{K_k}{(I_1)_0 L_{33} K_r} \quad , \tag{4.106}$$

and S_1, S_2, S_{22}, and K_k are given by equations (4.93), (4.99), (4.100), and (4.92), respectively.

The conditions under which equation (4.104) was derived are stated by (4.73), (4.74), (4.75), (4.80), and (4.102). These conditions are restated below, respectively, using where applicable expressions given by the equations (4.83) and (4.91), E_{ra} and M_{ra}, respectively:

$$k^2 = L_{23}^2(L_{22}L_{33})^{-1} \ll 1.0 \quad , \tag{4.107}$$

$$\left|(L_{33}L_{12d}-L_{23}L_{13d})K_v-L_{23}L_{12d}K_k\right| < \left|L_{22}R_3M_{ra}\times10^{-3}+L_{33}R_2K_r\right| , \tag{4.108}$$

$$\left| L_{12d}R_2^{-1}K_v\times10^3 \right| \ll \left| M_{ra} + \tau_{vv}E_{ra} \right| , \tag{4.109}$$

$$\left| M_{ra}^2 \right| > \left| L_{33}R_3^{-1}K_rE_{ra}\times10^4 \right| , \tag{4.110}$$

$$\left| L_{22}K_k \right| \gg \left| L_{23}K_v \right| . \tag{4.111}$$

4.1.1.2.3. Radial Low-Frequency Dynamics Function Δ/I_3

The high-frequency solution for equation (4.55) is given by equations (4.66) and (4.67). Assuming M_0 is zero, this equation becomes

$$I_3D = V_3R_2(s^2\tau_{vv}B_{31r} + sB_{dv} + B_{tk}) \quad , \tag{4.112}$$

where

$$B_{dv} = B_{31r} + \tau_{vv}B_{tk} - P_{12}(I_1)_0R_2^{-1}L_{12d} \quad . \tag{4.113}$$

The ratio of equations (4.103) and (4.112) results in a low-frequency perturbation dynamics function Δ/I_3. Comparison of equations (4.112) and (4.76) reveals that the quadratic term of (4.76) becomes equation (4.112) if in that quadratic term

τ_{cc} is replaced by τ_{vv}, and

B_d is replaced by B_{dv};

Comparison of equations (4.113) and (4.69) reveals that equation (4.69) [(4.82)] becomes equation (4.113) if in that equation

τ_{cc} is replaced by τ_{vv},

L_{13dk} is replaced by L_{12d},

R_3 is replaced by R_2,

B_{63k} is replaced by $(-P_{12})$. (4.114)

It follows that if the replacements indicated by (4.114) are carried out in the solution of the quadratic term of (4.76) [in equations (4.77)-(4.101)], a solution of equation (4.112) will be obtained.

Let eq. (4.112) be written

$$I_3D = \tau_{vv}B_{31r}R_2V_3(s-S_3)(s-S_{44s}) \quad . \tag{4.115}$$

Then, performing the indicated substitutions,

$$S_3 = -\frac{E_{ra}}{M_{rai}} \quad , \tag{4.116}$$

where E_{ra} is given by eq. (4.83) and

$$M_{rai} = \left(K_r - \frac{L_{12d}K_v}{R_2} \right)\times 10^3 + \frac{L_{22}}{R_2}E_{ra} \tag{4.117}$$

$$\equiv B_{dv}(I_1)_0^2\times 10^{10} \quad .$$

Referring to eqs. (4.96) and (4.100),

$$S_{44} = \frac{1}{L_{22}}\left(\frac{L_{12d}K_v}{K_r} - R_2 \right) - \frac{E_{ra}}{K_r \times 10^3} \quad . \tag{4.118}$$

Referring to eqs. (4.98) and (4.99),

$$S_4 = \frac{S_{44}}{(1-S_{44}\tau_r)} \quad , \tag{4.119}$$

$$(s-S_{44s}) = (s-S_4)(1-S_{44}\tau_r) \quad . \tag{4.120}$$

Substituting eq. (4.120) into eq. (4.115), using eqs. (3.30), (4.41a), and (4.43),

$$I_3D = \frac{\mu_0}{4\pi}L_{22}(I_1)_0^2K_r(1-S_{44}\tau_r)V_3 \frac{(s-S_3)(s-S_4)}{(1+\tau_r s)} \quad . \tag{4.121}$$

For the validity of this approximation, referring to eq. (4.110),

$$\left| M_{rai}^2 \right| > \left| \tau_{vv}K_rE_{ra} \times 10^4 \right| \quad . \tag{4.122}$$

Using equations (4.103) and (4.121),

$$\Delta\tau_{vv}(I_1)_0K_r(1-S_{44}\tau_r)(1+\tau_k s)(s-S_3)(s-S_4) = I_3K_k(1+\tau_{vv}s)(1+\tau_r s) \quad . \tag{4.123}$$

It is noted that eq. (4.123), the dynamics function Δ/I_3, is less reliable than eq. (4.104), the dynamics function Δ/V_3. This is obvious considering the statements of (4.114): the shift is made from control circuit parameters to the vacuum vessel parameters, which are much less reliable (or controllable) than the control circuit parameters. For these reasons and because of the problems associated with design of the control current drives, briefly stated in section 4.1.1., use of eq. (4.123) is not practical.

4.1.1.2.4. Radial Low-Frequency Dynamics Function I_3/V_3

Dynamics function I_3/V_3 is now easily obtained from equations (4.101) and (4.121),

$$I_3 G_3 (1+\tau_{vv} s)(s-S_1)(s-S_2) = V_3 (s-S_3)(s-S_4) \quad , \tag{4.124}$$

where

$$G_3 = \frac{L_{33}(1-S_{22}\tau_r)}{\tau_{vv}(1-S_{44}\tau_r)} \quad . \tag{4.125}$$

Equation (4.124) may be written as

$$I_3 Z_3 = V_3 \quad , \tag{4.126}$$

where

$$Z_3 = G_3 (1+\tau_{vv} s)(s-S_1)(s-S_2)(s-S_3)^{-1}(s-S_4)^{-1} \quad , \tag{4.127}$$

is defined as the effective control (coil) circuit perturbation impedance.

4.2. Approximated Vertical Plasma Equilibrium Perturbation Model

The approximated radial plasma equilibrium perturbation model, eq. (4.37), can be easily modified to represent an approximated vertical plasma equilibrium perturbation model.

Referring to fig. 2.1, to the first order of approximation, let [39,(11)]

$$B_y = -\Delta\left(\frac{\partial B_s}{\partial R}\right)_0 \quad , \tag{4.128}$$

where Δ (m) is a small positive displacement of the plasma current mass element M_0 in the positive vertical (z-axis) direction.

Using equation (2.31),

$$\left(\frac{\partial B_s}{\partial R}\right)_0 = -N\frac{B_{s0}}{R_0} \quad , \tag{4.129}$$

and hence

$$B_y = \frac{NB_{s0}}{R_0}\Delta \quad . \tag{4.130}$$

For vertical function, a value of B_s, equations (2.38) and (2.39), must be that of B_y. Therefore equation (2.39) becomes

$$B_s + \tau_k\dot{B}_s = \frac{NB_{s0}}{R_0}\Delta \quad , \tag{4.131}$$

equation (2.44) becomes

$$B_e + \tau_k\dot{B}_e = \frac{NB_{s0}}{R_0}\Delta - K_cI_3 \quad , \tag{4.132}$$

equation (3.43), the external magnetic field force perturbation, becomes, $(B_e)_0$ being equal to zero in this case,

$$B_{61} = 0 \quad , \tag{4.133}$$

and

$$(1+\tau_k s)F_e = -(I_1)_0\left(\frac{NB_{s0}}{R_0}\Delta - K_c I_3 \right) \tag{4.134}$$

$$= B_{62}\Delta + B_{63}I_3 \quad ,$$

$$B_{62} = -NB_{s0}\left(\frac{I_1}{R}\right)_0 \quad , \tag{4.135}$$

$$B_{63} = (I_1)_0 K_c \quad . \tag{4.136}$$

The forces F_i (2.6), F_t (2.24), F_v (2.27), and F_h (2.29) are zero; equation (3.48) becomes

$$s^2\Delta M_0 = \left(\frac{sB_{31}}{1+\tau_r s} + \frac{B_{62}}{1+\tau_k s} \right)\Delta + \frac{B_{63}}{1+\tau_k s}I_3 \quad . \tag{4.137}$$

Modified elements of equation (4.37) are

$$P_{12} = 0 \quad , \tag{4.138}$$

$$P_{15} = -(s^2 M_0 + sB_{31r} - B_{62k}) \quad ; \tag{4.139}$$

all other elements of the matrix remain the same. Referring to equations (4.40), (4.41), and (4.139), it is observed that

$$B_{tk} = -B_{62k} \quad , \tag{4.140}$$

$$B_{12} = 0 \quad , \tag{4.141}$$

$$B_{22t} = 0 \quad . \tag{4.142}$$

It is also observed that

$$L_{23} = 0 \quad , \tag{4.143}$$

since for vertical configuration the planes of the vacuum vessel and the magnetic field control coils are perpendicular to each other.

An approximated vertical plasma equilibrium perturbation model is obtained when modifications (4.133)-(4.136) and (4.138)-(4.143) are used in the equation (4.37).

4.2.1. Vertical High-Frequency Solution

Applying modifications (4.133)-(4.136) and (4.138)-(4.143) to equation (4.57), a second order equation describing high-frequency roots of the vertical characteristic equation (4.57) is obtained,

$$s^2 + s(\tau_k^{-1} + \tau_r^{-1} + \tau_{vv}^{-1} + \tau_{cc}^{-1}) + \frac{\mu_0}{4\pi} \frac{(I_1)_0^2}{M_0} \frac{K_r}{\tau_r} \quad . \tag{4.144}$$

By reference to equations (4.60) and (4.61), it is found that the vertical high-frequency roots are characterized by

$$Re \ (\text{rad/s}) = -0.5(\tau_k^{-1} + \tau_r^{-1} + \tau_{vv}^{-1} + \tau_{cc}^{-1}) \quad , \tag{4.145}$$

$$\omega_n^2 = \frac{\mu_0}{4\pi} \frac{(I_1)_0^2}{M_0} \frac{K_r}{\tau_r} \quad . \tag{4.146}$$

4.2.2. Vertical Low-Frequency Dynamics Functions

Applying modifications (4.133)-(4.136) and (4.138)-(4.143) to equations (4.68)-(4.101), section 4.1.1.2.1., it is found that for the vertical configuration

$$E_{ra} \ (\text{m}^{-2}) \equiv E_a \tag{4.147}$$

in equations (4.91), (4.93), and (4.100). With these changes the vertical low-frequency dynamics functions Δ/V_3, Δ/I_3, and I_3/V_3 are given by the same equations as the respective radial low-frequency dynamics functions, equations (4.104), (4.123), and (4.126), respectively.

5. TOKAMAK PLASMA DISPLACEMENT FEEDBACK CONTROL

A simplified schematic of a tokamak control is shown in fig. 5.1. A plasma radial displacement feedback control is shown without a similar plasma vertical displacement feedback control. The latter is of exactly the same configuration as the radial plasma displacement feedback control, with the displacement pickup coils #1 and #2 and the magnetic control field B_c having been rotated through an angle of 90 degrees.

A measure of the plasma current I_1 is obtained using a Rogowski coil and appropriate signal processing. A Rogowski coil is basically a toroidal solenoid having the plasma current at its axis of symmetry. The plasma current I_1 and its command (steady-state) value $(I_1)_0$ are used for adjustments and modifications of the gain and time constants of control loops as required [equations (2.38), (2.41), and (4.106), for example].

Measurement of the radial plasma displacement Δ is accomplished using two pickup coils and appropriate signal processing. This method of plasma displacement measurement is treated in detail in refs. [42, 44]. An vertical plasma displacement measurement is performed in a similar manner.

5.1. Control Field Drive

Generation of a (radial or vertical) magnetic control field B_c requires a control field drive. One such drive is shown schematically in fig. 5.2 . This is a direct current drive which employes a transistor bank (transistors in parallel) to control the current I_3 passing through an effective coil impedance Z_3 (4.127). Pulsed power drives may also be employed [63]; they increase mathematical complexity of

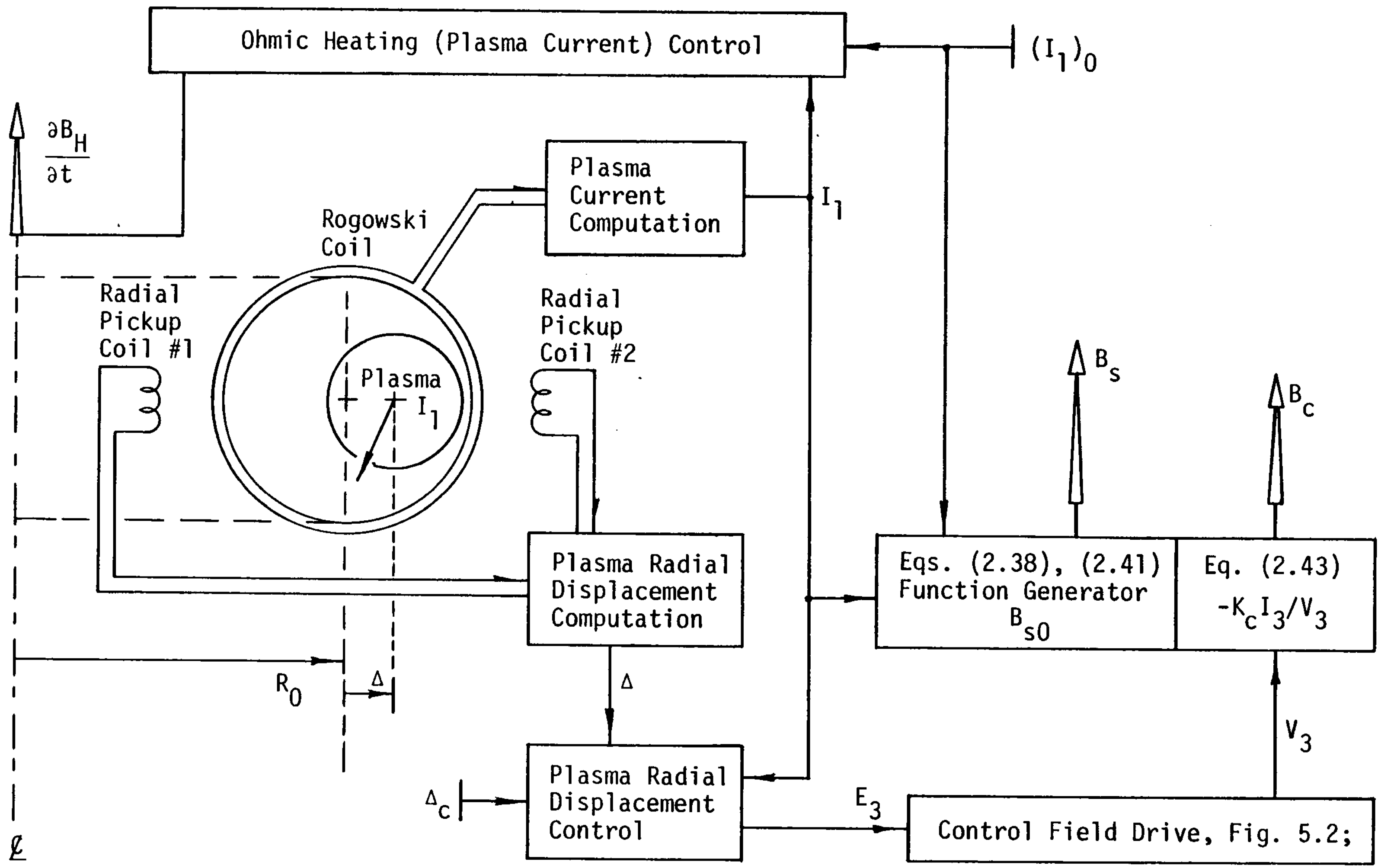

Figure 5.1. Tokamak plasma radial control, simplified schematic.

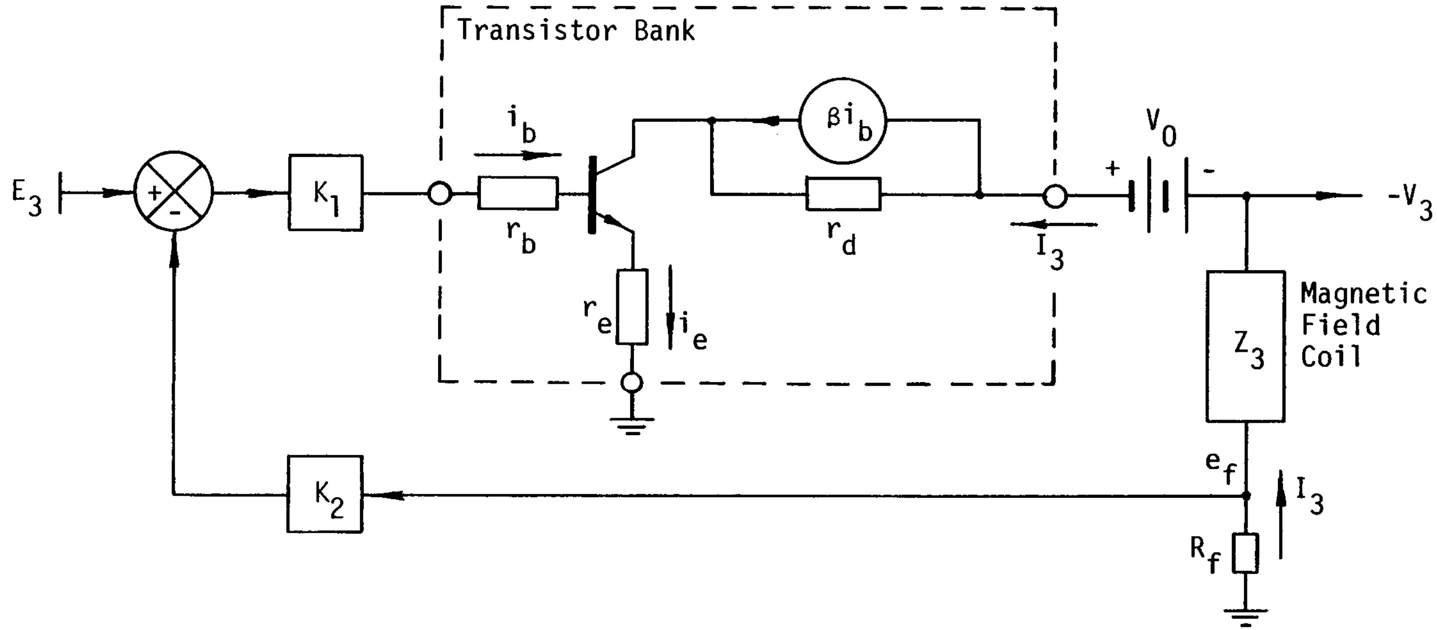

Figure 5.2. Magnetic control field drive, simplified schematic.

the analysis while contributing little to the basic understanding of the requirements of a magnetic control field drive. Such drives, however, are practical for large experimental tokamak ractors.

The transistor bank of the control field drive in fig. 5.2 is a common emitter configuration. As such it will normally have the following characteristics:

$$| I_3 | \gg | i_b | \quad , \tag{5.1}$$

$$r_d \gg r_b \gg r_e \quad . \tag{5.2}$$

Under the above conditions a perturbation transfer function of the control field drive is found to be

$$V_3(K_\beta + Z_3 r_b r_d^{-1}) = \beta K_1 Z_3 E_3 \quad , \tag{5.3}$$

where

$$K_\beta = (r_b + \beta r_e) - \beta K_1 K_2 R_f \tag{5.4}$$

and Z_3 is given by equation (4.127).

It is noted that it may be possible to have $K_\beta = 0$ in equation (5.3) by adjusting K_2 in (5.4) such that

$$K_1 = \frac{r_b + \beta r_e}{\beta K_2 R_f} \quad . \tag{5.5}$$

In such a case eq. (5.3) becomes

$$V_3 r_b r_d^{-1} = \beta K_1 E_3 \quad , \tag{5.6}$$

where it may be desirable to have

$$K_1 = \frac{r_b}{\beta r_d} \tag{5.7}$$

to obtain

$$V_3 = K_u E_3 \ , \qquad K_u = 1.0 \ . \tag{5.8}$$

Equating (5.5) and (5.7),

$$K_2 = \frac{(r_b + \beta r_e) r_d}{r_b R_f} \ . \tag{5.9}$$

5.2. Tokamak Dynamics Functions

Radial and vertical low-frequency dynamics functions have been derived in sections 4.1.1.2 through 4.2.2. It has been shown that the vertical dynamics functions are of the same form as the radial dynamics functions, the difference being only in numerical values of the coefficient E_{ra}, equation (4.134). Therefore there is no need to make a distinction between the radial and the vertical dynamics functions in considerations of analytical designs of tokamak plasma displacement feedback controls. Also, it has been stated in section 4.1.1.2.3 that use of the dynamics function Δ/I_3 may not be practical. For these reasons only the dynamics function Δ/V_3 will be considered.

5.2.1. Plasma Displacement Dynamics Function

The dynamics function Δ/V_3 is given by the equation (4.104),

$$\Delta(s - S_1)(s - S_2)(1 + \tau_k s) = V_3 G_0 (1 + \tau_r s) \ . \tag{5.10}$$

In this equation the time constant τ_k, the vacuum vessel penetration delay time constant for a magnetic field, would normally be comparatively small. That is, the separation ratios

$$(\tau_k |\ S_1\ |\ )^{-1} \quad \text{and} \quad (\tau_k |\ S_2\ |\ )^{-1} \tag{5.11}$$

are expected to be large, not less than 10.0. Under these conditions the effect of the time constant τ_k may be neglected, resulting in a further approximated dynamics function,

$$\Delta(s-S_1)(s-S_2) \;=\; V_3G_0(1+\tau_r s) \quad . \tag{5.12}$$

An analytical design of a plasma displacement feedback control system using the latter dynamics function (5.12) is simple, since the function is simple. Classical or modern control methods can easily be employed for this purpose.

5.2.1.1. Linear Optimal Control

Modern Control Theory is a vast array of analytical design procedures aimed to streamline and expand control system design of a wide class of control problems. *Optimal Control Theory* is a part of the Modern Control Theory. The *Maximum Principle of Pontryagin* dealing with Optimal Control was hypothesized in about 1956 and has since been developed into a rigorous theory. The principle can be stated as follows. For a given dynamics function

$$\dot{\mathbf{x}} \;=\; \mathbf{f}(\mathbf{x},\mathbf{u}) \tag{5.13}$$

and a performance index

$$S \;=\; \int_{t_0}^{T} F(\mathbf{x},\mathbf{u},\mathbf{r})dt \quad , \tag{5.14}$$

which is to minimized, the optimal control input $\mathbf{u}^{o}$ maximizes the scalar Hamiltonian function,

$$H(\mathbf{p},\mathbf{x},\mathbf{u}^{o},\mathbf{r}) = H_{\max} \quad , \tag{5.15}$$

where

$$H = \mathbf{p}^{T}\mathbf{f}(\mathbf{x},\mathbf{u}) - F(\mathbf{x},\mathbf{u},\mathbf{r}) \tag{5.16}$$

and the canonical Hamilton equations are

$$\dot{\mathbf{p}} = -\nabla_{\mathbf{x}}H \; ; \quad \dot{p}_i = -\frac{\partial H}{\partial x_i} \; ; \tag{5.17}$$

$$i = 1,\ 2,\ \ldots\ ,\ n \quad ;$$

$$\dot{\mathbf{x}} = -\nabla_{\mathbf{p}}H \; ; \quad \dot{x}_i = -\frac{\partial H}{\partial p_i} \; ; \tag{5.18}$$

$$i = 1,\ 2,\ \ldots\ ,\ n \quad .$$

In equations (5.13)-(5.18) the vector functions are defined as follows:

$\mathbf{x}$ is a state vector,

$\mathbf{u}$ is a control input vector,

$\mathbf{r}$ is a reference state vector,

$\mathbf{p}$ is a co-state vector.

Optimal Control Theory, in general and as defined above by the Pontryagin Maximum Principle, is applicable to a wide variety of control problems, including non-linear control problems.

Linear Optimal Control is a special sub-set of Optimal Control Theory; the dynamics function (5.13) is assumed to be linear,

$$\dot{\mathbf{x}} = \mathbf{f} = \mathbf{Ax}+\mathbf{Bu} \quad . \tag{5.19}$$

The performance index (5.14) is assumed to be (the reference state vector **r** is taken to be zero for simplicity)

$$S = \frac{1}{2}\mathbf{x}^{\mathrm{T}}\mathbf{Wx}\Big|_{t=T} + \frac{1}{2}\int_{t_0}^{T}(\mathbf{x}^{\mathrm{T}}\mathbf{Cx} + \mathbf{u}^{\mathrm{T}}\mathbf{Du})dt \quad , \tag{5.20}$$

where the weighting matrix **W** is assumed to be scalar, symmetric, and nonnegative definite. The matrices **A** and **B** in (5.19) and **C** and **D** in (5.20) may in general be time-varying functions. The weighting matrices **C** and **D** of (5.20) are assumed to be symmetric, nonnegative, and positive definite, respectively. Differentiating (5.20), its integrand is

$$F = \mathbf{x}^{\mathrm{T}}\mathbf{W}\dot{\mathbf{x}} + \frac{1}{2}\mathbf{x}^{\mathrm{T}}\mathbf{Cx} + \frac{1}{2}\mathbf{u}^{\mathrm{T}}\mathbf{Du} \quad ; \tag{5.21}$$

and the Hamiltonian (5.16) is then

$$H = (\mathbf{p}-\mathbf{Wx})^{\mathrm{T}}(\mathbf{Ax}+\mathbf{Bu}) - \frac{1}{2}\mathbf{x}^{\mathrm{T}}\mathbf{Cx} - \frac{1}{2}\mathbf{u}^{\mathrm{T}}\mathbf{Du} \quad . \tag{5.22}$$

To maximize the Hamiltonian (5.22) let

$$\nabla_{\mathbf{u}}H = 0 \quad , \tag{5.23}$$

$$\begin{aligned} \nabla_{\mathbf{u}}H &= \nabla_{\mathbf{u}}[(\mathbf{p}^{\mathrm{T}}-\mathbf{x}^{\mathrm{T}}\mathbf{W})\mathbf{Bu}] - \frac{1}{2}\nabla_{\mathbf{u}}(\mathbf{u}^{\mathrm{T}}\mathbf{Du}) \\ &= \mathbf{B}^{\mathrm{T}}(\mathbf{p}-\mathbf{Wx}) - \mathbf{Du}^{\mathrm{o}} = 0 \quad , \end{aligned} \tag{5.24}$$

from which the optimal control input is

$$\mathbf{u}^{\mathrm{o}} = \mathbf{D}^{-1}\mathbf{B}^{\mathrm{T}}(\mathbf{p}-\mathbf{Wx}) \quad . \tag{5.25}$$

Substituting eq. (5.25) into eq. (5.19),

$$\dot{\mathbf{x}}|_{\mathbf{u}=\mathbf{u}^{\circ}} = \mathbf{A}\mathbf{x} + \mathbf{B}\mathbf{D}^{-1}\mathbf{B}^{T}(\mathbf{p}-\mathbf{W}\mathbf{x}) \quad . \tag{5.26}$$

Using (5.22) in (5.17),

$$\begin{aligned}\dot{\mathbf{p}} &= -\nabla_{\mathbf{x}}[(\mathbf{p}^{T}-\mathbf{x}^{T}\mathbf{W})\mathbf{A}\mathbf{x}] + \frac{1}{2}\nabla_{\mathbf{x}}(\mathbf{x}^{T}\mathbf{C}\mathbf{x}) + \nabla_{\mathbf{x}}(\mathbf{x}^{T}\mathbf{W}\mathbf{B}\mathbf{u}) \\ &= -\mathbf{A}^{T}(\mathbf{p}-\mathbf{W}\mathbf{x}) + \mathbf{C}\mathbf{x} + \mathbf{W}\mathbf{B}\mathbf{u} \quad ,\end{aligned}$$

and substituting into (5.25),

$$\dot{\mathbf{p}}|_{\mathbf{u}=\mathbf{u}^{\circ}} = (\mathbf{W}\mathbf{B}\mathbf{D}^{-1}\mathbf{B}^{T} - \mathbf{A}^{T})(\mathbf{p}-\mathbf{W}\mathbf{x}) + \mathbf{C}\mathbf{x} \quad . \tag{5.27}$$

Let the state and co-state vectors be related,

$$\mathbf{p} = \mathbf{P}(t)\mathbf{x} \quad , \tag{5.28}$$

$$\dot{\mathbf{p}} = \dot{\mathbf{P}}\mathbf{x} + \mathbf{P}\dot{\mathbf{x}} \quad . \tag{5.29}$$

Substituting eq. (5.28) into eq (5.26),

$$\dot{\mathbf{x}} = [\mathbf{A} + \mathbf{B}\mathbf{D}^{-1}\mathbf{B}^{T}(\mathbf{P}-\mathbf{W})]\mathbf{x} \quad , \tag{5.30}$$

and eq. (5.30) into eq. (5.29),

$$\dot{\mathbf{p}} = \left(\dot{\mathbf{P}} + \mathbf{P}[\mathbf{A}+\mathbf{B}\mathbf{D}^{-1}\mathbf{B}^{T}(\mathbf{P}-\mathbf{W})]\right)\mathbf{x} \quad . \tag{5.31}$$

Substituting (5.28) into (5.27),

$$\dot{\mathbf{p}}|_{\mathbf{u}=\mathbf{u}^{\circ}} = [(\mathbf{W}\mathbf{B}\mathbf{D}^{-1}\mathbf{B}^{T}-\mathbf{A}^{T})(\mathbf{P}-\mathbf{W}) + \mathbf{C}]\mathbf{x} \quad . \tag{5.32}$$

Equating (5.31) and (5.32), the matrix Riccati differential equation is obtained,

$$\dot{\mathbf{P}} + \mathbf{PA} + [\mathbf{A}^T+(\mathbf{P}-\mathbf{W})\mathbf{BD}^{-1}\mathbf{B}^T](\mathbf{P}-\mathbf{W}) - \mathbf{C} = 0 \quad . \tag{5.33}$$

Solution of this equation provides the Riccati matrix $\mathbf{P}(t)$ to be used in equation (5.28). The Riccati matrix $\mathbf{P}(t)$ is a symmetric matrix [25, p. 762]. Substitution of (5.28) into (5.25) results in the optimal control input,

$$\mathbf{u}^o = \mathbf{D}^{-1}\mathbf{B}^T(\mathbf{P}-\mathbf{W})\mathbf{x} \quad . \tag{5.34}$$

An analytical solution of the non-linear matrix Riccati differential equation (5.33) is a formidable, if not an impossible, task even for low order systems. In all cases, however, it is possible to solve the Riccati equation employing a digital computer. Since the object of a control system is to produce a specified state vector $\mathbf{x}(t)$ at some terminal time $t=T$, regardless of any initial state vector $\mathbf{x}(t_0)$ at the initial time t_0, it is the terminal boundary condition that must be known and must be used in solution of the Riccati equation. Referring to eq. (5.34), since at the terminal time $\mathbf{u}^o=0$,

$$\mathbf{P}(T) = \mathbf{W} \quad . \tag{5.35}$$

With the terminal condition $\mathbf{P}(T)$ known, the Riccati equation (5.33) must be integrated backward in time until $\mathbf{P}(t_0)$ is reached.

Equations (5.33)-(5.35) are valid for either time-varying or time-invariant matrices **A**, **B** and **C**, **D** of equations (5.19) and (5.20), respectively, when the terminal time is finite, $T<\infty$.

In the case of infinite terminal time, $T=\infty$, and the time-varying matrices **A**, **B**, **C**, and **D**, the weighting matrix **W** loses its significance and is set to zero, resulting in the terminal condition $\mathbf{P}(T)=0$; the Riccati equation (5.33) is integrated backward in time using successively larger values of T, and its approximate solutions $\mathbf{P}(t,T)$ approach the desired solution $\mathbf{P}(t)$ as $T \to \infty$.

In the case of infinite terminal time, $T = \infty$, and the time-invariant matrices **A, B, C,** and **D**, with the matrix $\mathbf{W} = 0$, the Riccati matrix **P** becomes a time-invariant matrix, and satisfies the algebraic Riccati equation [$\dot{\mathbf{P}} = 0$ and $\mathbf{W} = 0$ in (5.33)],

$$\mathbf{PA} + \mathbf{A}^{\mathrm{T}}\mathbf{P} + \mathbf{PBD}^{-1}\mathbf{B}^{\mathrm{T}}\mathbf{P} - \mathbf{C} = 0 \quad . \tag{5.36}$$

In most practical cases a digital computer must be employed for solution of equation (5.36). It is of interest to note that the Riccati matrix of the equation (5.36) gives rise to a *Liapunov function,*

$$V(\mathbf{x}) = \mathbf{x}^{\mathrm{T}}\mathbf{P}\mathbf{x} \quad . \tag{5.37}$$

For the time-invariant (constant) matrices **A, B** and **C, D** of eqs. (5.19) and (5.20), respectively, the equations (5.26) and (5.27) form a set of two ordinary differential equations. This set may be written as

$$\dot{\mathbf{z}}(t) = \mathbf{E}\mathbf{z}(t) \quad , \tag{5.38}$$

where

$$\mathbf{z}^{\mathrm{T}} = [\mathbf{x},\ \mathbf{p}] \quad , \tag{5.39}$$

and

$$\mathbf{E} = \begin{bmatrix} (\mathbf{A}-\mathbf{BD}^{-1}\mathbf{B}^{\mathrm{T}}\mathbf{W}); & \mathbf{BD}^{-1}\mathbf{B}^{\mathrm{T}} \\ [\mathbf{C}-(\mathbf{WBD}^{-1}\mathbf{B}^{\mathrm{T}}-\mathbf{A}^{\mathrm{T}})\mathbf{W}]; & (\mathbf{WBD}^{-1}\mathbf{B}^{\mathrm{T}}-\mathbf{A}^{\mathrm{T}}) \end{bmatrix} \quad . \tag{5.40}$$

Since matrix $\mathbf{E}$ is a known scalar time-invariant matrix, equation (5.38) can be solved easily. The Laplace transformation of eq. (5.38) is

$$s\mathbf{Z}(s) - \mathbf{z}(0) = \mathbf{E}\mathbf{Z}(s) \quad , \tag{5.41}$$

and therefore

$$\mathbf{Z}(s) = [s\mathbf{I}-\mathbf{E}]^{-1}\mathbf{z}(0) \tag{5.42}$$

and its inverse transform is

$$\mathbf{z}(t) = \mathbf{\Phi}(t)\mathbf{z}(0) = \mathbf{\Phi}(t-t_0)\mathbf{z}(t_0) \quad , \tag{5.43}$$

where

$$\mathbf{\Phi}(t) = L^{-1}\left\{[s\mathbf{I}-\mathbf{E}]^{-1}\right\} \quad , \tag{5.44}$$

and $\mathbf{\Phi}(t-t_0)$ is a stationary system (time-invariant $\mathbf{E}$) transition matrix,

$$\mathbf{\Phi}(t-t_0) = \exp[(\mathbf{E})(t-t_0)] \quad . \tag{5.45}$$

One useful property of the transition matrix is that its inverse transition matrix is simply

$$\mathbf{\Phi}^{-1}(t-t_0) = \mathbf{\Phi}(t_0-t) \quad . \tag{5.46}$$

Using (5.39), let (5.43) be written

$$\begin{bmatrix} \mathbf{x}(t) \\ \mathbf{p}(t) \end{bmatrix} = \begin{bmatrix} \mathbf{\Phi}_{xx}(t-t_0); \; \mathbf{\Phi}_{xp}(t-t_0) \\ \mathbf{\Phi}_{px}(t-t_0); \; \mathbf{\Phi}_{pp}(t-t_0) \end{bmatrix} \begin{bmatrix} \mathbf{x}(t_0) \\ \mathbf{p}(t_0) \end{bmatrix} \quad . \tag{5.47}$$

The co-state vector $\mathbf{p}(t)$, required in the equation of the optimal control input (5.25), can be computed from equation (5.47) using the terminal condition of the state vector. The terminal and/or initial conditions of the state vector are generally known, $\mathbf{x}(T)$ and $\mathbf{x}(0)$, respectively. For determination of the optimal control input it is the terminal condition of the state vector that is of primary interest.

Assuming the terminal condition of the state vector, $\mathbf{x}(T)$, is known, let in equation (5.47) $t \rightarrow T$ and $t_0 \rightarrow t$; then

$$\mathbf{x}(T) = \mathbf{\Phi}_{xx}(T-t)\mathbf{x}(t) + \mathbf{\Phi}_{xp}(T-t)\mathbf{p}(t) \quad , \tag{5.48}$$

from which

$$\mathbf{p}(t) = \mathbf{\Phi}_{xp}^{-1}(T-t)[\mathbf{x}(T) - \mathbf{\Phi}_{xx}(T-t)\mathbf{x}(t)] \quad . \tag{5.49}$$

It must be noted that in equation (5.47) the partitioned matrices of the transition matrix $\mathbf{\Phi}(t-t_0)$ are not the transition matrices in their own right; therefore the inverse matrix of the equation (5.49), $\mathbf{\Phi}_{xp}^{-1}(T-t)$, must be computed using a normal matrix inversion procedure, and not the form of equation (5.46).

Substitution of the co-state vector $\mathbf{p}(t)$ of eq. (5.49) into eq. (5.25) results in the optimal control input vector $\mathbf{u}^0$.

5.2.1.1.1. Optimality Condition

For a linear system represented by (5.19),

$$\dot{\mathbf{x}} = \mathbf{Ax} + \mathbf{Bu} \quad , \tag{5.50}$$

and a performance index specified by (5.20),

$$S = \frac{1}{2}\mathbf{x}^{\mathrm{T}}\mathbf{Wx}\big|_{t=T} + \frac{1}{2}\int_{t_0}^{T}(\mathbf{x}^{\mathrm{T}}\mathbf{Cx} + \mathbf{u}^{\mathrm{T}}\mathbf{Du})dt \quad , \tag{5.51}$$

the optimal control input was found to be given by (5.34),

$$\mathbf{u}^{o} = -\mathbf{K}\mathbf{x} \quad , \tag{5.52}$$

where $\mathbf{K}$ is the optimal state-feedback gain matrix,

$$\mathbf{K} = -\mathbf{D}^{-1}\mathbf{B}^{T}(\mathbf{P}-\mathbf{W}) \quad , \tag{5.53}$$

with the Riccati matrix $\mathbf{P}$ satisfying equation (5.33).

For a command control of the state vector $\mathbf{x}$ let a command input be introduced,

$$\mathbf{u}_{c} = -\mathbf{K}_{c}\mathbf{x}_{c} \quad , \tag{5.54}$$

where $\mathbf{K}_c$ is a command gain matrix and $\mathbf{x}_c$ is a command-state vector.

In equation (5.50), then, let

$$\mathbf{u} = \mathbf{u}^{o} - \mathbf{u}_{c} \quad , \tag{5.55}$$

$$\mathbf{u} = \mathbf{K}_{c}\mathbf{x}_{c} - \mathbf{K}\mathbf{x} \quad . \tag{5.56}$$

Substituting (5.56) into (5.50), a closed-loop state vector differential equation is obtained,

$$\dot{\mathbf{x}} = (\mathbf{A}-\mathbf{B}\mathbf{K})\mathbf{x} + \mathbf{B}\mathbf{K}_{c}\mathbf{x}_{c} \quad . \tag{5.57}$$

Restricting attention to time-invariant systems [see (5.36)], the Laplace transformation of (5.57) results in a state vector transfer function,

$$\mathbf{x} = (s\mathbf{I}-\mathbf{A}+\mathbf{B}\mathbf{K})^{-1}\mathbf{B}\mathbf{K}_{c}\mathbf{x}_{c} \quad . \tag{5.58}$$

Using (5.52) and (5.54) this transfer function may also be written as

$$\mathbf{u}^{\mathrm{o}} = \mathbf{K}(s\mathbf{I}-\mathbf{A}+\mathbf{B}\mathbf{K})^{-1}\mathbf{B}\mathbf{u}_{\mathrm{c}} \quad . \tag{5.59}$$

Assuming a unity feedback equation (5.59) may also be written as

$$\mathbf{u}^{\mathrm{o}} = [\mathbf{I}+\mathbf{K}(s\mathbf{I}-\mathbf{A})^{-1}\mathbf{B}]^{-1}\mathbf{K}(s\mathbf{I}-\mathbf{A})^{-1}\mathbf{B}\mathbf{u}_{\mathrm{c}} \quad , \tag{5.60}$$

the open-loop relation being

$$\mathbf{u}^{\mathrm{o}} = -\mathbf{K}(s\mathbf{I}-\mathbf{A})^{-1}\mathbf{B}\mathbf{u} \quad , \tag{5.61}$$

derivable directly from (5.50) and (5.52).

The open-loop transfer function (5.61) may also be written as

$$\mathbf{D}^{1/2}\mathbf{u}^{\mathrm{o}} = -[\mathbf{D}^{1/2}\mathbf{K}(s\mathbf{I}-\mathbf{A})^{-1}\mathbf{B}\mathbf{D}^{-1/2}]\mathbf{D}^{1/2}\mathbf{u} \quad , \tag{5.62}$$

where $\mathbf{D}$ is the weighting matrix of the performance index (5.51) and the changed variables are

$$\mathbf{e}^{\mathrm{o}} = \mathbf{D}^{1/2}\mathbf{u}^{\mathrm{o}} \quad ,$$

$$\mathbf{e} = \mathbf{D}^{1/2}\mathbf{u} \quad ,$$

$$\mathbf{e}_{\mathrm{c}} = \mathbf{D}^{1/2}\mathbf{u}_{\mathrm{c}} \quad ,$$

$$\mathbf{e} = \mathbf{e}^{\mathrm{o}} - \mathbf{e}_{\mathrm{c}} \quad . \tag{5.63}$$

Letting the open-loop matrix of (5.62) be

$$\mathbf{M}_1(s) = \mathbf{D}^{1/2}\mathbf{K}(s\mathbf{I}-\mathbf{A})^{-1}\mathbf{B}\mathbf{D}^{-1/2} \quad , \tag{5.64}$$

and using (5.63), equation (5.62) is written as

$$\mathbf{e}^{\mathrm{o}} = -\mathbf{M}_1(s)\mathbf{e} \quad . \tag{5.65}$$

In terms of the changed variables of (5.63) and using (5.64) and (5.65), equation (5.60) becomes,

$$\mathbf{e}^o = \mathbf{M}_2^{-1}(s)\mathbf{M}_1(s)\mathbf{e}_c \quad , \tag{5.66}$$

where the *return difference matrix* is

$$\mathbf{M}_2(s) = \mathbf{I} + \mathbf{M}_1(s) \quad . \tag{5.67}$$

Similarly, equation (5.59) becomes

$$\mathbf{e}^o = \mathbf{M}_3(s)\mathbf{e}_c \quad , \tag{5.68}$$

where the closed-loop transfer matrix is

$$\mathbf{M}_3(s) = \mathbf{D}^{1/2}\mathbf{K}(s\mathbf{I}-\mathbf{A}+\mathbf{B}\mathbf{K})^{-1}\mathbf{B}\mathbf{D}^{-1/2} \quad . \tag{5.69}$$

By comparison of (5.66) and (5.68),

$$\mathbf{M}_3(s) = \mathbf{M}_2^{-1}(s)\mathbf{M}_1(s) \quad . \tag{5.70}$$

Several useful matrix relations arise from the equations (5.67) and (5.70); omitting for convenience the functional dependence indication (s),

$$\mathbf{M}_2 = \mathbf{I} + \mathbf{M}_1 \quad , \tag{5.71}$$

$$\mathbf{M}_3 = \mathbf{M}_2^{-1}\mathbf{M}_1 = \mathbf{M}_1\mathbf{M}_2^{-1} \quad , \tag{5.72}$$

$$\mathbf{M}_3 = \mathbf{I} - \mathbf{M}_2^{-1} \quad , \tag{5.73}$$

$$\mathbf{M}_3\mathbf{M}_1 = \mathbf{M}_1\mathbf{M}_3 \quad . \tag{5.74}$$

For example, from (5.64), (5.69), (5.71), and (5.73) it follows that

$$[\mathbf{I}+\mathbf{D}^{1/2}\mathbf{K}(s\mathbf{I}-\mathbf{A})^{-1}\mathbf{B}\mathbf{D}^{-1/2}]^{-1} = \mathbf{I}-\mathbf{D}^{1/2}\mathbf{K}(s\mathbf{I}-\mathbf{A}+\mathbf{B}\mathbf{K})^{-1}\mathbf{B}\mathbf{D}^{-1/2} \quad . \tag{5.75}$$

The open-loop transfer matrix (5.64),

$$\mathbf{M}_1 = \mathbf{D}^{1/2}\mathbf{K}(s\mathbf{I}-\mathbf{A})^{-1}\mathbf{B}\mathbf{D}^{-1/2} \quad ,$$

is written

$$\mathbf{M}_1 = \frac{\mathbf{N}_1}{q_1} \quad , \tag{5.76}$$

where

$$\mathbf{N}_1 = \mathbf{D}^{1/2}\mathbf{K}[\mathrm{adj}(s\mathbf{I}-\mathbf{A})]\mathbf{B}\mathbf{D}^{-1/2} \quad , \tag{5.77}$$

is the open-loop numerator transfer matrix and

$$q_1 = \det(s\mathbf{I}-\mathbf{A}) \quad , \tag{5.78}$$

is the matrix $(s\mathbf{I}-\mathbf{A})$ determinant; it is the open-loop characteristic polynomial of the system.

The inverse matrix $\mathbf{M}_1$ is then

$$\mathbf{M}_1^{-1} = q_1\mathbf{N}_1^{-1} = q_1\frac{\mathrm{adj}\,\mathbf{N}_1}{\det\mathbf{N}_1} \quad . \tag{5.79}$$

The return-difference matrix (5.67), (5.71),

$$\mathbf{M}_2 = \mathbf{I} + \mathbf{M}_1 \quad ,$$

is written, using (5.76),

$$\mathbf{M}_2 = \frac{\mathbf{N}_2}{q_2} = \frac{q_1\mathbf{I}+\mathbf{N}_1}{q_1} \quad , \tag{5.80}$$

so that

$$\mathbf{N}_2 = q_1\mathbf{I} + \mathbf{N}_1 \quad , \tag{5.81}$$

$$q_2 = q_1 \quad . \tag{5.82}$$

The inverse matrix $\mathbf{M}_2$ is then,

$$\mathbf{M}_2^{-1} = (\mathbf{I}+\mathbf{M}_1)^{-1} \quad , \tag{5.83}$$

$$\mathbf{M}_2^{-1} = q_1(q_1\mathbf{I}+\mathbf{N}_1)^{-1} = q_1\frac{\mathrm{adj}(q_1\mathbf{I}+\mathbf{N}_1)}{\det(q_1\mathbf{I}+\mathbf{N}_1)} \quad . \tag{5.84}$$

The closed-loop transfer matrix (5.69),

$$\mathbf{M}_3 = \mathbf{D}^{½}\mathbf{K}(s\mathbf{I}-\mathbf{A}+\mathbf{B}\mathbf{K})^{-1}\mathbf{B}\mathbf{D}^{-½} \quad ,$$

is written

$$\mathbf{M}_3 = \frac{\mathbf{N}_3}{q_3} \quad , \tag{5.85}$$

where

$$\mathbf{N}_3 = \mathbf{D}^{½}\mathbf{K}[\mathrm{adj}(s\mathbf{I}-\mathbf{A}+\mathbf{B}\mathbf{K})]\mathbf{B}\mathbf{D}^{-½} \tag{5.86}$$

is the closed-loop numerator transfer matrix and

$$q_3 = \det(s\mathbf{I}-\mathbf{A}+\mathbf{B}\mathbf{K}) \tag{5.87}$$

is the matrix $(s\mathbf{I}-\mathbf{A}+\mathbf{B}\mathbf{K})$ determinant; it is the closed-loop characteristic polynomial of the system.

The inverse matrix $\mathbf{M}_3$ is then

$$\mathbf{M}_3^{-1} = q_3\mathbf{N}_3^{-1} = q_3\frac{\mathrm{adj}\mathbf{N}_3}{\det\mathbf{N}_3} \quad . \tag{5.88}$$

Referring to (5.72),

$$\mathbf{M}_2 = \mathbf{M}_1\mathbf{M}_3^{-1} = \mathbf{M}_3^{-1}\mathbf{M}_1 \quad . \tag{5.89}$$

Substituting (5.76) and (5.88) into (5.89),

$$\mathbf{M}_2 = \frac{q_3}{q_1}\mathbf{N}_1\mathbf{N}_3^{-1} = \frac{q_3}{q_1}\mathbf{N}_3^{-1}\mathbf{N}_1 \quad . \tag{5.90}$$

Equating (5.80) and (5.90),

$$\mathbf{N}_2 = (q_1\mathbf{I}+\mathbf{N}_1) = q_3\mathbf{N}_3^{-1}\mathbf{N}_1 \quad . \tag{5.91}$$

The return-difference matrix $\mathbf{M}_2$ (5.67), (5.71) appears in an equation obtained by manipulating the algebraic Riccati equation (5.36) [31, (5.2-5)],

$$\mathbf{PA}+\mathbf{A}^{\mathrm{T}}\mathbf{P}+\mathbf{PBD}^{-1}\mathbf{B}^{\mathrm{T}}\mathbf{P} = \mathbf{C} \quad . \tag{5.92}$$

Adding and subtracting $s\mathbf{P}$ to the left side of (5.92), multiplying on the left by $\mathbf{D}^{-1/2}\mathbf{B}^T(-s\mathbf{I}-\mathbf{A}^T)^{-1}$ and on the right side by $(s\mathbf{I}-\mathbf{A})^{-1}\mathbf{BD}^{-1/2}$, using (5.53) [$\mathbf{W} = 0$],

$$\mathbf{K} = -\mathbf{D}^{-1}\mathbf{B}^{\mathrm{T}}\mathbf{P} \quad , \tag{5.93}$$

$$\mathbf{K}^{\mathrm{T}} = -\mathbf{PBD}^{-1} \quad ,$$

$$\mathbf{K}^{\mathrm{T}}\mathbf{D}^{1/2} = -\mathbf{PBD}^{-1/2} \quad , \qquad \mathbf{D}^{1/2}\mathbf{K} = -\mathbf{D}^{-1/2}\mathbf{B}^{\mathrm{T}}\mathbf{P} \quad ,$$

$$\mathbf{K}^{\mathrm{T}}\mathbf{DK} = \mathbf{PBD}^{-1}\mathbf{B}^{\mathrm{T}}\mathbf{P} \quad ,$$

and adding $\mathbf{I}$ to each side, equation (5.92) becomes,

$$[\mathbf{I}+\mathbf{D}^{-1/2}\mathbf{B}^{T}(-s\mathbf{I}-\mathbf{A}^{T})^{-1}\mathbf{K}^{T}\mathbf{D}^{1/2}]\ [\mathbf{I}+\mathbf{D}^{1/2}\mathbf{K}(s\mathbf{I}-\mathbf{A})^{-1}\mathbf{B}\mathbf{D}^{-1/2}] \tag{5.94}$$

$$= I \ + \ D^{-1/2}B^{T}(-s\mathbf{I}-\mathbf{A}^{T})^{-1}\mathbf{C}(s\mathbf{I}-\mathbf{A})^{-1}\mathbf{B}\mathbf{D}^{-1/2} \quad .$$

Transposing the first matrix of the left side of (5.94), using (5.64) and (5.67), with $s=j\omega$ and $*$ denoting the complex conjugate, $s^* = -s = -j\omega$, then

$$\begin{aligned}
&[\mathbf{I}+\mathbf{D}^{-1/2}\mathbf{B}^{T}(-s\mathbf{I}-\mathbf{A}^{T})^{-1}\mathbf{K}^{T}\mathbf{D}^{1/2}] \\
&\quad = [I+D^{1/2}K(-s\mathbf{I}-\mathbf{A})^{-1}\mathbf{B}\mathbf{D}^{-1/2}]^{T} \\
&\quad = I \ + \ M_1^{T}(s^*) \\
&\quad = M_2^{T}(s^*) \quad .
\end{aligned} \tag{5.95}$$

On the right side of (5.94) let

$$\mathbf{M}_4(s) \ = \ (s\mathbf{I}-\mathbf{A})^{-1}\mathbf{B}\mathbf{D}^{-1/2} \tag{5.96}$$

so that

$$\mathbf{M}_4^{T}(s^*) \ = \ \mathbf{D}^{-1/2}\mathbf{B}^{T}(-s\mathbf{I}-\mathbf{A}^{T})^{-1} \quad . \tag{5.97}$$

Equation (5.94) is written then, using (5.95), (5.67), (5.64), (5.97), and (5.96),

$$\mathbf{M}_2^{T}(s^*)\mathbf{M}_2(s) \ = \ \mathbf{I} \ + \ \mathbf{M}_4^{T}(s^*)\mathbf{C}\mathbf{M}_4(s) \quad . \tag{5.98}$$

Since in (5.98) for a positive semidefinite symmetric matrix $\mathbf{C}$ (5.20),

$$\mathbf{M}_4^{T}(s^*)\mathbf{C}\mathbf{M}_4(s) \ \geqslant \ 0 \quad , \tag{5.99}$$

equation (5.98) states that

$$\mathbf{M}_2^{T}(s^*)\mathbf{M}_2(s) \ \geqslant \ \mathbf{I} \quad , \tag{5.100}$$

which is the *optimality condition* [31, (7.3-24)] assuring that the control input (5.52),

$$\mathbf{u}^{o} = -\mathbf{K}\mathbf{x} \tag{5.101}$$

with

$$\mathbf{K} = -\mathbf{D}^{-1}\mathbf{B}^{T}\mathbf{P} \quad , \tag{5.102}$$

is optimal for the performance index (5.51), with $\mathbf{W} = 0$ and $\mathbf{T} = \infty$,

$$S = \frac{1}{2}\int_{t_0}^{\infty}(\mathbf{x}^{T}\mathbf{C}\mathbf{x}+\mathbf{u}^{T}\mathbf{D}\mathbf{u})dt \quad . \tag{5.103}$$

Referring to (5.90), the *optimality condition* (5.100) may also be written,

$$\frac{\overset{*}{q}_3 q_3}{\overset{*}{q}_1 q_1}\,(\mathbf{N}_1^{T*}[\ \mathbf{M}_3^{T*}\mathbf{N}_3]^{-1}\mathbf{N}_1) \geqslant \mathbf{I} \quad . \tag{5.104}$$

The optimality condition (5.104) holds for both the multiple- and single-input systems. For *single-input* systems the control input matrix **B** of (5.50) becomes a vector **b** and the control input vector **u** of (5.50) becomes a scalar u. The optimal gain matrix **K** of (5.52) becomes a transposed vector $\mathbf{k}^{T}$. Without any loss of generality the weighting matrix **D** of (5.103) may be assumed to be a unity matrix, since matrix **D** is significant only relative to matrix **C**, resulting in

$$S = \frac{1}{2}\int_{t_0}^{\infty}(\mathbf{x}^{T}\mathbf{C}\mathbf{x}+u^{2})\ dt \tag{5.105}$$

and

$$\mathbf{u}^{o} = -\mathbf{k}^{T}\mathbf{x} \quad , \tag{5.106}$$

$$\mathbf{k}^{\mathrm{T}} = -\mathbf{b}^{\mathrm{T}}\mathbf{P} \quad . \tag{5.107}$$

Under the above single-input system conditions the open-loop matrix (5.64) becomes

$$\mathbf{M}_1(s) = \mathbf{k}^{\mathrm{T}}(s\mathbf{I}-\mathbf{A})^{-1}\mathbf{b} \quad , \tag{5.108}$$

and the return-difference matrix (5.67) becomes

$$\mathbf{M}_2(s) = 1+\mathbf{k}^{\mathrm{T}}(s\mathbf{I}-\mathbf{A})^{-1}\mathbf{b} \quad . \tag{5.109}$$

Substituting (5.109) into (5.100), the optimality condition for single-input systems is [31, (5.2-10)],

$$|\ 1+\mathbf{k}^{\mathrm{T}}(s\mathbf{I}-\mathbf{A})^{-1}\mathbf{b}\ | \geqslant 1 \quad , \tag{5.110}$$

which states [31, p. 71] that the optimally designed closed-loop system possesses the *infinite gain margin property*: the Nyquist plot of $\mathbf{k}^{\mathrm{T}}(s\mathbf{I}-\mathbf{A})^{-1}\mathbf{b}$ avoids a circle of unit radius centered at $(-1+j0)$ in the complex s-plane for all real ω, $s=j\omega$, no matter how large the loop gain becomes. The *phase margin* is measured from a Nyquist plot point ($\omega \geqslant 0$) located at unit distance from the complex s-plane origin to the negative real axis of the complex s-plane. Therefore, equation (5.110) also states [31, p. 74] that the phase margin of an optimally designed closed-loop system is always not less than 60^o.

The single-input system conditions, (5.105)-(5.107), are also reflected in the following changes:

eqs. (5.76), (5.77), (5.78),

$$\mathbf{M}_1 = \frac{\mathbf{N}_1}{q_1} \rightarrow \frac{p_1}{q_1} \quad ,$$

$\mathbf{N}_1$ becomes the open-loop numerator polynomial p_1,

$$\mathbf{N}_1 \rightarrow p_1 = \mathbf{k}^{\mathrm{T}}[\mathrm{adj}(s\mathbf{I}-\mathbf{A})]\mathbf{b} \quad , \tag{5.111}$$

and

$$q_1 = \det(s\mathbf{I}-\mathbf{A}) \quad ; \tag{5.78}$$

eqs. (5.80), (5.81), (5.82), (5.111),

$$\mathbf{M}_2 = \frac{\mathbf{N}_2}{q_2} \rightarrow \frac{p_2}{q_2} \quad ,$$

$\mathbf{N}_2$ becomes the return-difference numerator polynomial p_2,

$$\mathbf{N}_2 \rightarrow p_2 = q_1+p_1 \quad , \tag{5.112}$$

and

$$q_2 = q_1 \quad ; \tag{5.113}$$

eqs. (5.85), (5.86), (5.87),

$$\mathbf{M}_3 = \frac{\mathbf{N}_3}{q_3} \rightarrow \frac{p_3}{q_3} \quad ,$$

$\mathbf{N}_3$ becomes the closed-loop numerator polynomial p_3,

$$\mathbf{N}_3 \rightarrow p_3 = \mathbf{k}^{\mathrm{T}}[\mathrm{adj}(s\mathbf{I}-\mathbf{A}+\mathbf{b}\mathbf{k}^{\mathrm{T}})]\mathbf{b} \quad , \tag{5.114}$$

$$p_3 = p_1 \quad , \tag{5.115}$$

and

$$q_3 = \det(s\mathbf{I} - \mathbf{A} + \mathbf{b}\mathbf{k}^{\mathrm{T}}) \quad , \tag{5.116}$$

$$q_3 = p_2 = q_1 + p_1 \quad . \tag{5.117}$$

Substituting (5.111) and (5.114) into (5.104), the optimality condition for single-input systems is simply [31, (7.4-4)],

$$q_3^* q_3 \geqslant q_1^* q_1 \quad . \tag{5.118}$$

Substituting (5.117) into (5.118), the optimality condition for single-input systems is also given by

$$(p_1^* q_3 + q_1^* p_1) \geqslant 0 \quad , \tag{5.119}$$

for all real ω, $s = j\omega$.

5.2.1.2. Tokamak Plasma Displacement Optimal Feedback Control

The approximated plasma displacement dynamics function is given by equation (5.12). It is simple enough to allow a direct application of the linear optimal control design procedure outlined in the preceding section by the equations (5.34) and (5.36). It is more practical and straightforward, however, to employ in this case a pole-positioning approach.

It is convenient to write (5.12) in a state-space form such that Δ is the first element of the state vector $\mathbf{x}$ [25, (4-194)],

$$\mathbf{x}^{\mathrm{T}} = [x_1, x_2] \quad , \quad x_1 = \Delta \quad , \tag{5.120}$$

$$\dot{\mathbf{x}} = \mathbf{A}\mathbf{x} + \mathbf{b}u \quad , \tag{5.121}$$

$$\mathbf{A} = \begin{bmatrix} 0; & 1 \\ -a_1; & -a_2 \end{bmatrix} , \qquad \mathbf{b} = \begin{bmatrix} b_1 \\ b_2 \end{bmatrix} , \tag{5.122}$$

where

$$u = V_3 ,$$

$$a_1 = S_1 S_2 ,$$

$$a_2 = -(S_1+S_2) ,$$

$$b_1 = \tau_r G_0 ,$$

$$b_2 = (1-\tau_r a_2) G_0 ,$$

$$x_2 = \dot{x}_1 - b_1 u . \tag{5.123}$$

Comparing equations (5.19) and (5.121), it is noted that for a single-input system the matrix **B** of (5.19) becomes a vector **b** and the vector **u** of (5.19) becomes a scalar u.

Equations (5.120)-(5.123) represent a simple time-invariant second order system. Therefore, in accordance with equations (5.34) and (5.36), the optimal control input is directly proportional to the state vector,

$$u^o = -\mathbf{k}^{\mathrm{T}} \mathbf{x} , \tag{5.124}$$

where

$$\mathbf{k}^{\mathrm{T}} = [k_1,\ k_2] \tag{5.125}$$

is a constant state-feedback gain vector.

For a command control of the state vector a command input is introduced,

$$u_c = -\mathbf{k}_c^T \mathbf{x}_c \quad , \tag{5.126}$$

where

$$\mathbf{k}_c^T = [k_{1c}, 0] \tag{5.127}$$

is a constant command gain vector and

$$\mathbf{x}_c^T = [x_{1c}, 0] \tag{5.128}$$

is a command state vector.

It is noted that in equations (5.127) and (5.128) the respective elements k_{2c} and x_{2c} are set to zero. This is done in accordance with a desire to control only one state of the state vector, namely the state $x_1 = \Delta$. In equation (5.128), then,

$$x_{1c} = \Delta_c \quad . \tag{5.129}$$

Using equations (5.124) and (5.126) the control input is written as

$$u = u^o - u_c \quad , \tag{5.130}$$

$$u = \mathbf{k}_c^T \mathbf{x}_c - \mathbf{k}^T \mathbf{x} \quad .$$

Substituting (5.130) into (5.121),

$$\dot{\mathbf{x}} = (\mathbf{A} - \mathbf{b}\mathbf{k}^T)\mathbf{x} + \mathbf{b}\mathbf{k}_c^T \mathbf{x}_c \quad , \tag{5.131}$$

and using Laplace transformation,

$$(s\mathbf{I} - \mathbf{A} + \mathbf{b}\mathbf{k}^T)\mathbf{x} = \mathbf{b}\mathbf{k}_c^T \mathbf{x}_c \quad ,$$

$$\mathbf{x} = (s\mathbf{I}-\mathbf{A}+\mathbf{b}\mathbf{k}^{\mathrm{T}})^{-1}\mathbf{b}\mathbf{k}_{\mathrm{c}}^{\mathrm{T}}\mathbf{x}_{\mathrm{c}} \quad . \tag{5.132}$$

In (5.132),

$$(s\mathbf{I}-\mathbf{A}+\mathbf{b}\mathbf{k}^{\mathrm{T}})^{-1} = \frac{\mathrm{adj}(s\mathbf{I}-\mathbf{A}+\mathbf{b}\mathbf{k}^{\mathrm{T}})}{\det(s\mathbf{I}-\mathbf{A}+\mathbf{b}\mathbf{k}^{\mathrm{T}})} \quad , \tag{5.133}$$

where, using (5.122) and (5.125),

$$\mathrm{adj}(s\mathbf{I}-\mathbf{A}+\mathbf{b}\mathbf{k}^{\mathrm{T}}) = \begin{bmatrix} (s+a_2+b_2k_2); & (1-b_1k_2) \\ -(b_2k_1+a_1); & (s+b_1k_1) \end{bmatrix} \quad , \tag{5.134}$$

and the closed-loop characteristic polynomial is

$$\begin{aligned} &\det(s\mathbf{I}-\mathbf{A}+\mathbf{b}\mathbf{k}^{\mathrm{T}}) \\ &\quad = s^2 + (a_2+b_1k_1+b_2k_2)s + [a_1+(b_2+b_1a_2)k_1-a_1b_1k_2] \quad . \end{aligned} \tag{5.135}$$

Writing (5.135) in standard form,

$$s^2 + \sigma_{21}\omega_0 s + \omega_0^2 = 0 \quad , \tag{5.136}$$

it follows that for a set of selected σ_{21} and ω_0,

$$\begin{aligned} k_1 &= [a_1b_1(\sigma_{21}\omega_0-a_2)+b_2(\omega_0^2-a_1)]D_1^{-1} \quad , \\ k_2 &= [b_1(a_1-\omega_0^2)+(b_2+b_1a_2)(\sigma_{21}\omega_0-a_2)]D_1^{-1} \quad , \end{aligned} \tag{5.137}$$

where

$$D_1 = a_1b_1^2 + b_2(b_2+b_1a_2) \quad . \tag{5.138}$$

In using eqs. (5.137) and (5.138) it may be an advantage to keep k_2 close to zero. For $k_2 = 0$ in eq. (5.137), σ_{21} and ω_0 are related by

$$\sigma_{21} = [a_2 - a_1 b_1 (b_2 + b_1 a_2)^{-1}]\omega_0^{-1} + b_1 (b_2 + b_1 a_2)^{-1} \omega_0 \quad . \tag{5.139}$$

For a value of σ_{21} larger (less) than the value computed using (5.139) the value of k_2 is larger (less) than zero.

Referring to (5.120)-(5.122), (5.127)-(5.129), and (5.132)-(5.136), the plasma displacement transfer function is

$$\Delta(s^2 + \sigma_{21}\omega_0 s + \omega_0^2) = \Delta_c k_{1c}[(s + a_2)b_1 + b_2] \quad , \tag{5.140}$$

from which it follows that for unity steady-state response,

$$k_{1c} = \omega_0^2 (a_2 b_1 + b_2)^{-1} \quad . \tag{5.141}$$

The optimality condition (5.119) must be satisfied for the selected values of σ_{21} and ω_0 used in computing k_1 and k_2, (5.137) and (5.138), respectively.

Referring to (5.111), (5.122), and (5.125),

$$\begin{aligned} p_1 &= \mathbf{k}^{\mathrm{T}}[\mathrm{adj}(s\mathbf{I} - \mathbf{A})]\mathbf{b} \\ &= [k_1(a_2 b_1 + b_2) - k_2 a_1 b_1] + s(k_1 b_1 + k_2 b_2) \quad . \end{aligned} \tag{5.142}$$

Referring to (5.78) and (5.122),

$$q_1 = \det(s\mathbf{I} - \mathbf{A}) = s^2 + a_2 s + a_1 \quad . \tag{5.143}$$

Referring to (5.116), (5.117), (5.135), and (5.136),

$$\begin{aligned} q_3 &= \det(s\mathbf{I} - \mathbf{A} + \mathbf{b}\mathbf{k}^{\mathrm{T}}) \\ &= q_1 + p_1 = s^2 + \sigma_{21}\omega_0 s + \omega_0^2 \quad . \end{aligned} \tag{5.144}$$

Using (5.143) and (5.144) in (5.118), the optimality condition for a second order system reduces to

$$(\omega_0^4 - a_1^2) \geqslant \omega^2[(a_2^2 - 2a_1) - (\sigma_{21}^2 - 2)\omega_0^2] \quad . \tag{5.145}$$

Assuming $\infty \geqslant \omega \geqslant 0$, the right side of equation (5.145) must be $\leqslant 0$; that is,

$$\sigma_{21} \geqslant [2 + (a_2^2 - 2a_1)\omega_0^{-2}]^{1/2} \quad . \tag{5.146}$$

The magnitude of σ_{21} satisfying (5.146) must be used in (5.137) and (5.138) for the second order system (5.140) to be optimal.

It is known that for a second order system (5.136) the ***Butterworth*** roots are defined by $\sigma_{21} = \sqrt{2}$. Comparing this with (5.146) it is noted that the Butterworth second order system is mathematically optimal only for $\omega_0 = \infty$; practically it is nearly optimal for

$$\omega_0 \gg (0.5a_2^2 - a_1)^{1/2} \quad . \tag{5.147}$$

Using equations (5.8) $[u \equiv E_3]$, (5.12), and (5.124)-(5.141), a block diagram of the optimal feedback control of a tokamak plasma displacement is shown in fig. 5.3.

5.2.1.3. Analog Implementation of Tokamak Plasma Displacement Feedback Control

Referring to fig 5.3, the required optimal feedback function $(k_1 + k_2 s)$ may be instrumented using a digital processor. Analog implementation of this function is not practical since it would require use of a differentiator. For analog implementation it is practical to replace the optimal feedback function of fig. 5.3 $(k_1 + k_2 s)$ by

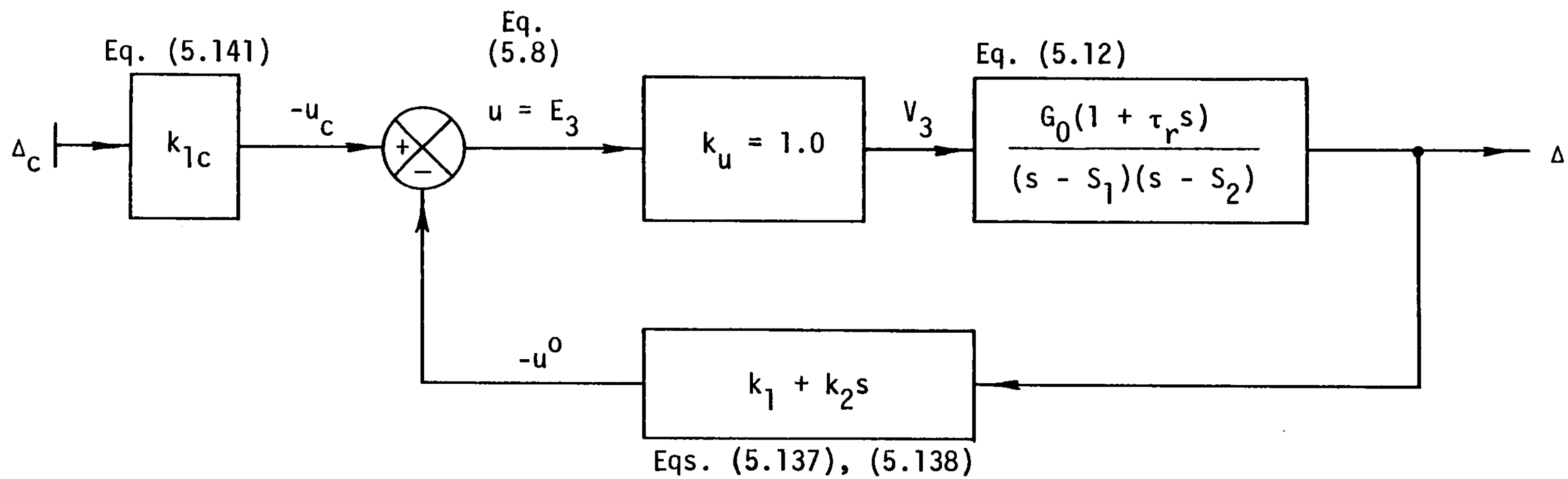

Figure 5.3. Tokamak plasma displacement optimal feedback control, block diagram.

$$\frac{k_1+k_2 s}{1+sT_3} \quad . \tag{5.148}$$

With this replacement the closed-loop transfer function (5.140) becomes

$$\Delta(s^3 + \sigma_{32}\omega_0 s^2 + \sigma_{31}\omega_0^2 s + \omega_0^3)T_3 = \Delta_c k_{1c} G_0 (1+sT_3)(1+\tau_r s) \quad , \tag{5.149}$$

where

$$T_3\omega_0^3 = a_1 + G_0 k_1 \quad , \tag{5.150}$$

$$T_3(\sigma_{31}\omega_0^2 - a_1) = a_2 + \tau_r G_0 k_1 + G_0 k_2 \quad , \tag{5.151}$$

$$T_3(\sigma_{32}\omega_0 - a_2) = 1 + \tau_r G_0 k_2 \quad , \tag{5.152}$$

and

$$k_{1c} = \omega_0^3 T_3 G_0^{-1} \tag{5.153}$$

for unity steady-state response.

For the selected values of σ_{31}, σ_{32}, and ω_0 from (5.150)-(5.153),

$$D_2 = [\sigma_{32}\omega_0 - a_2 + \tau_r(\tau_r\omega_0^3 - \sigma_{31}\omega_0^2 + a_1)]G_0 \quad , \tag{5.154}$$

$$k_1 = [\omega_0^3 + a_1(a_2 - \sigma_{32}\omega_0) + \tau_r(a_1(\sigma_{31}\omega_0^2 - a_1) - a_2\omega_0^3)]D_2^{-1} \quad , \tag{5.155}$$

$$k_2 = [\sigma_{31}\omega_0^2 - a_1 + a_2(a_2 - \sigma_{32}\omega_0) + \tau_r(a_1(\sigma_{32}\omega_0 - a_2) - \omega_0^3)]D_2^{-1} \quad , \tag{5.156}$$

$$T_3 = [1 + \tau_r(a_1\tau_r - a_2)]G_0 D_2^{-1} \quad . \tag{5.157}$$

For an optimally designed system the selected values of σ_{31}, σ_{32}, and ω_0 must be such that the optimality condition (5.118) [(5.119)] is satisfied.

For this system,

$$p_1 = G_0(1+s\tau_r)(k_1+k_2s) \quad , \tag{5.158}$$

$$q_1 = (s^2+a_2s+a_1)(1+sT_3) \quad , \tag{5.159}$$

$$q_3 = T_3(s^3+\sigma_{32}\omega_0s^2+\sigma_{31}\omega_0^2s+\omega_0^3) \quad , \tag{5.160}$$

so that

$$q_3^*q_3 = T_3^2[\omega^2(\omega^2-\sigma_{31}\omega_0^2)^2 + \omega_0^2(\omega_0^2-\sigma_{32}\omega^2)^2] \quad , \tag{5.161}$$

$$q_1^*q_1 = [a_1-\omega^2(a_2T_3+1)]^2 + \omega^2[a_2+T_3(a_1-\omega^2)]^2 \quad . \tag{5.162}$$

Rearranging components according to (5.118),

$$\begin{aligned}(\omega_0^6-a_1^2) \geqslant\ & \omega^4[1+T_3^2((a_2^2-2a_1)+\omega_0^2(2\sigma_{31}-\sigma_{32}^2))] \\ & + \omega^2[(a_2^2-2a_1)+T_3^2(a_1^2+\omega_0^4(2\sigma_{32}-\sigma_{31}^2))] \quad .\end{aligned} \tag{5.163}$$

Since (5.163) must hold for

$$\infty \geqslant \omega \geqslant 0 \quad ,$$

the left side of (5.163) must be

$$(\omega_0^6-a_1^2) \geqslant 0 \quad ; \tag{5.164}$$

the first term of the right side of (5.163) must be

$$0 \geqslant 1+T_3^2[(a_2^2-2a_1)+\omega_0^2(2\sigma_{31}-\sigma_{32}^2)] \quad ; \tag{5.165}$$

the second term of the right side of (5.163) must be

$$0 \geqslant (a_2^2-2a_1)+T_3^2[a_1^2+\omega_0^4(2\sigma_{32}-\sigma_{31}^2)] \quad . \tag{5.166}$$

From (5.165),

$$T_3^2[\omega_0^2(\sigma_{32}^2-2\sigma_{31}) \;-\; (a_2^2-2a_1)] \geqslant 1.0 \quad . \tag{5.167}$$

From (5.166),

$$T_3^2[\omega_0^4(\sigma_{31}^2-2\sigma_{32})-a_1^2] \geqslant (a_2^2-2a_1) \quad . \tag{5.168}$$

From (5.167),

$$\omega_0^2(\sigma_{32}^2-2\sigma_{31}) > (a_2^2-2a_1) \quad . \tag{5.169}$$

From (5.167),

$$\sigma_{32} \geqslant \left([T_3^{-2}+(a_2^2-2a_1)]\omega_0^{-2}+2\sigma_{31}\right)^{1/2} \quad . \tag{5.170}$$

From (5.168),

$$\sigma_{31} \geqslant \left([(a_2^2-2a_1)T_3^{-2}+a_1^2]\omega_0^{-4}+2\sigma_{32}\right)^{1/2} \quad . \tag{5.171}$$

The optimality condition (5.118) is satisfied if (5.167)-(5.171) hold; the third order system (5.149) is then optimal (characterized by an infinite gain margin and a phase margin of not less than 60^o).

For a third order system (5.149) the Butterworth roots are defined by

$$\sigma_{31} = \sigma_{32} = 2.0 \quad , \tag{5.172}$$

and the roots of other similar distributions are generally defined by

$$\sigma_{31} \geqslant \sigma_{32} > 1.0 \quad . \tag{5.173}$$

Referring to (5.167)-(5.171) and (5.172) it is observed that a third order Butterworth system (5.149) is not optimal, since none of eqs. (5.167) through

(5.169) is satisfied, assuming $(a_2^2-2a_1) \geqslant 0$. For $(a_2^2-2a_1) < 0$ eqs. (5.167) and (5.168) reduce to, respectively,

$$T_3^2 \geqslant (2a_1-a_2^2)^{-1} \quad , \tag{5.174}$$

$$T_3^2 \geqslant (2a_1-a_2^2)a_1^{-2} \quad , \tag{5.175}$$

where

$$a_1 > 0 \quad , \qquad 2a_1 > a_2^2 \quad , \tag{5.176}$$

and T_3 is given by (5.157).

6. ISX-A TOKAMAK HIGH-FREQUENCY OSCILLATIONS AND LOW-FREQUENCY DYNAMICS FUNCTIONS

For nominal numerical values of the ISX-A tokamak design and estimated parameters (listed in the Appendix), high-frequency oscillations parameters computed using eqs. (4.62)-(4.65), (4.132), and (4.133) are

Radial: $Re = -7405.3$ (rad/s) ,

$\omega_h = 0.820188 \times 10^6$ (rad/s) ,

$\zeta = 0.00903$.

Vertical: $Re = -3887.03$ (rad/s) ,

$\omega_h = 0.370649 \times 10^6$ (rad/s) ,

$\zeta = 0.0105$.

Amplitudes of these oscillations are of infinitesimal magnitudes.

High-frequency roots of the simplified perturbation model are due to a very low plasma mass. As the mass approaches zero, these roots approach infinity. High-frequency roots, real at virtual infinity, or oscillatory positively damped, however lightly, do not influence the low frequency stability of plasma motion. The approximated low-frequency radial and vertical dynamics (transfer) functions are given by equation (4.104),

$$\Delta(s-S_1)(s-S_2)(1+\tau_k s) = V_3 G_0(1+\tau_r s) \quad . \tag{6.1}$$

Using the ISX-A tokamak numerical data of the Appendix, the values of the parameters of these functions are as follows.

Radial function	Vertical function
$S_1 = 1.43$	$S_1 = -43.5$
$S_{22} = -1168.1$	$S_{22} = 502.5$
$S_2 = -164.12$	$S_2 = -337.84$
$S_3 = -188.53$	$S_3 = -99.25$
$S_{44} = 534.95$	$S_{44} = 849.55$
$S_4 = -963.75$	$S_4 = -2723.03$
$\tau_k = 0.14\times10^{-3}$	$\tau_k = 0.14\times10^{-3}$
$G_0 = 84.65$	$G_0 = -569.03$
$\tau_r = 5.24\times10^{-3}$	$\tau_r = 4.95\times10^{-3}$

It is observed that the smallest separation ratio of the characteristic equation roots for the radial function is $(\tau_k|S_2|)^{-1}=43.5$; for the vertical function, it is 21.1 . Therefore, for design purposes at least, the effect of the $(1+\tau_k s)$ term in equation (6.1) is negligible.

It is observed that the roots (poles) of the plasma motion dynamics function (6.1), S_1 and S_2, must be real-negative for plasma displacement stability.

Using ISX-A tokamak numerical data, for radial plasma motion root S_1 is real-positive, equal to 1.43 , and therefore an unstable root. Conditions necessary for radial S_1 to be a stable (real-negative) root are apparent from figs. 6.1 and 6.2. Radial S_1 becomes real-negative if either one of the following conditions or any of their proper combinations is true:

(a) N is less than -1.76,

(b) ρ is less than 0.953,

(c) $(I_1)_0$ is less than 1.03×10^5 A.

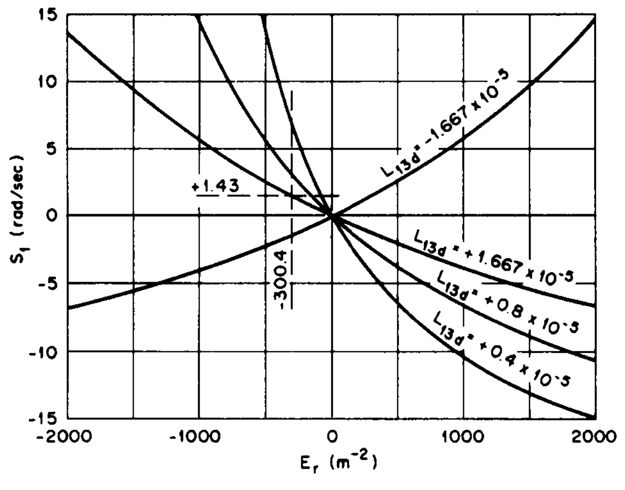

Figure 6.1. Radial root S_1.

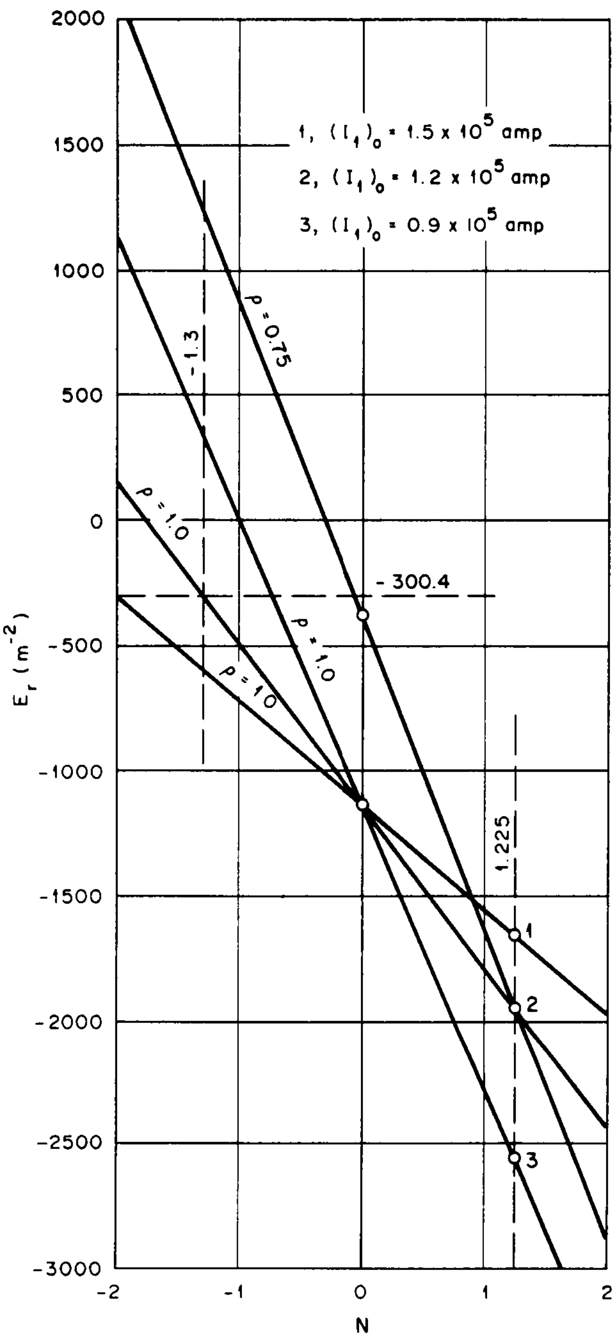

Figure 6.2. Radial parameter E_r.

Considering these conditions, it is observed that (a) is possible, (b) is very possible (the effect of the transformer iron core is known with a much lesser accuracy than 4.7%!), and (c) may be one of the experimental conditions.

Therefore, for radial plasma motion root S_1 may or may not be a stable root, depending on design uncertainties of a tokamak machine and its operating conditions.

For vertical plasma motion, figs. 6.3 and 6.4, root S_1 is real-negative, equal to -43.5, and is therefore a stable root.

Considering root S_2, eq. (4.99), it is noted that at $\tau_r = 0$ it is equal to S_{22}, fig. 6.5, and that radial $S_{22} = -1168.1$ is a stable root, while vertical $S_{22} = +502.5$ is an unstable root.

Both of these roots are operated on by τ_r, according to eq. (4.99), to produce stable radial and vertical roots S_2.

As is shown in fig. 6.6, an initially stable radial root S_{22} produces a stable radial root S_2 for any value of τ_r. Therefore, radial plasma displacement of the ISX-A tokamak may or may not be stable, depending entirely on the radial root S_1, as discussed previously.

An initially unstable vertical root S_{22} is converted to a stable vertical root S_2 only if

$$\tau_r > \frac{1}{\text{unstable vertical } S_{22}} \quad . \tag{6.2}$$

Referring to fig. 6.6, for vertical plasma position stability of the ISX-A tokamak, its vacuum vessel eddy-current time constant must be

$$\tau_r > 2.0\times 10^{-3}\,(\text{s}). \tag{6.3}$$

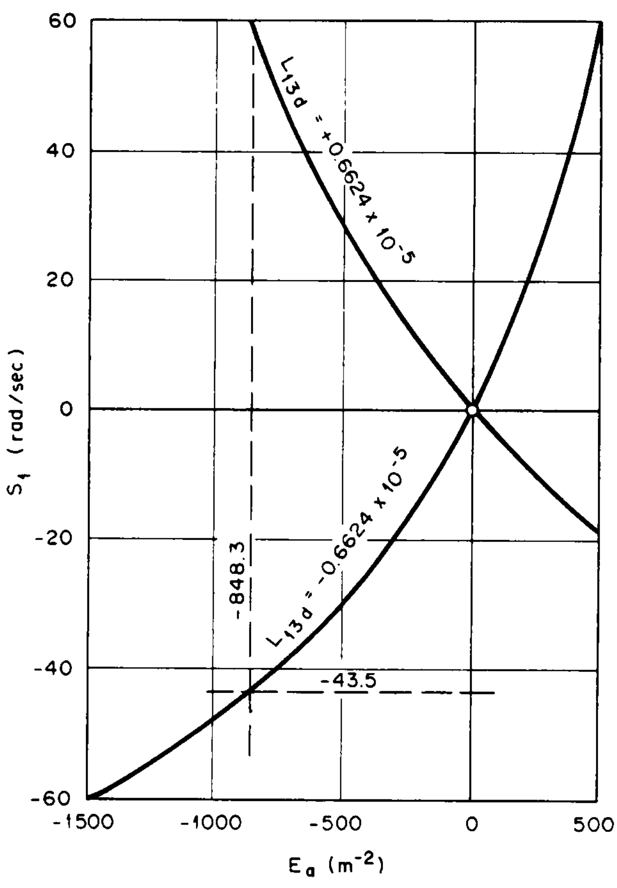

Figure 6.3. Vertical root S_1.

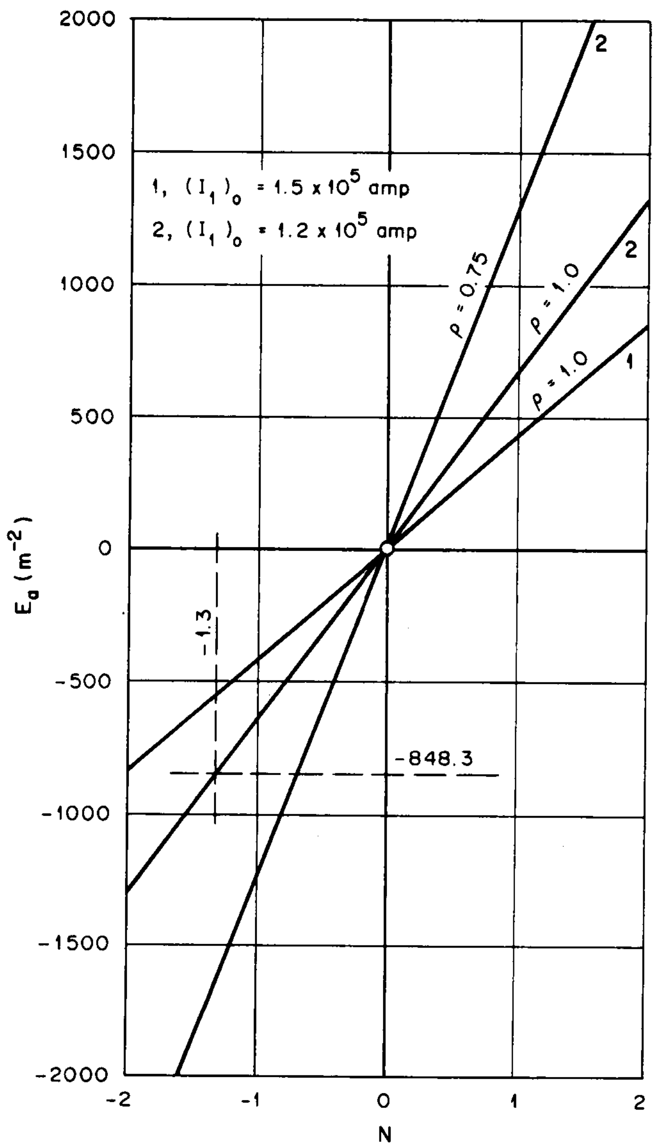

Figure 6.4. Vertical parameter E_a.

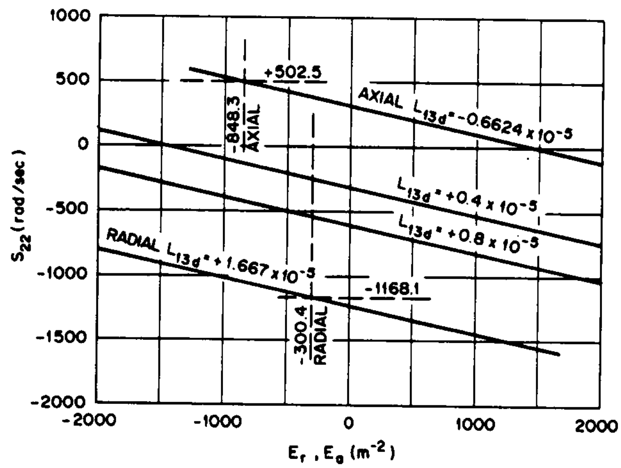

Figure 6.5. Radial and vertical (axial) root S_{22}.

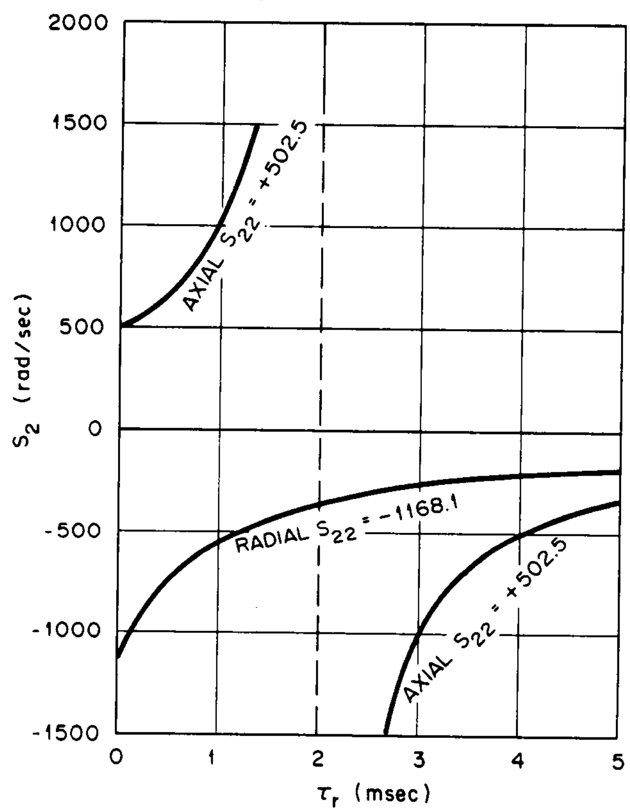

Figure 6.6. Radial and vertical (axial) root S_2.

Among the several ISX-A tokamak parameters estimated specifically for this work, a value of

$$\tau_r = 4.95\times 10^{-3}\,(\mathrm{s}) \tag{6.4}$$

had been arrived at. Therefore, the vertical plasma displacement of an ISX-A tokamak is expected to be stable.

The stability of both the radial and vertical plasma displacements of a tokamak, as discussed up to now, is based on an assumption of having

$$N = \text{negative number} \; (= -1.3)\,,$$

$$\text{radial } L_{13d} = \text{positive number} \; (= +1.667\times 10^{-5}),$$

$$\text{vertical } L_{13d} = \text{negative number} \; (= -0.6624\times 10^{-5}).$$

A careful consideration of figs. 6.1-6.6 reveals that reversing the signs of the above-stated quantities would result in a tokamak machine with a much better plasma displacement stability tolerance to magnitude variations of at least the parameters N, ρ, and $(I_1)_0$.

7. ISX-A TOKAMAK PLASMA DISPLACEMENT FEEDBACK CONTROL

Referring to eqs. (5.12), (5.123), and the Appendix, the ISX-A radial plasma displacement dynamics function is characterized by

$$G_0 = 84.65 \quad ,$$

$$a_1 = -234.69 \quad ,$$

$$a_2 = 162.69 \quad ,$$

$$\tau_r = 5.24\times10^{-3} \quad . \tag{7.1}$$

The eddy-current delay time constant τ_r was estimated using rough approximating methods. For this and other practical reasons, it is desirable to have a control over this time constant. The simplest control of this time constant is, of course, its cancellation via an appropriate adjustable time constant of the control field drive. That is, in equation (5.8) and in fig. 5.3 the gain constant k_u is modified to become

$$k_u = \frac{1}{1+\tau_r s} \quad . \tag{7.2}$$

With this modification eq. (5.12) becomes effectively a second order transfer function,

$$\Delta(s^2 + a_2 s + a_1) = E_3 G_0 \quad . \tag{7.3}$$

For a "burn" pulse of about 0.2 second it is assumed that a step-function rise time of 3.0×10^{-3} seconds (from 5% to 95%) is acceptable. Since the system

(5.140, 5.149) is of only the second or third order, an empirical rule holds approximately,

$$\omega_0 t_r \; = \; 2.0-3.0 \quad . \qquad (7.4)$$

For $t_r = 3\times10^{-3}$ seconds, then,

$$\omega_0 \; = \; 1000.0 \;\; \text{rad/s} \quad . \qquad (7.5)$$

Referring to (5.146), for the control system to be optimal ,

$$\sigma_{21} \; \geqslant \; 1.4237055 \quad . \qquad (7.6)$$

Choosing $\sigma_{21} \; = \; 1.6$, and using (7.1) and (7.5) in eqs. (5.137) and (5.138) it is found that, referring to fig. 5.3 ,

$$k_1 \; = \; 1.181612\times10^4 \quad , \qquad (7.7)$$

$$k_2 \; = \; 16.79445 \quad ,$$

$$k_{1c} \; = \; 1.181335\times10^4 \quad ,$$

and the step-function response is characterized by the rise time of 3.0×10^{-3} seconds and a maximum overshoot of 1.57% at 5.4×10^{-3} seconds .

For an analog implementation of the ISX-A tokamak plasma displacement feedback control eqs. (5.148) and (7.2) are used in fig. 5.3, resulting in fig. 7.1 .

Choosing $\sigma_{31} = \sigma_{32} = 2.6$ and using (7.1) and (7.5) in eqs. (5.154)-(5.157) and (5.153), it is found that, referring to fig. 7.1,

$$k_1 \; = \; 4849.65 \quad , \qquad (7.8)$$

$$k_2 \; = \; 10.6811 \quad ,$$

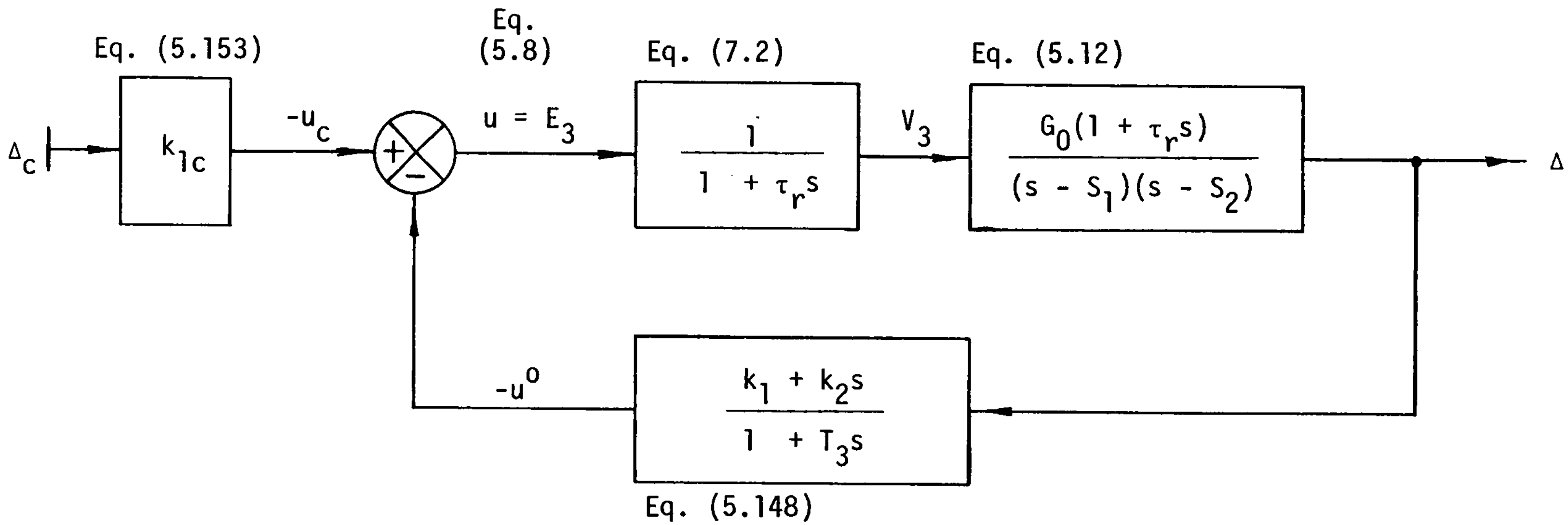

Figure 7.1. ISX-A tokamak plasma displacement feedback control, analog implementation diagram.

$$T_3 = 4.1029\times10^{-4} \quad , \tag{7.8}$$

$$k_{1c} = 4846.88 \quad .$$

For these values of parameters a step-function response is characterized by the rise time of 3.8×10^{-3} seconds and a maximum overshoot of 0.36% at 7.2×10^{-3} seconds. This analog implementation is not *optimal* in a strict mathematical sense. Optimality conditions (5.167) and (5.170) are not satisfied. Practically, however, this design does have an infinite gain margin: at a gain increase of 60.0 dB the step-function response is characterized by the rise time of 5.7×10^{-3} seconds and no overshoot; the system in fact becomes more damped.

A theoretical design step-function response of the ISX-A tokamak radial plasma displacement feedback control system and its corresponding actual hardware response are shown in fig. 7.2 . Discounting minor plasma disruptions, measurement noise, and the actual response record's inaccuracies and nonlinearities, they are in excellent agreement.

An actual hardware ISX-A tokamak *vertical* plasma displacement feedback control system, designed using the same technique, performed just as well as the radial control system.

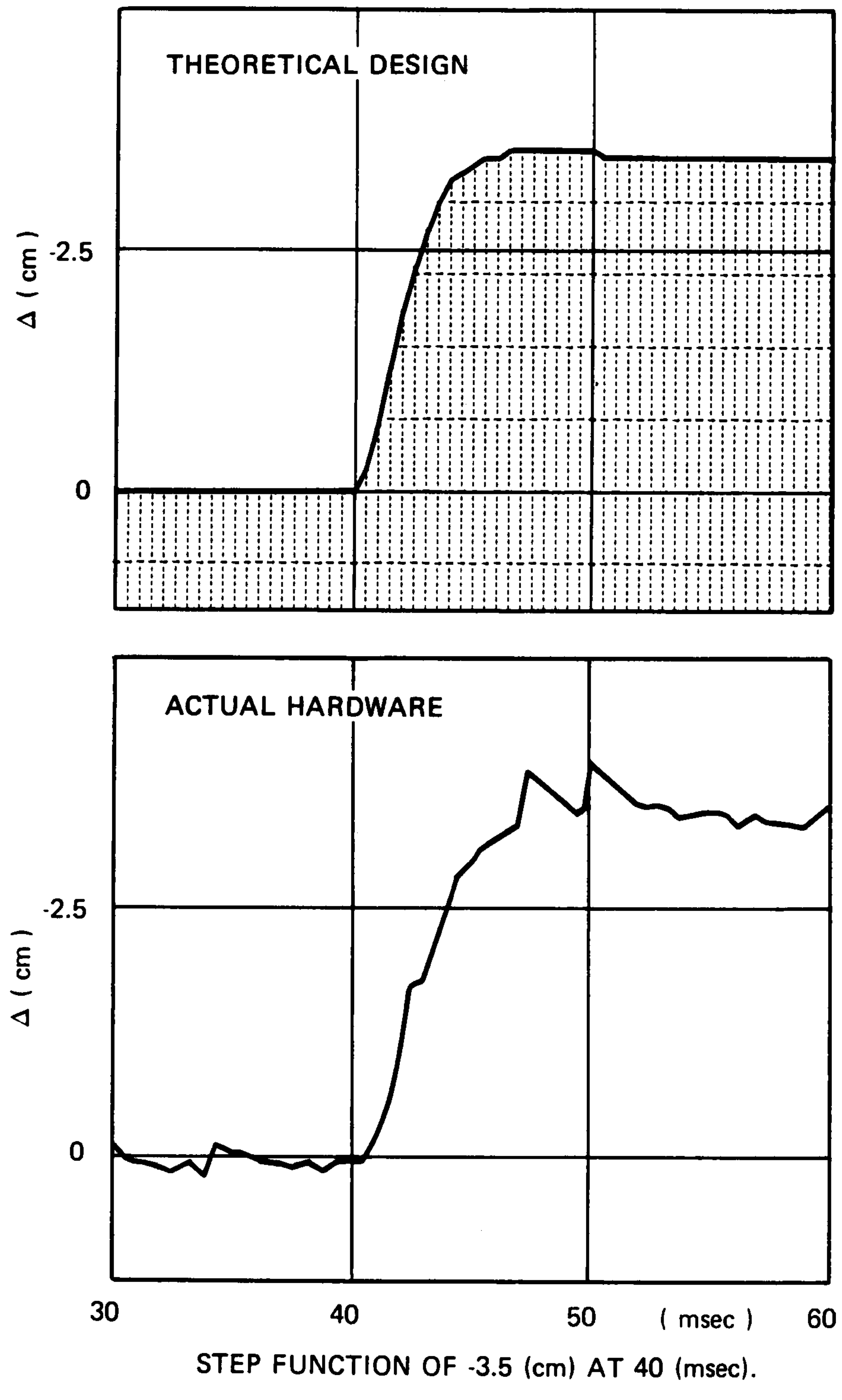

Figure 7.2. ISX-A tokamak radial plasma displacement feedback control, step function response.

8. CONCLUSIONS

A tokamak which does not have a conducting shell, or a tokamak which operates with a long time-pulse, on the order of many seconds, or a steady-state tokamak must employ an active plasma displacement feedback control to keep a plasma torus centered in its vacuum vessel. Analytical design of a tokamak plasma displacement feedback control system requires knowledge of the plasma displacement dynamics of the tokamak. A *unique* low-frequency plasma displacement dynamics transfer function of a tokamak has been developed in a *symbolic* form. This function allows studies of the tokamak plasma equilibrium in terms of its major parameters. One of the major parameters governing plasma equilibrium position stability has been shown to be the *vacuum vessel eddy-current time constant*. It has been shown that for a vacuum vessel eddy-current time constant exceeding a certain value the vertical plasma displacement is stable, in spite of an intentional vertical instability design represented by a negative decay index.

Knowledge of a tokamak plasma displacement dynamics transfer function permits an ordered analytical synthesis of plasma displacement feedback control systems, without too much guesswork. Application of optimal control theory results in a simple plasma displacement feedback control. Feedback control has been considered in view of an optimality condition and the practicality of hardware implementation. A practical plasma displacement feedback control has been designed, and computer simulation and experimental results have been found to be in excellent agreement, supporting all of the analytical developments.

LIST OF REFERENCES

LIST OF REFERENCES

[1] Bishop, Amasa S., PROJECT SHERWOOD, Addison-Wesley, Reading, Mass. (1958).

[2] Artsimovich, L. A., "Research on Controlled Thermonuclear Reactions in the USSR", Proc. of the Second United Nations International Conference on the Peaceful Uses of Atomic Energy, Geneva, 1-13 September 1958, Vol. 31, p. 6.

[3] Teller, Edward, "Peaceful Uses of Fusion", ibid., Vol. 31, p. 27.

[4] Thonemann, P. C., "Controlled Thermonuclear Research in the United Kingdom", ibid., Vol. 31, p. 34.

[5] Tuck, James L., "Review of Controlled Thermonuclear Research at Los Alamos for mid 1958", ibid., Vol. 32, p. 3.

[6] Butt. E. P., et al., "The Design and Performance of ZETA", ibid., Vol. 32, p. 42.

[7] Thompson, W. B., "Theoretical Problems Suggested by ZETA", ibid., Vol. 32, p. 65.

[8] Dolgov-Saveliev, G. G., et al., "Investigations of the Stability and Heating of Plasmas in Toroidal Chambers", ibid., Vol. 32, p. 82.

[9] Alfven, H., "Magnetohydrodynamics and the Thermonuclear Problem", ibid., Vol. 31, p. 3.

[10] Biermann, L., "Recent Work on Controlled Thermonuclear Fusion in Germany (Federal Republic)", ibid., Vol. 31, p. 21.

[11] Aymar, R., et al., "Experimental Studies of the Pinch Phenomenon", ibid., Vol. 32, p. 92.

[12] Andreoletti, J., et al., "High Intensity Discharges in Deuterium in a Metal Wall Torus", ibid., Vol. 32, p. 100.

[13] Siegbahn, Kai, Ohlin, Per, "Toroidal Discharges in Deuterium with External Magnetic Field", ibid., Vol. 32, p. 113.

[14] Jukes, J. D., MAN-MADE SUN, Abelard-Schuman, London and New York (1959).

[15] Bezbatchenko, A. L., et al., "A High-Current Electrodeless Discharge in a Toroidal Chamber with a Longitudinal Magnetic Field", Plasma Physics and the Problems of Controlled Thermonuclear Reactions, Volume IV, Pergamon Press (1960), p. 135.

[16] Glasstone, S., Lovberg, R. H., CONTROLLED THERMONUCLEAR REACTIONS, Van Nostrand Reinhold Co., New York (1960).

[17] Rose, D. J., Clark, M., Jr., PLASMAS AND CONTROLLED FUSION, The MIT Press and John Wiley & Sons, Inc., New York (1961).

[18] Spitzer, L., Jr., PHYSICS OF FULLY IONIZED GASES, Interscience Publishers, NewYork (1962).

[19] Shafranov, V. D., "Equilibrium of a Toroidal Pinch in a Magnetic Field", Soviet Atomic Energy 13 (1963) 1149.

[20] Kalman, R. E., "When is a Linear Control System Optimal?", Transactions of the ASME Ser. D: Journal of Basic Engineering, Vol. 86, pp. 51-60, March 1964.

[21] Artsimovich, L. A., Mirnov, S. V., Strelkov, V. S., "Investigation of Ohmic Heating of the Plasma in the "Tokamak-3" Toroidal Assembly", Soviet Atomic Energy, Consultants Bureau, Volume 17, No. 1, p. 886, July, 1964.

[22] Mirnov, S. V., "Probe Method of Measuring the Displacement of the Current Pinch in Cylindrical and Toroidal Chambers", ibid., p. 929.

[23] Artsimovich, L. A., "Controlled Thermonuclear Fusion and High-Temperature Plasma Physics Research in the USSR", Proc. of the Third International Conference on the Peaceful Uses of Atomic Energy, Geneva, 31 August - 9 September 1964, Volume 15, 17.

[24] Artsimovich, L. A., CONTROLLED THERMONUCLEAR REACTIONS, Gordon and Breach Science Publishers, Inc., New York (1964).

[25] Athans, Michael, Falb, Peter L., OPTIMAL CONTROL, McGraw-Hill Book Company, New York (1966).

[26] Shafranov, V. D., "Plasma Equilibrium in a Magnetic Field", Reviews of Plasma Physics 2 , Consultants Bureau, New York (1966) 103.

[27] Sage, A. P., OPTIMAL SYSTEMS CONTROL, Prentice-Hall, Inc., Englewood Cliffs, New Jersey (1968).

[28] Arsenin, V. V., et al., "Suppression of Plasma Flute Instability by Means of a Feedback Circuit", Proc. Plasma Physics and Controlled Nuclear Fusion Research, 3rd Int. Conf., Novosibirsk, USSR, 1-7 August 1968, Vol. II, 515.

[29] Church, M. J., et al., "Stabilisation of Ion Cyclotron Instabilities by Electron Heating and Flute Instability by Feedback in Magnetic Well/Mirror Geometries", Proc. of 3rd European Conference on Controlled Fusion and Plasma Physiscs, Symposium on Beam-Plasma Interactions, Utrecht, The Netherlands, 23-27 June 1969, 12.

[30] Furth, H. P., Rutherford, P. H., "Feedback Control Problems in Tokamaks", AIP Conf. Proc. Feedback and Dynamic Control of Plasmas, New York, 1970, Number 1, 74.

[31] Anderson, Brian D. O., Moore, John B., LINEAR OPTIMAL CONTROL, Prentice-Hall, Inc., Englewood Cliffs, New Jersey (1971).

[32] Greene, J. M., et al., "Tokamak Equilibrium", Physics of Fluids 14 (1971) 671.

[33] Artemenkov, L. I., et al., "Experiments on Equilibrium in the Uncased TO-1 Tokamak Device by Means of a Feedback System", Proc. Plasma Physics and Controlled Nuclear Fusion Research, 4th Int. Conf., Madison, USA, 17-23 June 1971, Vol. I, 359.

[34] Mukhovatov, V. S., Shafranov, V. D., "Plasma Equilibrium in a Tokamak", Nuclear Fusion 11 (1971) 605.

[35] Artsimovich, L. A., "Tokamak Devices", Nuclear Fusion 12 (1972) 215.

[36] Artemenkov, L. I., et al., "Experiments on the TO-1 Tokamak having an Automatic System for Controlling the Equilibrium", in Controlled Fusion and Plasma Physics, (6th Europ. Conf. Moscow, 1973), Paper 1.7.1.

[37] Hugill, J., et al., "Plasma Equilibrium in Cleo-Tokamak", ibid., Paper 1.7.2.

[38] Merckel, G. U., "Computer Controlled Feedback Stabilization of an MHD Plasma Instability", Ph.D. Thesis, The University of Tennessee, August 1973.

[39] Hugill, J., Gibson, A., "Servo-Control of Plasma Position in Cleo-Tokamak", Nuclear Fusion 14 (1974) 611.

[40] Furth, H. P., "Tokamak Research", Nuclear Fusion 15 (1975) 487.

[41] Arsenin, V. V., "Stabilization of Flute Waves in an Open Cofiguration by a Magnetic Feedback System", ibid., p. 237.

[42] Miskell, R. V., "A Control Srategy for Plasma Equilibrium in a Tokamak", Oak Ridge Report No. Y-1988, August 1975.

[43] Allgeyer, R., et al., "The Design of the ASDEX Tokamak", Proc. 6th Symposium on Engr. Problems of Fusion Research, San Diego, Calif., November 18-21, 1975, 378.

[44] Anderson, J. L., Bailey, J. M., Booth, R. S., Colchin, R. J., Miskell, R. V., "Feedback Control for Plasma Equilibrium in ORMAK", Nuclear Fusion 16 (1976) 629.

[45] Schneider, F., Gresser, F., "Investigations on the Feedback System of ASDEX", Proc. of the 9th Symposium on Fusion Technology, Garmish-Partenkirchen (FRG), June 14-18, 1976, 783.

[46] Bombi, F., Ciscato, D., "Plasma Position and Shape Control in JET", ibid., 789.

[47] Edelbaum, T. N., et al., "Fusion Reactor Control Study", 1st Annual Report, Electric Research Institute, Report ER-533, Palo Alto, California, July 1977.

[48] Gran, R., et al., "Plasma Position Control for TFTR using Modern Control Theory", Proc. 7th Symposium on Engr. Problems of Fusion Research, Knoxville, TN, October 25-28, 1977, Volume I, 104.

[49] Suzuki, Y., et al., "Control System of Plasma Position and Cross-Sectional Shape in Large Tokamak Device", ibid., 112.

[50] Dei-Cas, R., et al., "Slow and Fast Feedback Circuits for the Plasma Equilibrium in the T.F.R. 600 Tokamak", ibid., 478.

[51] Schneider, F., "Novel Method of Determining the Plasma Position and its Application to the ASDEX Feedback System", Fusion Technology 1978, Proc. of the 10th Symposium, Padova, Italy, 4-9 September 1978, Volume 2, 1013.

[52] Gerhauser, H., "Calculations on Feedback Control of Plasma Position in the Textor Vessel and the Role of the Response Time Behaviour of the Control System", Proc. of the Tenth Symposium on Fusion Technology 1978, Volume 2, p. 951, Padova, Italy, 4-9 September 1978.

[53] Bobbio, S., et al., "Stabilizing Passive Shell and Active Feedback Windings for 'RFP' Configurations", ibid., p. 1007.

[54] Ninomiya, H., et al., "Studies of Eddy Currents in JT-60", Proc. of the 8th Symposium on Engineering Problems of Fusion Research, Volume IV, p. 1867, San Francisco, California, November 13-16, 1979.

[55] Cotsaftis, M., "Non Linear Equilibrium and Stability of a Toroidal Plasma Inside its Vessel", ibid., p. 1884.

[56] Yoshioka, K., et al., "Computer Aided Design for Plasma Control of the JT-60", ibid., p. 1894.

[57] Matsuzaki, Y., et al., "Direct Digital Control of Plasma Position in JFT-2 Tokamak without Shell", ibid., p. 1899.

[58] Cosler, A., et al., "Design, Fabrication and Testing of Magnetic Field Diagnostic Components for Implantation into the Textor Tokamak", ibid., p. 1903.

[59] Gran, R., et al., "A Survey of the TFTR Feedback Control Design", Proc. of the 8th Symposium on Engineering Problems of Fusion Research, San Francisco, Calif., Nov. 13-16, 1979, Volume IV, 1854.

[60] Chao, Y. A., et al., "A Practical Method for Analyzing the Feedback Control of the Position of a Tokamak Plasma", ibid., 1869.

[61] Blum, J., Dei Cas, R., "Static and Dynamic Control of Plasma Equilibrium in a Tokamak", ibid., 1873.

[62] Ogata, A., Ninomiya, H., "Use of Modern Control Theory in Plasma Control at Neutral Beam Injection", ibid., 1887.

[63] Gran, R., et al., "TFTR Plasma Control System Analysis with Power Supply Dynamics and Diagnostic Filtering", ibid., 1887.

[64] Lerner, Eric J., "Magnetic Fusion Power", IEEE Spectrum, Dec. 1980, 44.

[65] Miyamoto, Kenro, PLASMA PHYSICS FOR NUCLEAR FUSION, MIT Press, Cambridge, Mass. (1980).

[66] Stacey, Weston M., Jr., FUSION PLASMA ANALYSIS, John Wiley & Sons, New York (1981).

[67] Dolan, Thomas James, FUSION RESEARCH, Pergamon Press, New York (1982).

APPENDIX

APPENDIX

ISX-A TOKAMAK CHARACTERISTICS

The Impurity Study Experiment (ISX) tokamak was a joint project of General Atomic Company, San Diego, California, and Oak Ridge National Laboratory (ORNL) and was the first (-A) experimental tokamak in a series of experiments exploring the effects of impurities in high temperature hydrogen plasmas and the magnetic flux conservation concept (developed at ORNL), which may be used to increase the "beta" of the tokamak discharge.

In a tokamak, such as ISX-A, three magnetic field components are employed to hold the plasma in the shape of a torus. They are shown schematically in fig. 2.1. A toroidal magnetic field (B_T) is obtained using 18 water-cooled coils powered by a 120,000-ampere solid state power supply. A second field component is the poloidal field (B_P), which is produced by up to 200,000 amperes of current flowing in the plasma itself. The current also provides about 600,000 watts of resistive (ohmic) heating for the plasma. Finally, to achieve equilibrium, a vertical field (B_{s0}) is necessary; this is provided by toroidal windings powered by storage batteries. The plasma is produced within a stainless steel vacuum vessel. The vessel is all welded construction with metal vacuum seals and is bakeable to 400 degrees Celsius. The use of ultrahigh vacuum technology serves to minimize the amount of impurities present in the discharge, a crucial requirement of successful tokamak operation. Beyond the vacuum vessel are two concentric fiberglass cylinders which support the vertical field windings. The primary windings induce the plasma current (I_1) and form the primary of a large transformer; they are supplied by a capacitor bank and storage batteries. An iron core threading the center of the torus carries the magnetic flux, inducing the current in the plasma which acts as the secondary of the transformer.

Major parameters of ISX-A tokamak are:

Toroidal magnetic field $\approx$ 1.8 tesla,

Vertical magnetic field $\approx$ 200 gauss (0.02 tesla),

Plasma current $\approx$ 40,000 to 200,000 amperes,

Ohmic heating power $\approx$ 600,000 watts,

Peak electron temperature $\approx$ 1200 electron volts,

Peak ion temperature $\approx$ 400 electron volts,

Plasma density $\leqslant 4 \times 10^{19}$ particles/m^3,

Plasma volume $\approx$ 1000 liters,

Experiment time $\approx$ 0.2 seconds.

Figure A1 shows schematically arrangement of the ISX-A tokamak toroidal, ohmic heating, and vertical field coils relative to the iron core center line. Figure A2 is a photograph of the ISX-A tokamak as it looked in February 1977 when initial operation took place.

Representative numerical data of the ISX-A tokamak for a steady-state discharge ("burn" phase) are given below. The subscript "0" denoting a nominal steady-state quantity, where it would be applicable, is omitted for simplicity. The data apply to both the radial and vertical degrees of freedom, except where noted.

$$I_1 = 1.2 \times 10^5 \,(\mathrm{A}) \,,$$

$$\dot{I}_1 = 0 \,,$$

$$I_2 = 200.4 \,(\mathrm{A}) \,,$$

$$\dot{I}_2 = 0 \,,$$

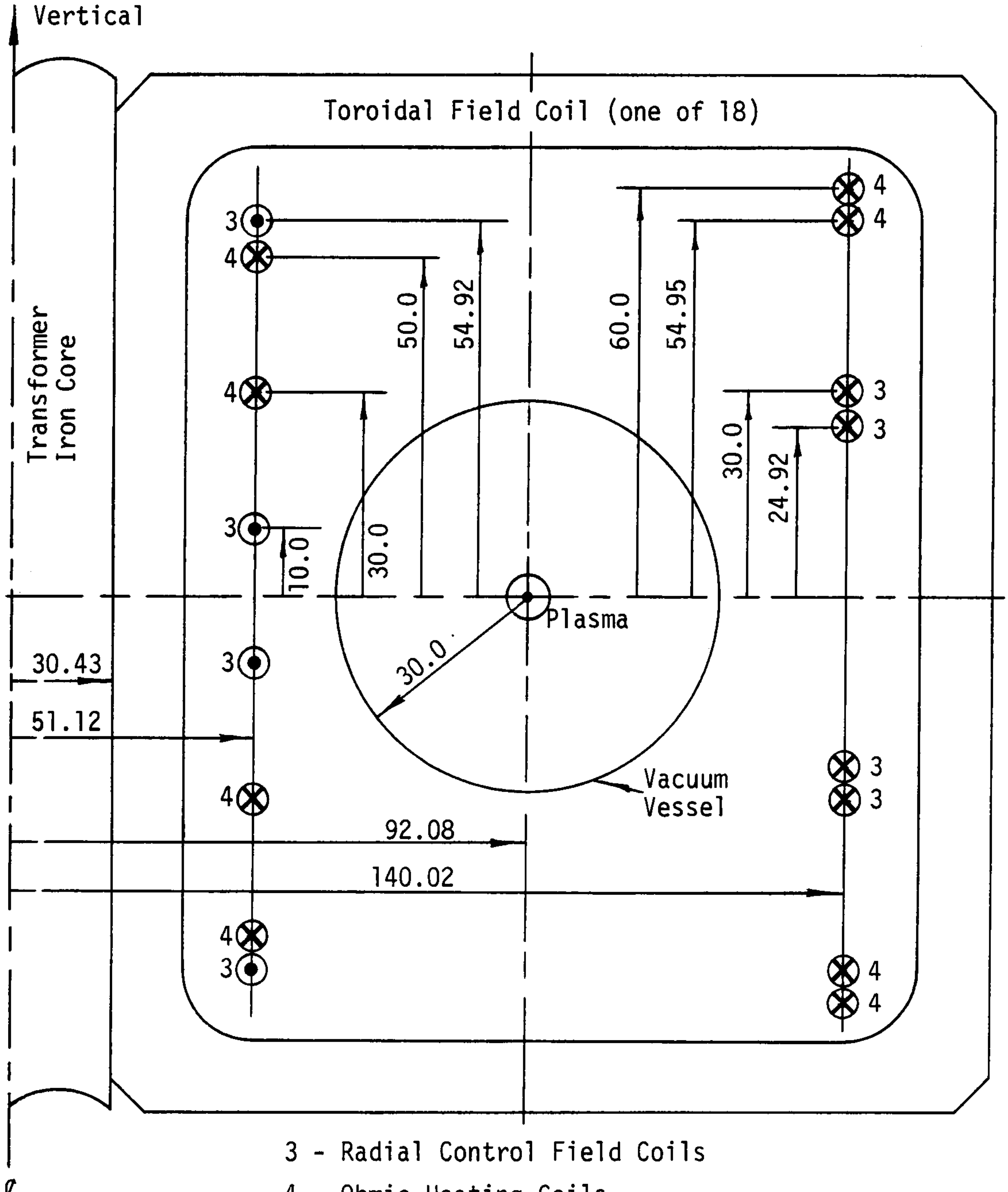

3 - Radial Control Field Coils
4 - Ohmic Heating Coils
Measurements are in centimeters

Figure A1. ISX-A tokamak toroidal, radial control field, and ohmic heating coils. Schematic diagram.

ISX

FUSION ENERGY

THE IMPURITY STUDY EXPERIMENT

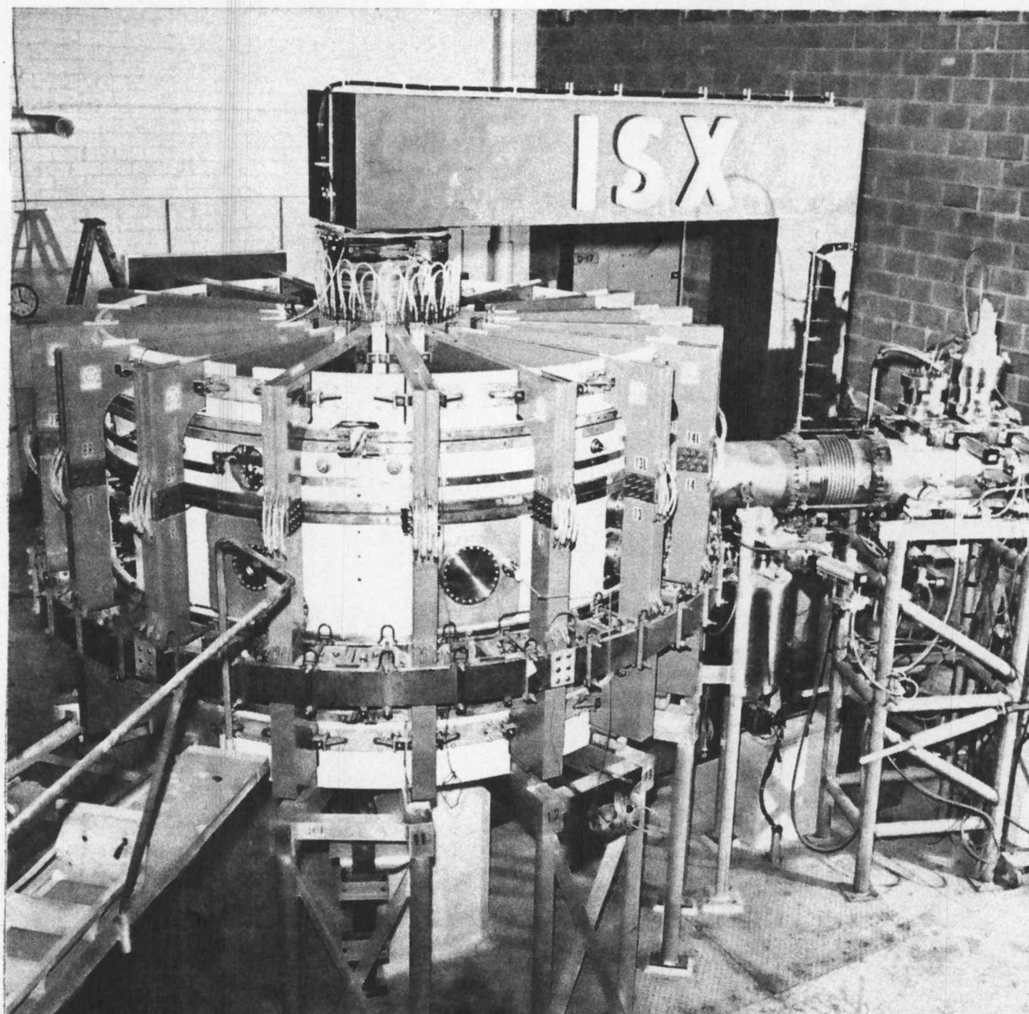

OAK RIDGE NATIONAL LABORATORY

OPERATED BY UNION CARBIDE CORPORATION FOR THE ENERGY RESEARCH AND DEVELOPMENT ADMINISTRATION

Figure A2. ISX-A tokamak.

I_4 is not required since $K_h = 0$,

$\dot{I}_4$ is not required since $L_{14d} = 0$,

$L_{11} = 2.273\times10^{-5}$ (H) ,

$L_{22} = 2.273\times10^{-5}$ (H) ,

$L_{33} = 8.429\times10^{-5}$ (H) , $= 1.65\times10^{-5}$ (H) vertical ,

$L_{44} = 1.424\times10^{-3}$ (H) ,

$L_{12} = 2.273\times10^{-5}$ (H) ,

$L_{13} = 2.110\times10^{-7}$ (H) , $= 0.0$ vertical ,

$L_{14} = 1.736\times10^{-4}$ (H) ,

$L_{23} = 2.110\times10^{-7}$ (H) , $= 0.0$ vertical ,

$L_{24} = 1.736\times10^{-4}$ (H) ,

$L_{34} = 4.716\times10^{-6}$ (H) ,

$L_{11d} = 3.3644\times10^{-5}$ (H/m) ,

$L_{12d} = 1.6818\times10^{-5}$ (H/m) ,

$L_{13d} = 1.6670\times10^{-5}$ (H/m) , $= -6.624\times10^{-6}$ (H/m) vertical ,

$L_{14d} = 0.0$,

$R_2 = 7.0\times10^{-3}(\Omega)$,

$R_3 = 2.2\times10^{-3}(\Omega)$, $= 2.0\times10^{-3}(\Omega)$ vertical ,

$R_4 = 14.2\times10^{-4}(\Omega)$,

$K_c = 2.87\times10^{-6}$ (T/A) , $= 5.2\times10-7$ (T/A) vertical ,

$K_k = 28.7\ (\mathrm{m}^{-1})$, $= 5.2\ (\mathrm{m}^{-1})$ vertical ,

$K_r = 4.707\times10^{-3}\ (\mathrm{s/m}^2)$, $= 3.103\times10^{-3}\ (\mathrm{s/m}^2)$,

$K_i = (13.223\rho + 1)$, $0 \geqslant \rho \geqslant 1.0$,

$K_h = 0.0$,

$K_n = 0$ for design ,

$K_v = 3.279\ (\mathrm{m}^{-1})$, $= 0.0$ vertical ,

$\tau_t = 0.14\times10^{-3}\ (\mathrm{s})$,

$\tau_k = 0.14\times10^{-3}\ (\mathrm{s})$,

$\tau_r = 5.237\times10^{-3}\ (\mathrm{s})$, $= 4.950\times10^{-3}\ (\mathrm{s})$ vertical ,

$N = -1.3$,

$l_i = 0.5$,

$kT = 1.0\times10^{-16}\ (\mathrm{J/particle})$,

$n = 2.0\times10^{19}\ (\mathrm{nuclei/m^3})$,

$M_0 = 6.57\times10^{-9}\ (\mathrm{kg})$,

$R = 0.92\ (\mathrm{m})$,

$a = 0.25\ (\mathrm{m})$,

$r_c = 0.3\ (\mathrm{m})$.

VITA

Oleg Burenko was born in Jusowka, Ukraine on August 15, 1925. In May 1945, at the end of World War II in Europe, he found himself in Germany where beginning in 1946 he engaged in continuing his education at the universities in Regensburg and Karlsruhe. In July 1949 he immigrated to the United States of America and after entering Ohio State University in March 1951, he received a Bachelor of Science degree in Electrical Engineering in June 1953. In 1954 he became a member of Sigma Xi and Eta Kappa Nu honor societies. In March 1955 he received a Master of Science degree in Electrical Engineering. During the time period 1953 through 1975 he was employed at the Ohio State University Electrical Engineering Department, Convair Missile Division, Martin Marietta Aerospace, General Precision Aerospace, and Northrop Nortronics in various positions ranging from Research Associate to Research Scientist, in areas of aerospace vehicle flight control analysis, development, research, consulting, and supervision. He is a registered Professional Engineer in the State of Florida. In November 1975 he joined Oak Ridge National Laboratory. While employed full-time, he entered graduate school at The University of Tennessee, Knoxville, as a part-time student and was admitted to candidacy in March 1982. He received the Doctor of Philosophy degree in Engineering Science with a specialization in systems dynamics and feedback control theory in June 1983.